TECHNICAL OPERATIONS RESEARCH

FINAL REPORT
THE EFFECT OF LIMITED STRIPS OF CONTAMINATION ON THE DOSE RATE IN A MULTISTORY WINDOWLESS BUILDING

By
John F. Batter
Albert W. Starbird
Nancy-Ruth York

Report No. TO-B 62-58
Contract No. OCD-OS-62-43
August, 1962

Submitted to

Office of Civil Defense
Department of Defense
Washington, D. C.

techops

TECHNICAL OPERATIONS Incorporated

FINAL REPORT

THE EFFECT OF LIMITED STRIPS OF CONTAMINATION ON THE DOSE RATE IN A MULTISTORY WINDOWLESS BUILDING

By

John F. Batter, Albert W. Starbird, and Nancy-Ruth York

Report No. TO-B 62-58

Contract No. OCD-OS-62-14

August, 1962

Submitted to

Office of Civil Defense
Department of Defense
Washington, D. C.

Burlington, Massachusetts

FOREWORD

This is the fifth and final report on the effects of limited fields of contamination on the dose rate within a multistory structure as determined by modeling techniques under Contract No. OCD-OS-62-14. The model structure represented a 6-story windowless building of different wall and floor mass thicknesses. Preliminary raw data are presented in Volume I (Report No. TO-B 62-26) containing data on a model with 20 psf walls and floors; Volume II (TO-B 62-29), a model with 80 psf walls and floors; Volume III (TO-B 62-40), a model with 0 psf walls and 20 psf floors; and Volume IV (TO-B 62-49), a model with 20 psf walls and 80 psf floors. These interim reports were issued upon the completion of the model experiments for each of the four structures to make these data immediately available to the National Shelter Survey Computer Program. Final analysis, results, and recommendations on the four 6-story structures investigated are presented in this report.

ACKNOWLEDGMENTS

The authors gratefully acknowledge the valued efforts of Mr. Milton Dwonczyk, Mr. Robert MacNeil, Mr. Richard J. Brodeur, and Mr. David McLaughlin for their untiring efforts in the performance of the experiments described in this report.

ABSTRACT

This final report of a series of five evaluates the effects of limited fields of contamination on the dose rate within multistory structures. Comparisons are made between experimentally determined results and those obtained through use of the OCD "Guide for Architects and Engineers," the National Shelter Survey Computer Program, and the OCD Manual entitled "The Design and Review of Structures for Protection from Fallout Gamma Radiation."

The National Shelter Survey Computer Program method for correction to account for near-field limited strips of contamination contains appreciable error, because it does not differentiate between thin- and thick-floor correction factors. Recommended experimentally obtained multiplicative correction factors for both thin and thick floors are presented. Further investigation of the effects of floor thickness and floor-edge scattering is recommended. An improved computation procedure for determining the fraction of infinite-field dose rate obtained from far-field limited strips of contamination is described. Agreement is excellent between experimentally measured and computed infinite-field dose rates. The measured dose rates in the basement are higher than predicted by computational procedures. Further below-ground-level investigation is recommended on a full-scale basement. Excellent agreement is shown between results obtained from the modeling technique on a phantom structure and previous full-scale results.

TABLE OF CONTENTS

TABLE OF CONTENTS (Cont'd.)

LIST OF ILLUSTRATIONS

LIST OF ILLUSTRATIONS (Cont'd.)

LIST OF TABLES

LIST OF TABLES (Cont'd.)

LIST OF TABLES (Cont'd.)

CHAPTER 1

INTRODUCTION

In the event of a nuclear attack on the United States, the shelter from fallout afforded by urban structures may prevent excessive radiation casualties and thus prove to be decisive in our ability to recover quickly. The essentially infinite field of fallout contamination from a nuclear explosion is interrupted in urban areas by many multistoried structures. To compute the shelter afforded by such structures, therefore, the effect of finite fields of contamination must be taken into account.

Finite-field computational procedures of the previous guides published by the Office of Civil Defense ("Guide for Architects and Engineers"[1] and "The Design and Review of Structures for Protection from Fallout Gamma Radiation"[2]) and the National Shelter Survey Computer Program[3] are based on analytical interpretations of the angular distribution of radiation penetrating slabs. The purpose of this study has been to evaluate these analytical procedures and to provide experimental data from which improved techniques may be developed.

Full-scale experimentation upon real structures, while desirable, is considerably less economical than model experimentation, and presents excessive experimental difficulties: the finding or construction of a suitable test structure surrounded by enough flat, cleared land to perform experiments; the exclusion of nonauthorized personnel during the experiment; the use of intense radiation sources; and the monitoring and guarding of the security of the experimental area, to mention a few. The concept of radiation modeling was therefore used to devise a program flexible enough to ensure the rapid accumulation of accurate data, without incurring inordinate costs, on the effects of limited strips of contamination on structures typical of an urban complex.

The basic structure selected as typical of what might be found in an urban area was a 6-story building of 36 x 48 foot plan area. This structure, scaled to 1/12 size, was constructed of iron plates so that its wall and floor thicknesses could be easily varied. A field of contamination was then created about the structure, using cobalt-60 as the fallout simulant. This field was divided into thirty-two separate experimental areas surrounding one quadrant of the structure. The size of each

area was chosen to represent typical sizes of parking lots, roadways, and other ground level spaces where fallout might accumulate in an urban area.

The data obtained from these experiments were published in preliminary form at the conclusion of the investigation on each structure type so that the results could be used immediately in the National Shelter Survey Computer Program.[4-7] These data are now collected in final form, and a comprehensive analysis is performed on the effects of limited fields of fallout contamination on urban-type structures.

A complete description of the experiment, including the modeling technique, the scale-model facility, and the operational procedures, is given in Chapter 2. Chapter 3 presents the results of tests on a phantom version of the model structure to determine the accuracy of the experimental techniques. Experimental data and analysis are presented in Chapters 4 and 5 for above-ground and below-ground positions, respectively. Conclusions and recommendations gained from this study are contained in Chapter 6.

CHAPTER 2

DESCRIPTION OF EXPERIMENT

THE MODELING TECHNIQUE

Theoretically, the internal radiation-dose distribution inside a structure from radiation sources located outside a structure will be exactly reproduced in a geometrically similar scale model if the densities of all materials comprising the structure, the surrounding ground, and the atmosphere are increased by the scale factor. Perfect scaling therefore requires that: (1) All physical dimensions be linearly scaled by the same factor, (2) Each absorbing surface attenuate radiation to the same degree as the original surface, independent of the scaling factor, and (3) The specific scattering and absorption properties of all materials remain unchanged. These basic rules of modeling show that densities of all materials should be increased by the same scaling factor that reduces linear dimensions.

In practice, however, limitations in increasing densities by a factor large enough to be useful in reducing building dimensions make it difficult to achieve this ideal. For modeling to have sufficient advantage over full-size structure experimentation, scaling by a factor of about 10 must be used. A scale factor of 12 was chosen for the 6-story model building used in the experiment covered in this report. The actual scaling rules followed in this experiment were somewhat relaxed from those defining perfect modeling. Iron was substituted for concrete and other building materials to increase density without radically changing the atomic number and the corresponding cross sections of the material. This permitted an increase in average density of approximately 3 as compared to the desired factor of 12. However, prior modeling experiments[8,9] have shown that realistic results can be obtained if the wall thickness does not exceed 10% of the average dimensions of any given room. Hence, wall thicknesses may be increased above those indicated by the scale factor without distorting the dose distribution within the structure. Since it is impractical to scale the densities of the ground or atmosphere surrounding the models, skyshine and ground penetrations were not properly reproduced in the experiment and must be allowed for by analytical procedures. However, since

skyshine comprises a maximum of 10% of the dose rate for a zero thickness building and attenuates more rapidly than direct or structure-scattered radiation, the error due to neglect of skyshine should be small. The model building is thick enough so that most of the radiation within the structure is direct radiation from the gamma-ray source or from radiation scattered by the walls and ceiling of the building itself.

SCALE-MODEL FACILITY

A facility for conducting gamma-ray experiments on model buildings was constructed for the Office of Civil Defense by Technical Operations, Inc., during the spring of 1960. It was built on a 6-acre site in Burlington, Massachusetts, adjacent to the firm's main office building. This site is ideal for carrying out gamma-ray experiments because the terrain provides a natural barrier between the facility and the main building, and the company's other radiographic and shop facilities are nearby. The facility was also situated far enough away from other buildings in the area to allow safe use of radioactive materials of high enough source strength to permit reasonable experimentation time. Figure 1 shows a plan view of the model facility.

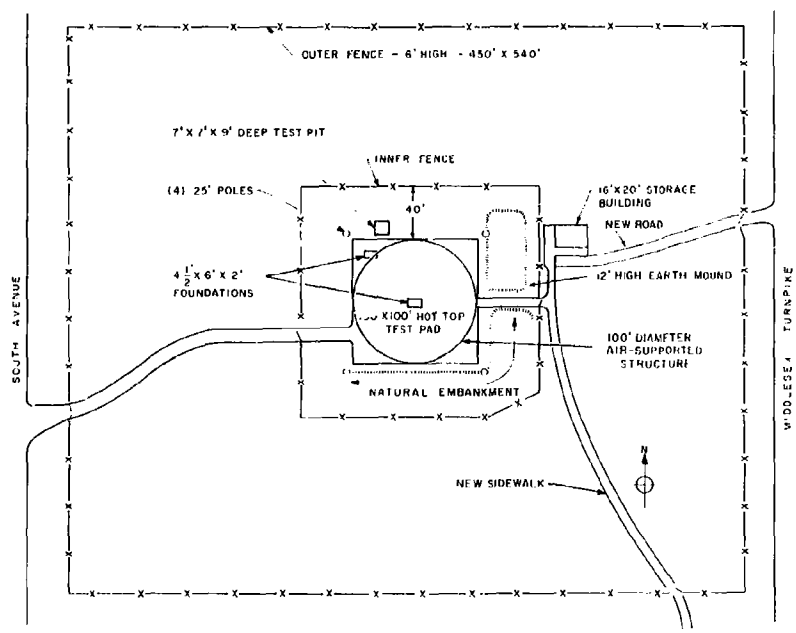

Figure 1. Plan View of Model Facility

An outer personnel-protection fence 6 feet high with two locked service gates and a personnel entrance gate (with alarm) was constructed around the site. "Caution, Radiation Area" signs were posted on this fence at 50-foot intervals. A 100 x 100 foot flat test pad with asphalt surface was constructed near the center of the enclosed area. Two concrete foundations 4-1/2 x 6 x 2 feet deep were recessed flush in the pad to permit testing of model buildings with basements. One foundation was located at the center of the pad, permitting 360^{o} area spread and source ring experiments, and the other was positioned near one corner of the pad for quarter-symmetry experiments. An inner fence was erected at a minimum distance of 40 feet from the edge of the pad to serve as a high-radiation (100 mr/hr) area boundary. This fence was connected to an audible alarm that was triggered if anyone climbed the fence. "Caution, High-Radiation Area" signs were attached to this fence at 50-foot intervals. Chain gates were provided for the two entrances to the test pad. A 25-foot pole was erected at each corner of the pad for flood lighting and stringing cables over the pad. On the east side of the pad, a 12-foot earth mound was formed from boulders and other fill material removed during rough grading of the pad. The mound provides excellent protection for operating personnel during radiation experiments. Behind the mound, a 16 x 20 foot control and storage building was erected. This building and a paved path to the pad were constructed at pad level to permit wheeling heavy lead source containers from the storage area to the test pad.

During the fall of 1961, a hemispherical, air-supported structure, 45 feet high with a 100-foot diameter base, was erected over the test pad to permit all-weather, year-round operation (Figure 2). Birdair, Inc., of Buffalo, New York, fabricated and installed this vinyl-coated nylon structure. A pressure of 1-1/2 inches of water supplied by two 1-horsepower air blowers keeps the balloon-type building inflated. A ballast skirt attached to the balloon and filled with 90 tons of sand anchors the structure to the test pad. Access is through an air-locked entry near the control and utility building. A concrete-block radiation shield 16 inches thick was also installed in the hemispherical shelter adjacent to the air-locked exit so that an operator could remain in the test area during exposure if desired. A 350,000 BTU/hr oil heater removes the chill inside the structure during cold weather.

Figure 2. Entrance of Air-Supported Structure

The placement of the balloon over the test pad area made necessary a new access road to the storage and control shack. This road (from Middlesex Turnpike to the control shack) is shown as "New Road" in Figure 1. Since the hemispherical balloon prevented use of the corner pit, all arrangements of the multistory model building were erected over the center pit.

MODEL STRUCTURE

Shielding experiments were conducted on a 6-story, steel model structure with basement, representing a full-scale building 36 feet wide by 48 feet long. This structure had no doors or windows because the effect of such apertures on dose rate was not a part of this investigation. The experimental structure was scaled to 1/12 full-size, thus creating a 36 by 48 inch rectangular cross-section building 6 feet high.

The model building was designed around a basic single story of 1/2-inch thick steel. Six of these stories were stacked vertically to form a 6-story structure. Allowance was provided for increasing floor thickness in 1/2-inch increments and for bolting layers of 1/2-inch thick steel plates to the sides of the model. In this way, wall and floor thicknesses were increased to a maximum of 2 inches of steel. A single 4 x 6 foot x 1/2 inch thick steel plate served as an easily removable rear wall, allowing quick access to instrumentation within the model structure.

The model structure rests on a lead and concrete foundation outlining a basement 2 feet deep, 4-1/2 feet long, and 4 feet wide. The basement was 1-1/2 feet wider than the model on the rear side, to allow access to the basement instrumentation. The lip of the basement on the two sides facing the areas of simulated contamination was increased in mass density by making the inner top section of these walls of lead brick to a thickness of 4 inches and a depth of 8 inches. A 1/2-inch thick rectangular plate, 3-1/2 x 7 feet, resting on all but the rear wall of the test pit provided the first 20 psf for the ground floor of the model building and at the same time transferred most of the weight load to the walls of the pit. Figure 3 illustrates the basement, support plate, and model structure arrangement.

Experiments were conducted on five versions of the model structure: one phantom building, and four buildings with different wall and floor thicknesses. The phantom building arrangement consisted of an open basement, with the model building and its support plate removed. The four building variations represented the following structure mass thicknesses:

1. 0 psf wall, 20 psf floor
2. 20 psf wall, 20 psf floor
3. 20 psf wall, 80 psf floor
4. 80 psf wall, 80 psf floor.

The zero wall structure with 1/2-inch thick floors (Figure 4) consisted of 6 floors on a 12-inch spacing supported by three corner tie rods with spacers. The 20 psf wall and floor structure was constructed by stacking the 6-unit floor assemblies vertically on the support plate in alignment with the basement. The 1/2-inch thick support plate for both of these versions served as the first floor, giving a first-floor surface height of 1/2-inch above ground level. The distance from the floor level to the ceiling was 11-1/2 inches.

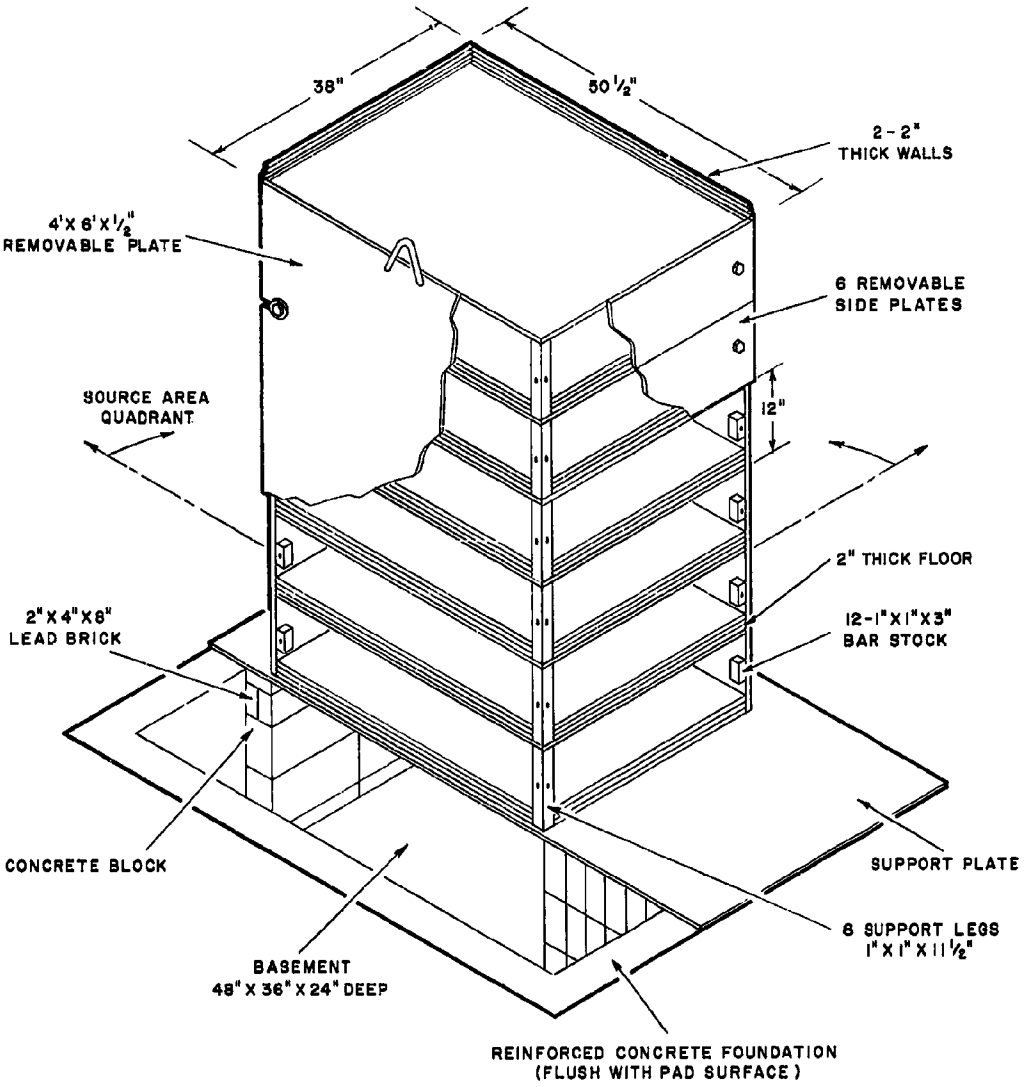

Figure 3. Typical Model Six-Story Structure Arrangement (80 psf Walls and Floors)

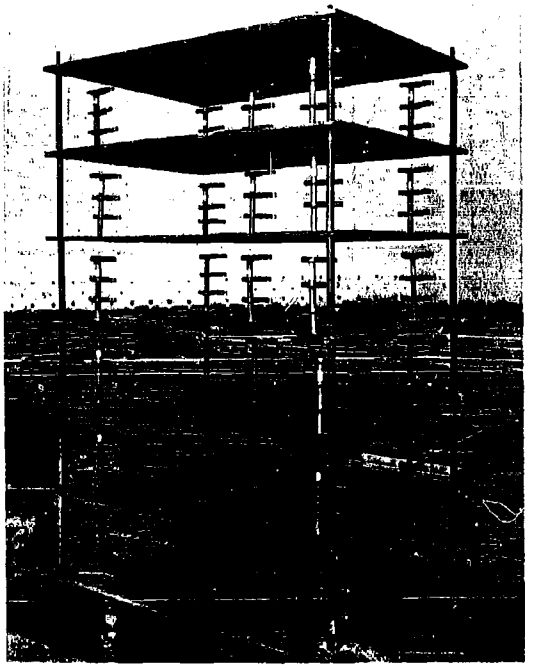

Figure 4. Model Structure: 0 psf Wall, 20 psf Floor

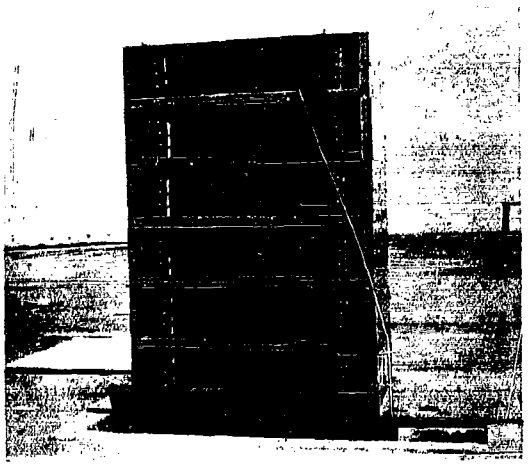

Figure 5. Model Structure: 20 psf Wall, 80 psf Floor

Floor mass thickness for cases 3 (Figure 5) and 4 was increased to 80 psf by adding three floor plates 1/2-inch thick to each story of the basic structure, thus making each floor 2 inches thick (80 psf). The first floor surface was thus 2 inches above ground level and the floor-to-ceiling distance was 10 inches. The 80 psf wall and floor case (Figure 3) was constructed by bolting on three thicknesses of 1/2-inch thick plate to the building sides facing the simulated contamination area.

EXPERIMENTAL AREAS

Preliminary investigations of the dimensions of roadways, parking areas, and other flat areas at ground level in a built-up area indicated that in a real situation contaminated areas in general would have dimensions of multiples of approximately 50 feet. Thus, since the modeling method requires that the areas of simulated contamination be scaled by the same factor as the structure, and since a scale factor of 12 was selected as the largest practical factor, the experimental areas are 4 feet wide. They are rectangular and parallel to the building walls. Since the structures exhibited quarter symmetry, areas of contamination were also simulated in one quadrant. Instrumentation was symmetrically placed so that, by proper addition of readings, does rates identical to what would have been obtained from a full annulus could be achieved.

SIMULATION OF CONTAMINATED AREAS

Figure 6 shows the simulated contaminated areas selected for experimentation. Twenty-nine of the area segments were rectangular and arranged so that a series of equivalent rectangular source annuli could be obtained through summation of dose rates from individual areas. Areas 25 and 26 completed a quadrant 47.7 feet in radius, while Area 27 provided a quarter annulus 2-1/2-feet wide to give data useful in the analytical estimate of the dose rate values that would be obtained if the source field were extended to greater diameters (far-field effects). Areas of contamination were simulated by judicious orientation of cobalt-60 sources over each area. Contamination in areas close to the model was simulated through placement of point sources at evenly spaced points, while simulation of contaminated areas located 4 feet or more from the model was created by pumping a source at constant speed through prepositioned tubing.

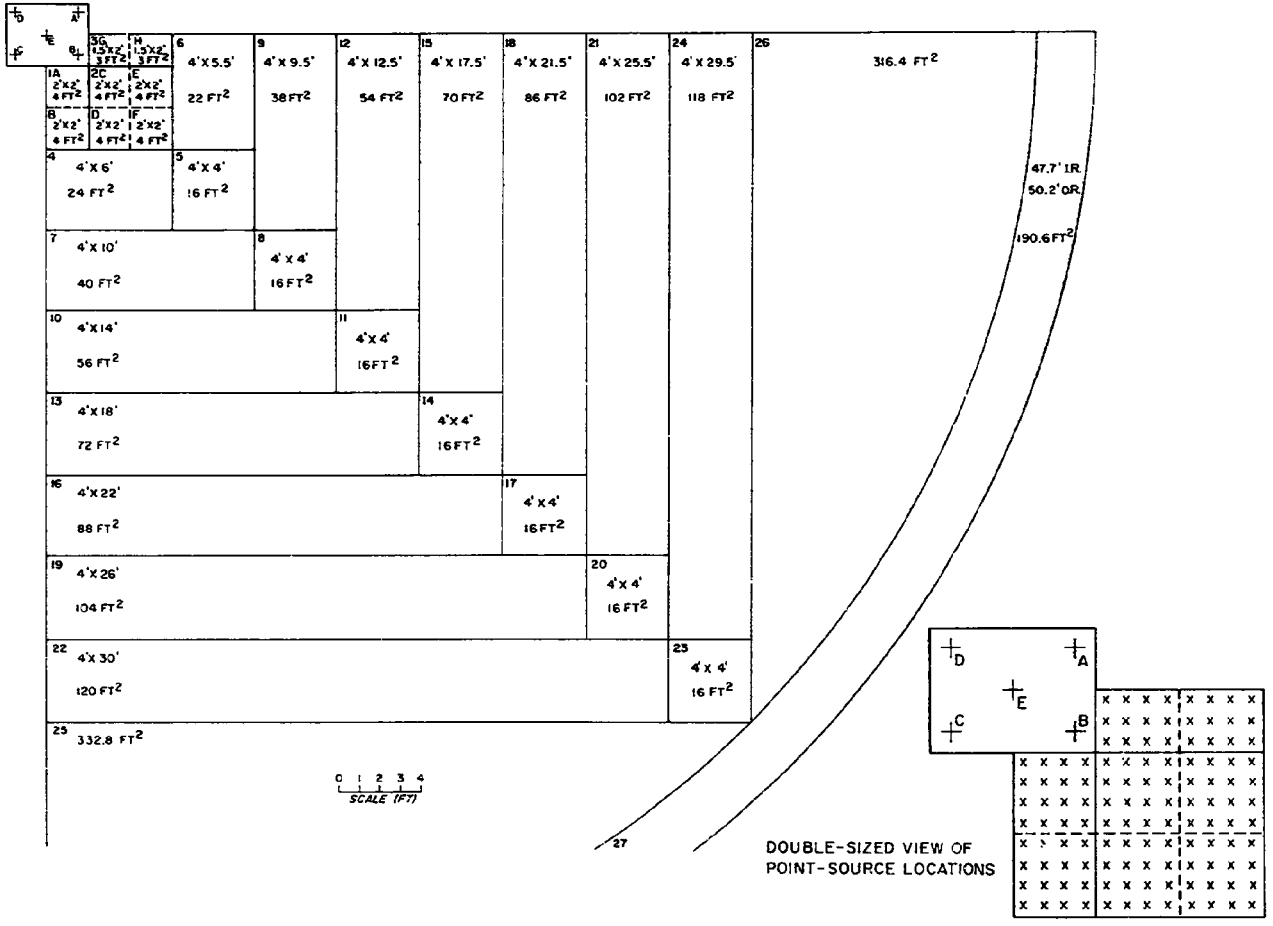

Figure 6. Areas of Simulated Fallout Contamination

PUMPED SOURCE

A uniform source density was simulated in Areas 4 through 27 by pumping a 24-curie cobalt-60 source through properly arranged polyethylene tubing. The tubing was spaced so that the source traveling at a uniform velocity through the tubing would spend an equal amount of time in each square foot of the area to be simulated. The detectors in the model integrate the effects of radiation from each increment of tubing as the source passes through it, thus presenting in effect an essentially uniform source area density. The tubing has an internal diameter of 0.267 inch, with a 1/8-inch wall thickness. It was not feasible to use this pumped-source method in the small 2 x 2 foot areas close to the model, since the minimum radius to which the tubing can be bent without interfering with source-capsule movement is 1 foot.

The tubing for Areas 4, 5, and 6 was more densely placed than on remaining areas because of its proximity to the model, where closer tube spacing is required for accurate simulation of a uniform source density. Tubing loops for these areas were arrayed so that the maximum distance between two parallel runs of tubing was 6 inches. The tubing for each area was in one continuous length, with all bend radii of 1 foot, and was mounted on 1/4-inch plywood panels for ease of removal. Four complete tubing circuits were required to obtain adequate exposure times without reducing pump output below the limits necessary to ensure positive uniform source motion. The removable 4 x 4 foot panel for Area 5 was also used for Areas 8 and 11 (4 x 4 feet).

The tubing for the remaining rectangular area panels was arranged in similar fashion. This tubing, however, is spaced at 1-foot intervals and consists basically of two offset loops, each containing three wraps of tubing. Tubing in Areas 25 and 26 was continuous, with 1-foot spacing, while Area 27 contained three loops of tubing running the full length of the quarter annulus, spaced at 10-inch intervals. The tubing leads from the source container to the source areas were roughly 3 feet long and were shielded with canvas bags of lead shot to a minimum thickness of 6 inches to prevent the presence of the source within the leads from contributing unwanted dosage values at the model building.

The equipment required for pumping an encapsulated source through area spreads of polyethylene tubing is similar to that previously developed and used by Technical Operations Research for model and full-scale building tests. This type of equipment was described in detail in previous reports[8-11] and will therefore not be covered in detail in this report.

A schematic of the hydraulic system for source circulation is shown in Figure 7. Water from the reservoir is drawn into the appropriate pump or pumps and then forced through the source container. This operation drives the source out of the container, through the polyethylene tubing, and back to the storage container at the conclusion of the exposure. A Hills-McCanna two-feed metering pump is used for an accurate flow control between 0.36 and 13.6 gph. For maximum versatility, one feed of the pump has a capacity of 3.6 gph and the other 10.0 gph. Output of these pumps can be rapidly changed through a micrometric adjustment of the pump stroke. Flow from the pumps passes into a 3-way solenoid valve wired for remote operation.

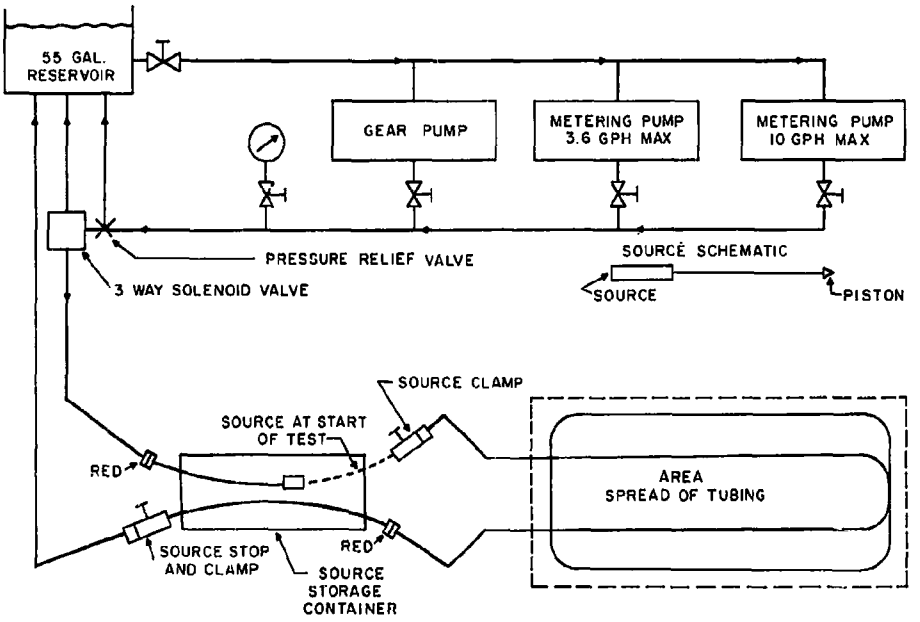

Figure 7. Diagram of Source Circulation System

This valve allows either bypassing the pump output directly to the reservoir or diverting the flow to the source storage container and hence into the area spread of tubing. The source container is a 1000 pound lead-filled steel shell mounted on wheels. Two stainless-steel tubes of the same internal dimensions as the polyethylene tubes pass lengthwise through the center of the container.

POINT SOURCES

Rod-mounted point sources were manually placed on Areas 1A, 1B, 2C, 2D, 2E, 2F, 3G, and 3H (Figure 6) to simulate contaminated areas. Both 0.215 curie and 0.520 curie cobalt-60 sources were used for the point-source work. The larger source reduced exposure times at more shielded locations (particularly the upper three floors of the model) to reasonable levels. Point-source locations were marked on 1/2-inch thick plywood. These positions were spaced at 6-inch intervals from each other, but only 3 inches from the area boundary; thus the 2 x 2 foot areas have a total of 16 point-source positions. The source was manually placed at each position for equal lengths of time. The source rod was 14 feet long, limiting dose rates to the handler to about 35 mr/hr. After placing the source, the handler immediately retired to a region having a much lower dose-rate level.

A 24 curie cobalt-60 source (the same source that was also pumped through polyethylene tubing) was used as a point source on Areas 14, 17, 20, and 23 (4 x 4 foot areas). These areas were small enough and sufficiently removed from the model building to warrant simulation of a uniform source density by placing the source at the center of these areas. For these point-source exposures, a cranked, cable-type, source-positioning retrieval unit was coupled to the source container. Point-source exposures were then made by cranking the source out through polyethylene tubing to a stop position at the center of a 4 x 4 foot area. At the end of an exposure, the source was cranked back into the source container.

INSTRUMENTATION

Measurements in the model building were made with Landsverk L-81 (2 r) dosimeters, Victoreen Model 239 (10 mr) stray radiation chambers, and Victoreen Model 362 pocket dosimeters (200 mr). The 2 r dosimeters were used at the

beginning of this experimental series, but because of the long exposure times necessary to produce reasonable readings for the more distant areas, and because they proved less accurate than the 200 mr dosimeters, they were not used in later experiments. Charger-reader instruments used in conjunction with all these dosimeters were compact portable units specifically designed and constructed by the Radiation Products Division of Technical Operations, Inc., for field experiment. This unit displays the total electrical charge required to return a dosimeter to the voltage to which it was charged before the exposure.

All basement measurements were made with 10 mr dosimeters. The bulk of the measurements above ground level were made with the 200 mr dosimeters; however, 10 mr dosimeters were used in extremely low dose-rate locations on the upper floors of the model. These instruments were always mounted horizontally and parallel to the source area, thus ensuring that a minimum dose-rate gradient existed over the dosimeter length. Dosimeters were placed to form five vertical building traverses, one at each corner plus a center traverse. The corner positions were located 6 inches perpendicularly from the walls. The detectors above ground level were spaced at 3, 6, and 9 inches above the floor in structures with 20 psf floors and 2-1/2, 5, and 7-1/2 inches above each floor for structures with 80 psf floors. Basement detectors were in general located 3, 9, and 15 inches below the first floor. However, additional detectors were also placed 1, 6, 12, and 18 inches below, and 1/4 inch above, ground level at the center position for a more complete traverse. The inch-below-ground-level measurement was obtained by taping a 10 mr dosimeter 2 inches in diameter to the basement ceiling. All dosimeter stands were constructed of phenolic tubing 3/4 inch in diameter by 1/32 inch thick to minimize their effect on the readings. Calibration checks with these stands showed that there was no measurable gamma-ray attenuation or backscattering by the stand material.

CALIBRATION

The radiation doses determined in this series of experiments were measured by the Tech/Ops charger-readers using primarily 10 mr and 200 mr full-scale ionization chambers. Since the output of these charger-readers is presented upon an arbitrary scale ranging from 0 to 100, they were calibrated by subjecting the chambers to a

cobalt-60 source previously calibrated at the National Bureau of Standards. Calibration of the chambers was performed on an essentially mass-less calibration range with source-to-detector distance equal to 1/4 of the source and detector-to-ground distance to minimize ground-scattering effects. With this arrangement, the expected total dosage is within 1% of free-air values.[12] Since instrument reading is a function of the density of the air within the cavity of the chamber, results were corrected to standard conditions of temperature and pressure for comparison with previous calibration data.

OPERATIONAL PROCEDURES

All personnel working at the model facility were equipped with both 200 mr direct-reading dosimeters and film badges. Both the air-supported structure and the combination control, office, and storage building were continuously monitored by Tech/Ops Model 492 "Gammalarms." In addition, during all radiation experiments, two portable survey meters were used for personnel monitoring.

Operation with a point source was simple and straightforward. Dosimeters were charged and placed in position in the model building. One person attached the point source to a 14-foot handling rod and placed the source at the required location while being monitored by a second person at a safe distance. The operators retired behind a concrete barrier for the duration of the exposure. After the exposure was completed, the source was replaced in its storage container, and the dosimeters read and replaced for the next run.

For safety, area-source simulation with the pumped source requires that a dummy run (using an identical source capsule but without radioactivity) be made first to ensure that the source tubing has not been damaged. For the active run, one person installed the source container in the tubing loop while a second person monitored from a distance. During this operation, all pumps were turned off and the bypass valve placed in the bypass position. Tubing leads were attached and the pressure tube from the pump was connected last. After making certain that other persons had cleared the area, or were behind the concrete barrier, the operator retracted the source clamps. The appropriate metering pump was turned on, and the solenoid valve switch was activated to connect the output of the pump to

the source container. Exit times of the source from both the source container and the shielded leads from the container to the area spread could be observed by the survey meter. In addition, the "Gammalarm" would change from a steady green light to a flashing red light. Exact exit of the source from the source area was determined either by actual observation with a 20-power spotting scope from behind the barrier or by a proximity device that rang an alarm as the source passed through the last length of tubing.

When the source had returned to the container, the solenoid valve was switched to the bypass position and the pump (or pumps) turned off. One person then monitored while a second individual with a survey meter approached the source container and closed the source clamp on the return tube, thus fastening the source in a position near the center of the container. The return connection from the area was then opened to relieve any water pressure that might be acting on the source piston or capsule. At this stage, dosimeters within the model were read and replaced if another run were to be made.

Part of the dosimeters might then be exposed for additional lengths of time by repeating the procedure described above if required to obtain measurable dose levels accurately. The source container is prepared (as previously described) for further runs and after use is secured by attaching source positioning plugs and locking.

CHAPTER 3

PHANTOM STRUCTURE

The method of source simulation in the outer experimental areas, pumping the source through a maze of closely-spaced tubing, is a compromise with the ideal situation of bare sources uniformly distributed upon a flat plane. Therefore, it is necessary to evaluate the attenuation effects of the inner rows of tubing when the source is in its outermost positions. Since this "tubing attenuation" increases near the ground level, and thus affects the ratio of upper-story to first-floor data, results must be obtained for all the experimental areas over the entire range of building heights. To obtain the data, the multistory model was removed from the test area and a vertical array of dosimeters was located at the center of the former model location (see Figure 8). These dosimeters were then exposed to each of the simulated contaminated areas, and dose rates as functions of height were determined. The data obtained from each area are presented in Table 1.

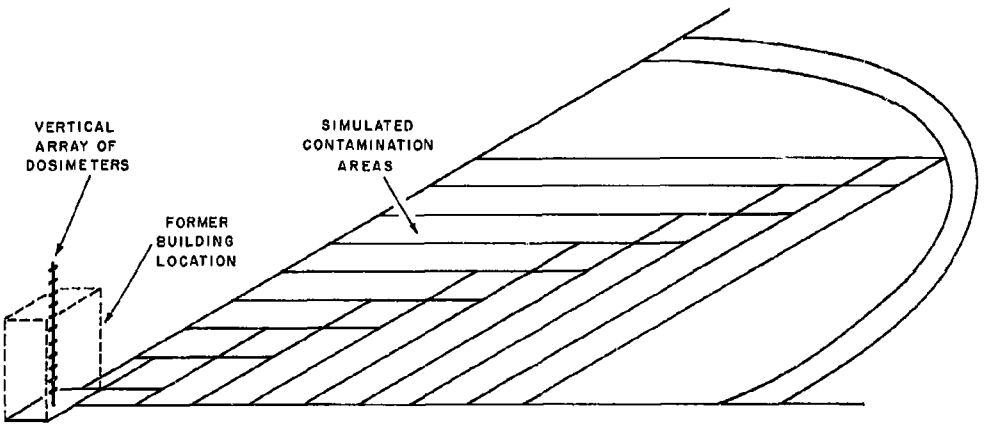

Figure 8. Phantom Building Experiment

TABLE 1

DOSE RATE VS HEIGHT FOR THE PHANTOM STRUCTURE
(Normalized to 1 curie/ft^2 cobalt-60)
(r/hr)

Area	Detector Height - Inches													
	3	6	9	12	18	24	30	36	42	48	54	60	66	72
1A	7.70*	7.62	7.36	6.86	5.84	4.83	4.18	3.30	2.79	2.29	1.82	1.54	1.39	1.17
1B	2.64	2.97	2.86	2.75	2.64	2.42	2.20	1.98	1.76	1.54	1.54	1.32	1.21	0.99
2C	3.39	3.39	3.39	3.29	3.23	2.97	2.54	2.33	1.98	1.73	1.55	1.34	1.23	1.06
2D	1.77	1.91	1.91	1.88	1.84	1.70	1.63	1.52	1.38	1.24	1.17	1.06	.99	.85
2E	1.58	1.69	1.71	1.66	1.64	1.56	1.50	1.35	1.27	1.19	1.06	1.00	.90	.79
2F	1.12	1.22	1.25	1.20	1.20	1.14	1.12	1.04	.98	.90	.85	.82	.77	.69
3G	4.05	4.16	4.05	3.84	3.41	2.88	2.45	2.13	1.78	1.49	1.28	1.07	.96	.82
3H	1.53	1.67	1.67	1.63	1.56	1.46	1.35	1.21	1.11	.97	.90	.83	.76	.66
4	3.46	3.93	4.12	4.12	4.21	4.21	4.21	4.02	3.88	3.70	3.56	3.56	3.28	3.00
5	1.28	1.47	1.56	1.56	1.60	1.62	1.68	1.62	1.60	1.58	1.55	1.56	1.53	1.41
6	3.19	3.68	3.79	3.84	3.95	3.90	3.95	3.79	3.68	3.52	3.41	3.25	3.25	2.92
7	2.25	2.71	2.91	2.87	2.95	2.95	3.10	2.98	2.95	2.95	2.87	2.95	2.83	2.71
8	.57	.67	.68	.68	.70	.72	.74	.74	.76	.74	.74	.76	.74	.70
9	2.14	2.46	2.62	2.62	2.74	2.74	2.86	2.82	2.78	2.74	2.74	2.74	2.74	2.60
10	1.78	2.02	2.16	2.13	2.16	2.27	2.23	2.27	2.23	2.23	2.23	2.30	2.23	2.13
11	.36	.38	.39	.36	.39	.39	.41	.40	.40	.40	.40	.42	.42	.38
12	1.75	2.01	2.08	2.12	2.19	2.19	2.26	2.23	2.23	2.23	2.23	2.23	2.23	2.12
13	1.19	1.45	1.58	1.58	1.64	1.66	1.72	1.74	1.74	1.74	1.77	1.82	1.79	1.74
14	.24	.25	.25	.25	.26	.26	.27	.27	.27	.27	.27	.28	.28	.26
15	1.24	1.45	1.55	1.55	1.60	1.60	1.68	1.68	1.68	1.65	1.68	1.73	1.73	1.65
16	.88	1.18	1.25	1.30	1.34	1.34	1.41	1.39	1.41	1.41	1.41	1.41	1.44	1.41
17	.17	.17	.18	.17	.18	.18	.18	.18	.18	.18	.18	.19	.19	.18
18	.94	1.24	1.30	1.33	1.37	1.37	1.46	1.44	1.46	1.46	1.48	1.53	1.53	1.46
19	.83	1.07	1.16	1.18	1.21	1.25	1.28	1.28	1.28	1.30	1.32	1.35	1.35	1.32
20	.11	.12	.12	.12	.12	.12	.13	.13	.13	.13	.13	.13	.13	.13
21	.84	1.07	1.17	1.17	1.23	1.24	1.28	1.28	1.28	1.28	1.28	1.30	1.32	1.28
22	.74	.96	1.04	1.06	1.08	1.08	1.13	1.13	1.13	1.15	1.16	1.20	1.20	1.15
23	.10	.09	.09	.09	.09	.09	.10	.10	.10	.10	.10	.10	.10	.09
24	.70	.88	.96	.97	1.00	1.03	1.06	1.06	1.06	1.08	1.09	1.12	1.12	1.08
25	1.68	1.69	1.83	2.08	1.92	1.96	2.08	2.08	2.12	2.12	2.20	2.20	2.20	2.20
26	1.06	1.48	1.62	1.69	1.78	1.79	1.90	1.90	1.90	1.94	1.94	1.97	2.01	1.97
27	.39	.59	.74	.87	.87	.94	.97	1.04	1.00	1.00	1.03	1.00	1.03	1.00

*Estimated

The effect of tubing attenuation in each of the experimental areas could be determined if all tubing were removed and each area source of contamination were replaced with a base array of closely spaced sources. This procedure, however, is impractical because of the large number of sources required for adequate simulation in each area and the excessive exposures that operators would be subjected to in placing and retrieving these sources. Therefore the results from point-source-to-detector readings obtained with varying detector heights and source-to-detector distances were integrated numerically over each area.

Rexroad[13] has performed experimentation of this type and has presented his data as experimentally obtained dose rates and buildup factors. However, there exists some doubt as to the exact strength of the source he used and, hence, the accuracy of his buildup-factor measurements in regions of small source-to-detector distances. Rexroad calibrated his cobalt source at an 11-foot height with source and detector approximately 6 feet apart. Allowance for air and ground scatter was then estimated by placing a small lead shield approximately 4 inches thick between the source and the detector and then reading the scattered dose. The difficulty in such a measurement is that the scatter introduced by the edges of the shield is usually greater than the air and ground scatter one is attempting to measure. Thus Rexroad obtains a scatter component of 5.1% of direct beam, while Clarke,[12] in measurements taken in similar geometry without the lead shield, reports less than 1% air and ground scatter. Since source calibration is dependent on direct beam results, Rexroad's source may thus be as much as 4.1% stronger than he states. Because of these uncertainties, it was decided that a fundamental measurement of the buildup factor in the range from 1 to 50 foot distances was required.

To obtain this measurement, the following procedure was used. A source and detector were mounted on a thin aluminum beam (see Figure 9) so that accurate source-to-detector distance could be maintained. The output of the detector was fed through an amplifier and read on a digital voltmeter to four-place accuracy. Free-field calibration was then obtained by elevating the source and detector to a distance 12 feet above, and parallel to, the ground while varying the source-to-

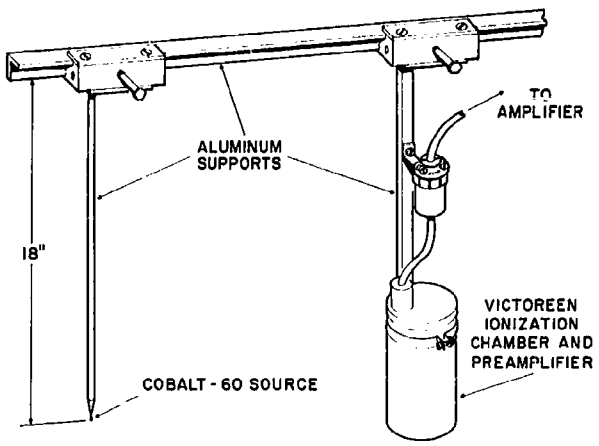

Figure 9. Source and Detector Arrangement

detector distance. The effects of air and ground scattering for the various source-to-detector distances were estimated using the results of Clarke.[12] The total dose was then measured with the source placed 3/8 inch above the ground (a macadam pad, approximately 2 inches thick on gravel), while the detector was varied about the source through an arc extending from vertical to a point 82.5° from vertical. This procedure was used out to source-to-detector distances of 14 feet. To extend source-to-detector distance beyond 14 feet, the detector was mounted on a thin, vertical aluminum stand at heights of 1, 3, and 6 feet above the ground. Data were taken in this fashion out to a maximum horizontal source-to-detector distance of 50 feet.

The data obtained from this experiment were then analyzed by computing the direct beam radiation at each position and dividing the experimentally measured radiation by this direct beam to obtain the buildup factor. These resultant buildup factors are presented in Table 2 as a function of detector height above the ground versus horizontal source-to-detector distance.

TABLE 2

COBALT-60 BUILDUP FACTORS

(Source 3/8 inch above the ground)

Horizontal Source-to-Detector Distance (ft)	Vertical Detector Height Above Ground (ft)		
	1	3	6
0	1.049	1.079	1.109
1	1.068	1.081	1.110
2	1.100	1.085	1.111
3	1.130	1.110	1.115
4	1.145	1.125	1.122
5	1.148	1.142	1.136
6	1.152	1.150	1.144
7	1.155	1.155	1.148
8	1.157	1.160	1.150
9	1.156	1.165	1.154
10	1.155	1.168	1.160
11	1.154	1.170	1.168
14	1.148	1.171	1.178
16	1.138	1.172	1.183
18	1.135	1.173	1.192
20	1.135	1.174	1.196
25	1.135	1.175	1.200
30	1.135	1.176	1.200
35	1.135	1.175	1.200
40	1.135	1.174	1.200
45	1.135	1.172	1.200
50	1.135	1.170	1.200

It may be noted from Table 2 and Ref. 13 that the relative agreement between these data and those obtained by Rexroad[13] improves as source-to-detector distance increases. This would be as expected if a minor error in source calibration were introduced, and further confirms the inadequacy of obtaining scatter-direct ratios by substituting a shield between source and detector.

The data obtained from the scatter experiment may now be compared with those obtained in the phantom structure experiment if they are numerically integrated over the phantom structure areas of interest. The results of this integration for full annuli are illustrated in Figure 10 for several of the experimental areas of interest. From these data it may be seen that there are two points of disagreement. First, a discrepancy of approximately 25% exists for positions above about 1 foot in height. These positions in general are not affected by the tubing attenuation and, thus, the discrepancy must be attributed either to an error in source calibration or to self-absorption by the source. Figure 11 illustrates the relative output of the source as a function of angular displacement. This figure, and the observation that during the simulation of contaminated areas the source travels in essentially random azimuthal paths, shows that the major portion of this discrepancy may be related to the differing amounts of self-absorption existing between the "radiation center" of the tube source and the detector.

The second discrepancy between the phantom structure and integrated ground-scatter data occurs at altitudes below about 1 foot and is attributable directly to the attenuation provided by the inner lengths of the source tubing when the source is in the extreme radial position in each source area. This effect varies with the annular area simulated and is a maximum when the source is in the outermost areas. In this position, the maximum amount of tubing is placed in direct line of sight between the source and detector.

It is thus necessary to apply a correction factor to the model results previously published[4-7] in preliminary form to account for the anisotropy of the source and the line-of-sight attenuation provided by the inner lengths of tubing when the source is in its outer-most position. This factor is presented in Table 3 as a function of both height and annular radius. Note that since areas of contamination Numbers 1,

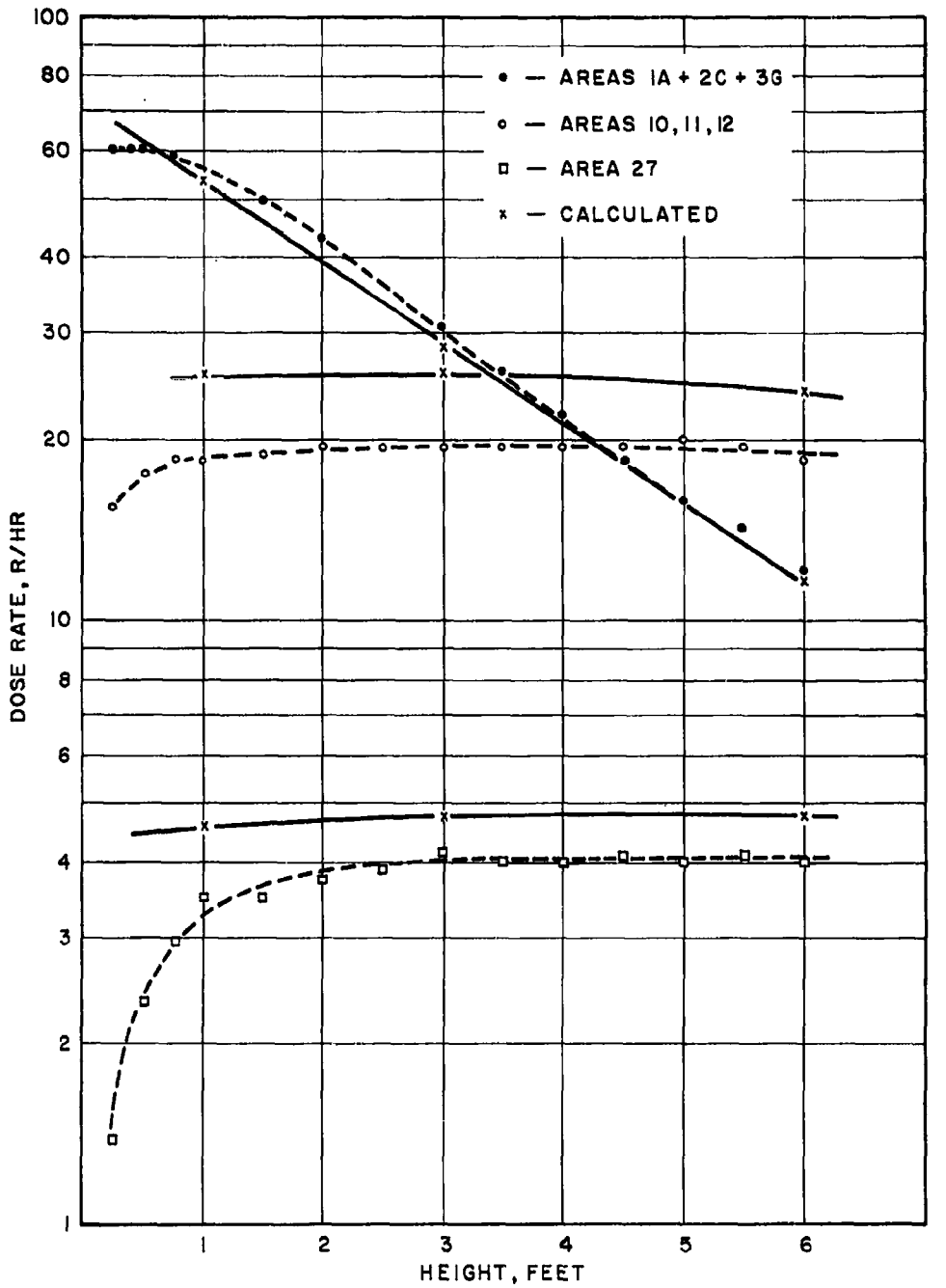

Figure 10. Vertical Dose-Rate Distributions in Phantom Building

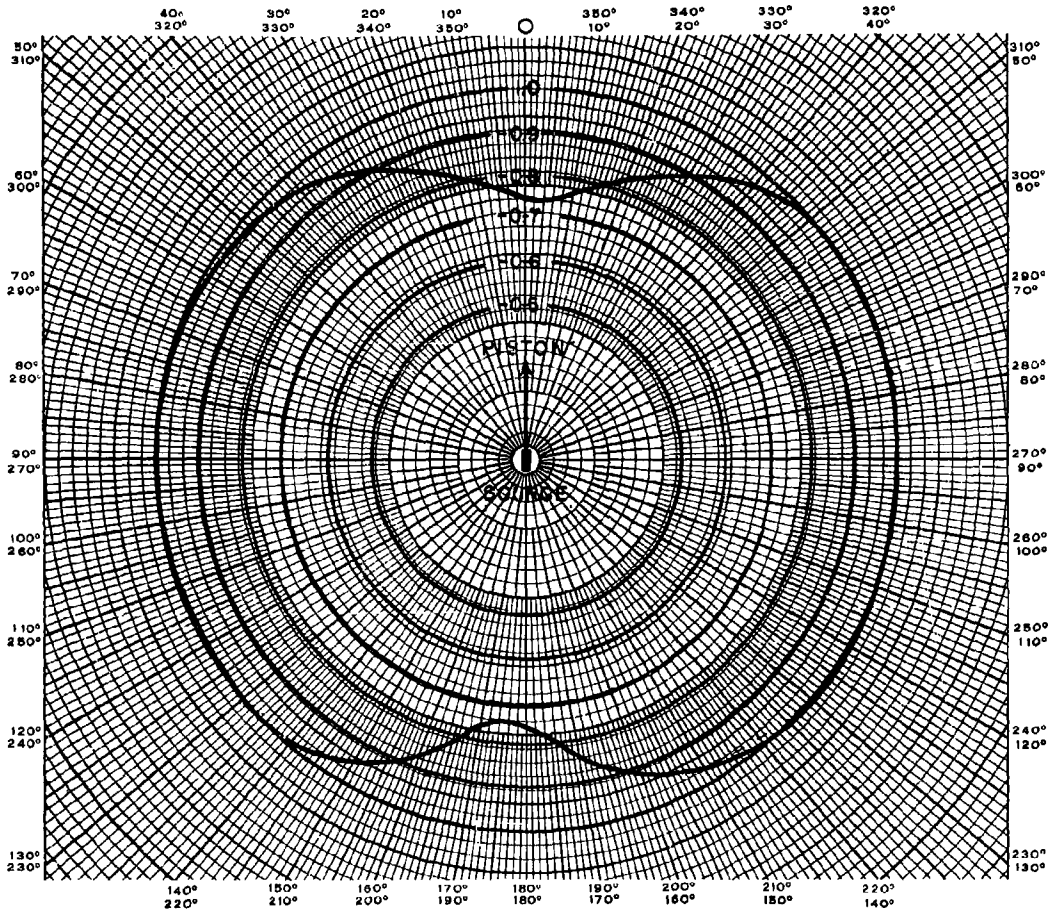

Figure 11. Variation of Relative Source Strength with Azimuth

2, and 3 were simulated using a small isotropic point source rather than the tube source, the correction factor for these areas is nearly equal to 1.

In properly scaling structures so that model tests may be performed, it is impracticable to scale the atmosphere. Results obtained from model tests must, therefore, be treated analytically to correct for this density difference artifically. The tests performed upon the phantom structure together with the experimental results previously published[13] provide an ideal method of checking the mathematical

TABLE 3

MULTIPLICATIVE FACTOR TO CORRECT MODEL DATA FOR ANISOTROPY OF SOURCE AND TUBING ATTENUATION

Floor	Detector Height (inches)	EXPERIMENTAL AREAS (See Figure 6)										
		1,2,3		4,5,6	7,8,9	10,11,12	13,14,15	16,17,18	19,20,21	22,23,24	25,26	27
		A,C,G,	B,D,E,F,H									
1	3	1.0	1.3	1.7	1.7	1.7	1.8	1.9	1.9	1.9	2.0	3.0
	6	1.0	1.2	1.6	1.5	1.5	1.6	1.6	1.6	1.6	1.7	2.0
	9	1.0	1.2	1.5	1.4	1.4	1.5	1.5	1.5	1.5	1.6	1.6
2	3	1.0	1.1	1.3	1.3	1.4	1.4	1.4	1.4	1.4	1.5	1.3
	6	1.0	1.1	1.3	1.3	1.3	1.4	1.4	1.4	1.4	1.5	1.3
	9	1.0	1.1	1.3	1.3	1.3	1.4	1.4	1.4	1.4	1.5	1.3
3	3	1.0	1.1	1.3	1.3	1.3	1.3	1.3	1.3	1.3	1.4	1.2
	6	1.0	1.1	1.3	1.3	1.3	1.3	1.3	1.3	1.3	1.4	1.2
	9	1.0	1.1	1.3	1.3	1.3	1.3	1.3	1.3	1.3	1.4	1.2
4	3	1.0	1.1	1.3	1.3	1.3	1.3	1.3	1.3	1.3	1.4	1.2
	6	1.0	1.1	1.3	1.3	1.3	1.3	1.3	1.3	1.3	1.4	1.2
	9	1.0	1.1	1.3	1.3	1.3	1.3	1.3	1.3	1.3	1.4	1.2
5	3	1.0	1.1	1.3	1.3	1.3	1.3	1.3	1.3	1.3	1.4	1.2
	6	1.0	1.1	1.3	1.3	1.3	1.3	1.3	1.3	1.3	1.4	1.2
	9	1.0	1.1	1.3	1.3	1.3	1.3	1.3	1.3	1.3	1.4	1.2
6	3	1.0	1.1	1.3	1.3	1.3	1.3	1.3	1.3	1.3	1.4	1.2
	6	1.0	1.1	1.3	1.3	1.3	1.3	1.3	1.3	1.3	1.4	1.2
	9	1.0	1.1	1.3	1.3	1.3	1.3	1.3	1.3	1.3	1.4	1.2

manipulations required to correct for improper atmospheric density. Thus, if a scaling factor of 12 is accepted, the phantom building 3-inch position should be directly comparable with the 3-foot data in Reference 13.

The method of analytical correction of model to full-scale data used in this series of reports is as follows. The attenuation of radiation reaching a structure is a function of the geometry and mass thickness of the structure and the attenuation and scattering properties of the atmosphere. Since the model accurately represents the full-scale structure in geometry and mass thickness, the difference between model and full-scale results is a function only of the ratio of the scattering and attenuation properties of the real and "model" atmosphere.

The scattering and attenuation properties of the atmosphere for cobalt radiation have been experimentally measured by many investigators.[13-15] Their data

for dose rate from a point source in general, may be represented by an analytical expression of the form:

$$I = I_o \frac{e^{-\mu r}}{r^2}(1 + a_1\mu r + a_2(\mu r)^2 + \ldots) \qquad (1)$$

where:

I_o = dose rate at a unit distance from a source

r = distance from the source

μ = total cross section

$(1 + a_1\mu r + a_2(\mu r)^2 + \ldots)$ = dose buildup factor

$a_1, a_2, a_3 \ldots$ = experimentally measured constants.

Various investigators have evaluated the constant a_1 as varying from about 0.55 several feet above the ground-air interface to about 1.0 at altitudes of 50 feet or more for values of $\mu r \geq 0.1$. A more exact analytical fit of the data may be obtained by adding terms of the form $a_n(\mu r)^n$. However, since in general these buildup factors have been measured over paths essentially parallel to the ground and, in radiation penetrating a structure, the radiation predominantly traverses angular paths, the increase in accuracy obtained in computing the ratio of model to full-scale results using additional terms is unwarranted in view of the lack of accuracy of angular buildup data and the increased complexity of computation required.

This representation of the dose-buildup factor is admittedly crude; however, it is probably adequate when used as a ratio to compare model with full-scale experiments. The major problems which have arisen from use of this approximation are attributable to its poor representation of the scattered portions of the dose at

small distances ($\mu r \leq 0.1$). However, as shown below, the actual ratio that must be computed to compare data obtained from a model with those obtained from a full-scale structure is that of total dose from a full-scale annular contaminated field to that from the corresponding model field. Thus, for close-in field locations, while the dose due to scattered radiation may be seriously in error, it is but a few per cent of the total dose for both model and full-scale conditions. Hence, the ratio may be accepted as valid.

The total dose arriving at a position located in a structure at the center of a contaminated annular area with radii r_i, r_o (see Figure 12) may be written as:

$$D(h, r_i \rightarrow r_o) = I_o G(X_e, h, a, b \ldots) \int_{r=r_i}^{r=r_o} \frac{2\pi\sigma B(\mu\sqrt{r^2 + h^2}) e^{-\mu\sqrt{(r^2 + h^2)}}\, rdr}{(r^2 + h^2)} \qquad (2)$$

where

$D(h, r_i \rightarrow r_o)$ = dose rate at detector position of interest

h = detector height

r_i = inner radius of contaminated annulus

r_o = outer radius of contaminated annulus

I_o = dose rate at a unit distance from a 1-curie source

$G(X_e, h, a, b \ldots)$ = geometric and barrier shielding introduced by the structure at height h

X_e, a, b, = barrier thickness and geometric factors describing the structure

σ = source density in curies per unit area

$B(\mu\sqrt{r^2 + h^2})$ = air buildup factor $\cong 1 + 0.55\mu\sqrt{r^2 + h^2}$

μ = total linear coefficient for air

which upon integration reduces to:

$$D(h, r_i \rightarrow r_o) = 2\pi\sigma \, I_5 G(X_e, h, a, b \ldots) \left[E_1(\mu\rho_i) + 0.55e^{-\mu\rho_i} - E_1(\mu\rho_o) - 0.55e^{-\mu\rho_o} \right] \quad (3)$$

where

$\rho_i = \sqrt{r^2 + h^2}$

$\rho_o = \sqrt{r_o^2 + h^2}$

E_1 = the familiar exponential integral.

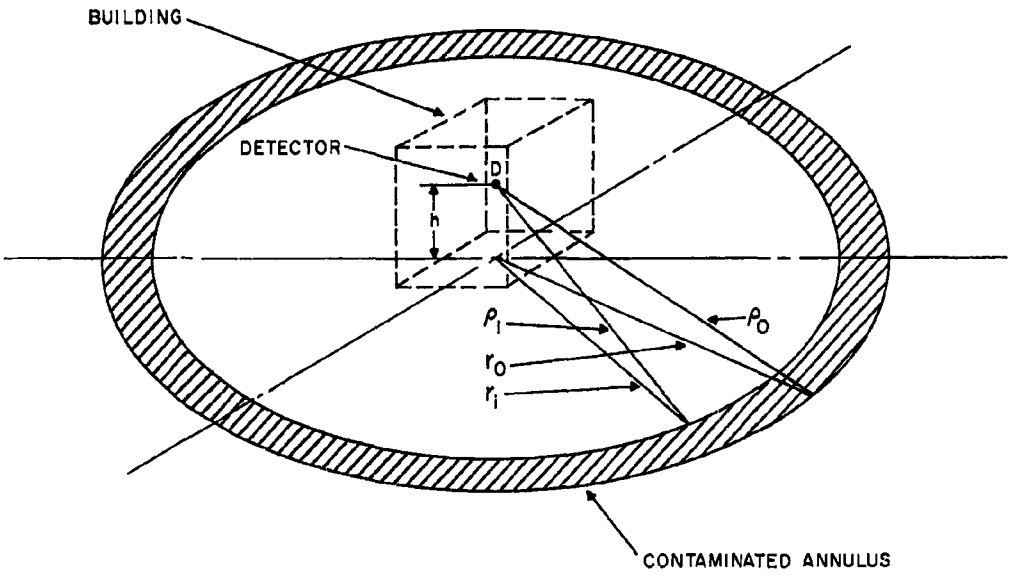

Figure 12. Schematic Diagram of Building Contaminated by an Annular Contaminated Field

The dose rates for the model and full-scale structure are both represented by the equation given above. Thus, if we take as the dimensions of interest the actual dimensions of the model, the corresponding equation for the full-scale structure would simply have each linear dimension multiplied by the scale factor "S." If the model structure is assumed to represent a 1/12-scale model (S = 12) of an actual structure, the ratio of the dose that would be obtained from a full-scale test to that of the model test may be written as:

$$R = \frac{D_{FS}(h, r_i \rightarrow r_o)}{D_M(h, r_i \rightarrow r_o)} = \frac{E_1(12\mu\rho_i) - E_1(12\mu\rho_o) + 0.55\left[e^{-12\mu\rho_i} - e^{-12\mu\rho_o}\right]}{E_1(\mu\rho_i) - E_1(\mu\rho_o) + 0.55\left[e^{-\mu\rho_i} - e^{-\mu\rho_o}\right]} \quad (4)$$

where

$D_{FS}(h, r_i \rightarrow r_o)$ = dose that would be measured in a full-scale building

$D_M(h, r_i \rightarrow r_o)$ = dose as measured in the model structure

ρ_i, ρ_o = actual model source area dimensions.

The data from model experiments may then be multiplied by this ratio to get values that would have been obtained from a full-scale experiment. Performing this manipulation for the phantom structure and applying the required correction for tubing attenuation and source anisotropy (see Table 4), we obtain data from the 3-inch model height (equivalent to 3 feet full scale) for a source annulus extending from 1.95 to 50.2-foot radius (equivalent to 23.4 to 602-foot radius full scale) that indicates a full scale dose rate of 257 r/hr.

The resultant value of 257 r/hr compares quite favorably with that previously obtained by Rexroad[13] of 260 r/hr for the same field size. Thus, the accuracy of the scaling correction for improper atmospheric density is adequate.

TABLE 4

FULL-SCALE PHANTOM STRUCTURE DOSE RATES

Source Area (See Figure 6)	Model Radii (ft)		Ratio of Full-Scale to Model Data	Correction Factor (Table 3)	Dose Rate	
	r_i	r_o			Phantom	Corrected to Full Scale
1A, 2C, 3G	1.95	4.08	0.98	1.0	15.14	14.8
1B, 2D, 2E, 2F, 3H	4.08	6.46	0.96	1.3	8.56	10.7
4,5,6	6.46	11.0	0.91	1.7	7.93	11.9
7,8,9	11.0	15.5	0.85	1.7	4.96	7.2
10,11,12	15.5	20.0	0.80	1.7	3.89	5.3
13,14,15	20.0	24.6	0.75	1.8	2.67	3.6
16,17,18	24.6	29.0	0.69	1.9	1.99	2.6
19,20,21	29.0	33.6	0.63	1.9	1.78	2.1
22,23,24	33.6	38.0	0.57	1.9	1.54	1.7
25,26	38.0	47.7	0.60	2.0	2.74	3.8
27	47.7	50.2	0.48	3.0	0.39	.6
					Total	64.3
						x 4*
					Full-scale dose	257 r/hr

*The factor of 4 is introduced by the quarter symmetry used in this experiment.

CHAPTER 4

ANALYSIS OF ABOVE-GROUND DATA

INTRODUCTION

The upper floors of multistory urban structures have been found to be useful in providing potential shelter from fallout radiation in the event of a nuclear attack. Most urban structures, however, are partially shielded by surrounding structures from the essentially infinite field of fallout contamination created by a nuclear detonation. Experimental measurements have been made to: (1) verify the computational procedures presently used to estimate the effects of limited fields of contamination on the dose rate within multistory structures and (2) to provide a basis for refining these procedures. Comparisons are made between the experimentally determined dose rates and those determined from computational procedures used in the National Shelter Survey Computer Program (NSSCP),[3] the "Guide for Architects and Engineers" (GAE),[1] and the engineering manual "Design and Review of Structures for Protection from Fallout Gamma Radiation."[2]

CONVERSION OF MODEL DATA TO FULL-SCALE DATA

Shielding results obtained from experimentation on model structures may be considered to be exact replicas of full-scale experiments if three basic laws of scaling are obeyed:

1. All dimensions must be scaled geometrically by the same factor.
2. Each absorbing surface must attenuate radiation to the same degree as the original surface independent of scaling factor.
3. The specific scattering and absorption factors must remain unchanged.

The principal difficulties lie in the interpretation of experimental evidence obtained on model structures arising from the third scaling rule. First, to increase the density of the building materials, the model is constructed of iron while

the attenuation curves presented in the "Guide for Architects and Engineers" have been computed for material with the scattering and absorption properties of water. Since an accurate reproduction of the relative scattering and absorption properties at all applicable radiation energies is required, some ambiguity exists in selecting the criteria for computing model wall thicknesses. Three points of comparison to full-scale walls can be made:

1. Mass thickness may be matched.
2. Broad-beam absorption data for flat slabs can be applied.
3. Electron density may be maintained.

To illustrate, we observe that a wall of iron 20 psf thick is equivalent to:

1. A wall of water 20 psf thick if criterion No. 1 is accepted.
2. A wall of water 29 psf thick if criterion No. 2 is accepted.
3. A wall of water 16.8 psf thick if criterion No. 3 is accepted.

A wall of iron 80 psf thick is equivalent to:

1. A wall of water 80 psf thick if criterion No. 1 is accepted.
2. A wall of water 86 psf thick if criterion No. 2 is accepted.
3. A wall of water 67.2 psf thick if criterion No. 3 is accepted.

When iron is used as a substitute for more common materials, it effectively removes much of the lower-energy gamma rays. Thus, it is critical to use detectors that are within a few per cent of linearity in dose down to an energy level of 70-100 kev.

A second ramification of the third scaling rule becomes apparent during consideration of modeling of the atmosphere and ground. It is difficult, if not impossible, to increase the density of the atmosphere and ground to the extent required for perfect scaling. Results obtained from model experiments must therefore be treated analytically to correct for the difference between the scattering and attenuation properties of the real and the model atmosphere.

Experiments performed on the model are for simulated finite fields of radiation that extend to a radius of 50.2 feet from the center of the model structure. Thus, extension of the model results to an infinite field of contamination must also be

handled analytically. In addition, allowance must be made for the attenuation of gamma rays by the polyethylene tubing used in the model experiments and for any effective anisotropy of the cobalt-60 source.

The atmospheric density-correction factors to be used in converting 1/12-scale model dose rates to full-scale values are determined from the following equation as developed in Chapter 3, Eq. (4) of this report (see p. 29):

$$R = \frac{D_{FS}(h, r_i \rightarrow r_o)}{D_M(h, r_i \rightarrow r_o)} = \frac{E_1(12\mu\rho_i) - E_1(12\mu\rho_o) + 0.55\left[e^{-12\mu\rho_i} - e^{-12\mu\rho_o}\right]}{E_1(\mu\rho_i) - E_1(\mu\rho_o) + 0.55\left[e^{-\mu\rho_i} - e^{-\mu\rho_o}\right]} \qquad (1)$$

where

$D_{FS}(h, r_i \rightarrow r_o)$ = dose that would be measured in a full-scale building

$D_M(h, r_i \rightarrow r_o)$ = dose as measured in the model structure

ρ_i, ρ_o = actual model source area dimensions.

These ratios of full-scale to model results for the 1/12-scale models (S=12) are given in Table 5 for the range of detector heights used. The data obtained from model experiments may then be multiplied by the appropriate ratio from Table 5 to obtain values that would have been obtained from a full-scale experiment.

TABLE 5

RATIO OF FULL-SCALE TO MODEL RESULTS

Source Area (See Figure 6)	Model Radii (feet)		Detector Height in Model (feet)					
	r_i	r_o	1/2	1-1/2	2-1/2	3-1/2	4-1/2	5-1/2
1A, 2C, 3G	1.95	4.22	0.98	0.98	0.97	0.97	0.97	0.96
1B, 2D, 2E, 2F, 3H	4.22	6.46	.96	.96	.96	.95	.94	.93
4,5,6	6.46	11.0	.91	.90	.90	.90	.89	.87
7,8,9	11.0	15.5	.85	.85	.85	.85	.84	.84
10,11,12	15.5	20.0	.80	.80	.80	.79	.79	.78
13,14,15	20.0	24.6	.75	.75	.75	.74	.74	.74
16,17,18	24.6	29.0	.69	.69	.69	.68	.68	.68
19,20,21	29.0	33.6	.63	.63	.63	.63	.63	.63
22,23,24	33.6	38.0	.57	.57	.57	.57	.57	.56
25,26	38.0	47.7	.69	.65	.63	.62	.61	.61
27	47.7	50.2	.48	.48	.48	.48	.48	.48

ESTIMATE OF FAR-FIELD RADIATION

The additional amount of radiation that would have been obtained if the contaminated field had been simulated out to an infinite radius is determined as follows. Returning to Eq. (3) of Chapter 3 (see p. 28) for the dose rate from an annular area, we may write the approximate far-field fraction, in terms of the model, as the ratio of the dose from radiation originating beyond the outer radius used in the experiment to the dose originating from a certain annular source area. This annular area is located at a distance from the structure where the angular distribution of radiation striking the structure from the annulus is essentially the same as that which would arise from sources located at large distances from the structure:

$$\frac{D_M(r_o \rightarrow \infty)}{D_M(r_i \rightarrow r_o)} = \frac{E_1(\mu\rho_o) + 0.55e^{-\mu\rho_o}}{E_1(\mu\rho_i) - E_1(\mu\rho_o) + 0.55\left(e^{-\mu\rho_i} - e^{-\mu\rho_o}\right)} \tag{2}$$

where

ρ_o = slant distance from detector to maximum outer radius of the outer field simulated

ρ_i = slant distance to the inner radius of the outer field simulated.

In a similar fashion, the actual far-field dose to be expected from a full-scale structure may be estimated if the dose rate from an outlying contaminated annulus is known. In the present study, however, since only a model experiment has been performed, we must estimate this contribution from the outer annulus of the model experiment. As shown in Eq. (1) and Table 5, the ratio of full-scale dose to model dose for the outer annulus is about 0.48 (Area 27). Thus, the far-field dose rate in the full-size structure written in terms of the experimentally obtained dose from the outer model annulus and the model dimensions is:

$$\begin{aligned} D_{FS}(r_o \rightarrow \infty) &= D_M(r_i \rightarrow r_o)\left[\frac{D_{FS}(r_o \rightarrow \infty)}{D_M(r_i \rightarrow r_o)}\right] \\ &= D_M(r_i \rightarrow r_o)\left[\frac{E_1(12\mu\rho_o) + 0.55e^{-12\mu\rho_o}}{E_1(\mu\rho_i) - E_1(\mu\rho_o) + 0.55(e^{-\mu\rho_i} - e^{-\mu\rho_o})}\right] \end{aligned} \tag{3}$$

where

$D_M(r_i \rightarrow r_o)$ = dose obtained experimentally from the outer annulus surrounding the model

$D_{FS}(r_o \rightarrow \infty)$ = dose that would be obtained from contamination existing beyond the outer radius of a full-scale structure

ρ_i = model slant distance from the detector location to the inner radius of the outer contaminated annulus

ρ_o = model slant distance from the detector location to the outer radius of the outer contaminated annulus

if the scale factor "S" is assumed to be equal to 12. The resultant ratio of full-scale far-field dose to outer-annulus model dose and the actual far-field dose expected is shown in Table 6.

TABLE 6

FAR-FIELD CORRECTIONS

Dosimeter Height in Model (ft)	Ratio of Full-Scale Far-Field Dose to Dose from Outer-Annulus of Model
1/2	5.5
1-1/2	5.5
2-1/2	5.6
3-1/2	5.6
4-1/2	5.7
5-1/2	5.8

PRESENTATION OF EXPERIMENTAL DATA

In addition to the correction ratios given in Tables 5 and 6 for the conversion of model data to full-scale dose rates and for the far-field contributions, allowance must be made for the effects of anisotropy of the cobalt-60 source radiation field

and for gamma-ray attenuation by the water-filled polyethylene tubing. Table 3 (p. 25) presents the correction values that must be applied to the experimental data on the 6-story model structures to allow for these effects. These values were determined from measurements on a phantom version of the model steel structures and were covered in detail in Chapter 3. None of the data previously reported on the four multistory steel models[4-7] includes these correction values. These data must, therefore, be multiplied by the appropriate correction factor from Table 3 to allow for reduction of the radiation field due to source anisotropy and tubing attenuation.

The data obtained from the central and corner positions presented in Volumes I through IV have been corrected for source anisotropy and tubing attenuation, converted to full-scale results, and normalized to the uniform source density (2.01 millicuries/ft^2) that would produce a dose rate of 1.0 r/hr 3 feet above an infinite smooth plane. These normalized data are plotted in cumulative form in Figures 13 through 20 as functions of the width of the contaminated fields divided by the dosimeter heights for both center and corner positions. These figures replace similar uncorrected preliminary cumulative data plots previously reported in Volumes I through IV.[4-7] The presentation of these data on separate graphs for each floor-height position, rather than on a common graph, is dictated by the difference in the effect of the floor shadow on the source field.

The data (in general) for each structure follow a common curve for all floors at small values of W_c/h ($W_c/h \leq 10$) with the exception of those taken on the first floor when the floor thickness was 80 psf. The dose rate measured on the first floor of the thick-floor structures was always found to be significantly higher than that measured at similar locations on the upper floors. This is attributed to the shadowing effect of the thick floor below the detector. Thus, direct radiation from close-in contaminated areas is attenuated by the floor in upper-floor positions, whereas the first-floor detectors are not similarly affected.

Further evidence of floor-shadow effects is illustrated in Figures 13, 15, and 17 for dosimeters 3 feet above floor level at the center of the building where a noticeable dip in the dose-rate curves occurs for W_c/h values between 3 and 7.5. This perturbation is most pronounced for the 0 psf wall building, is still noticeable for the 20 psf wall building, but does not appear for the 80 psf case. This is presumably due to the diffuseness of the radiation emerging from thick walls. The effect

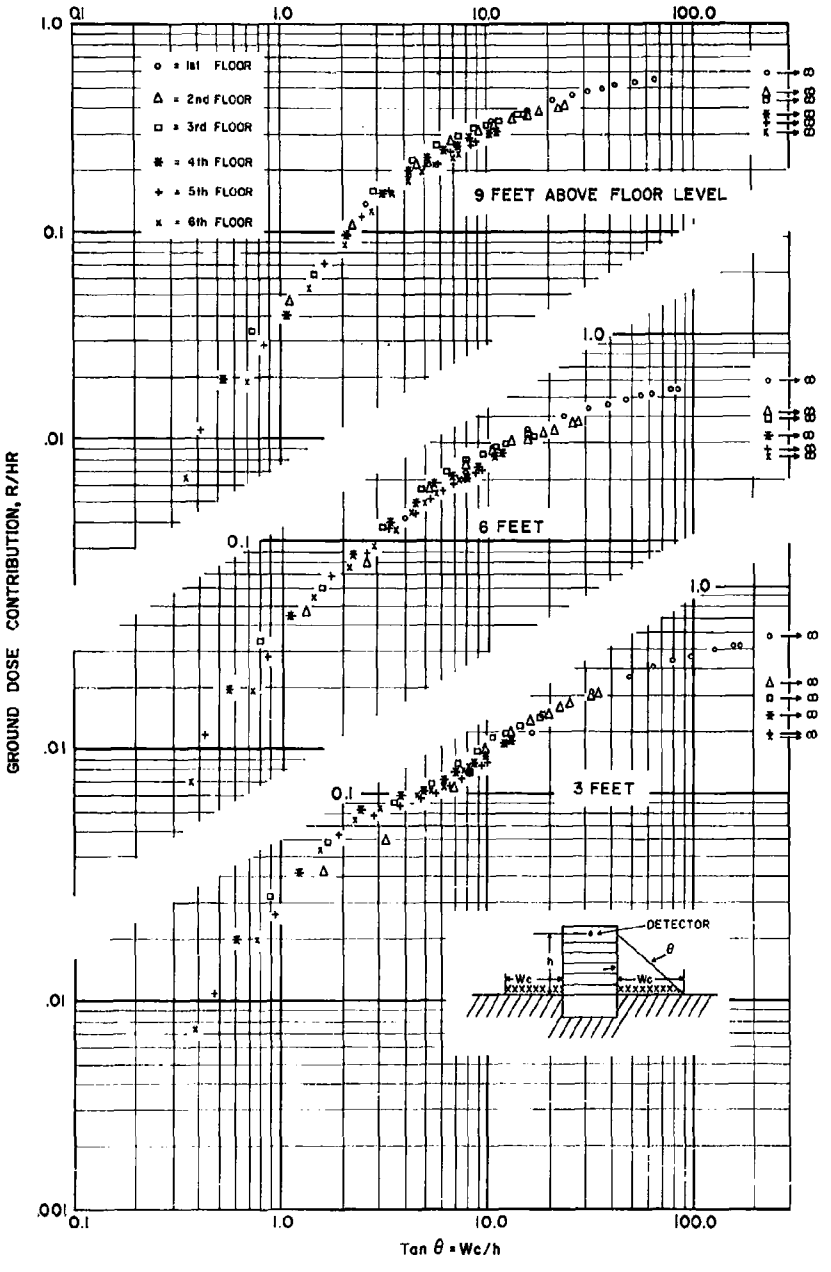

Figure 13. Full-Scale Dose Rate vs. W_c/h for Center Position of Building with 0 psf Walls and 20 psf Floors

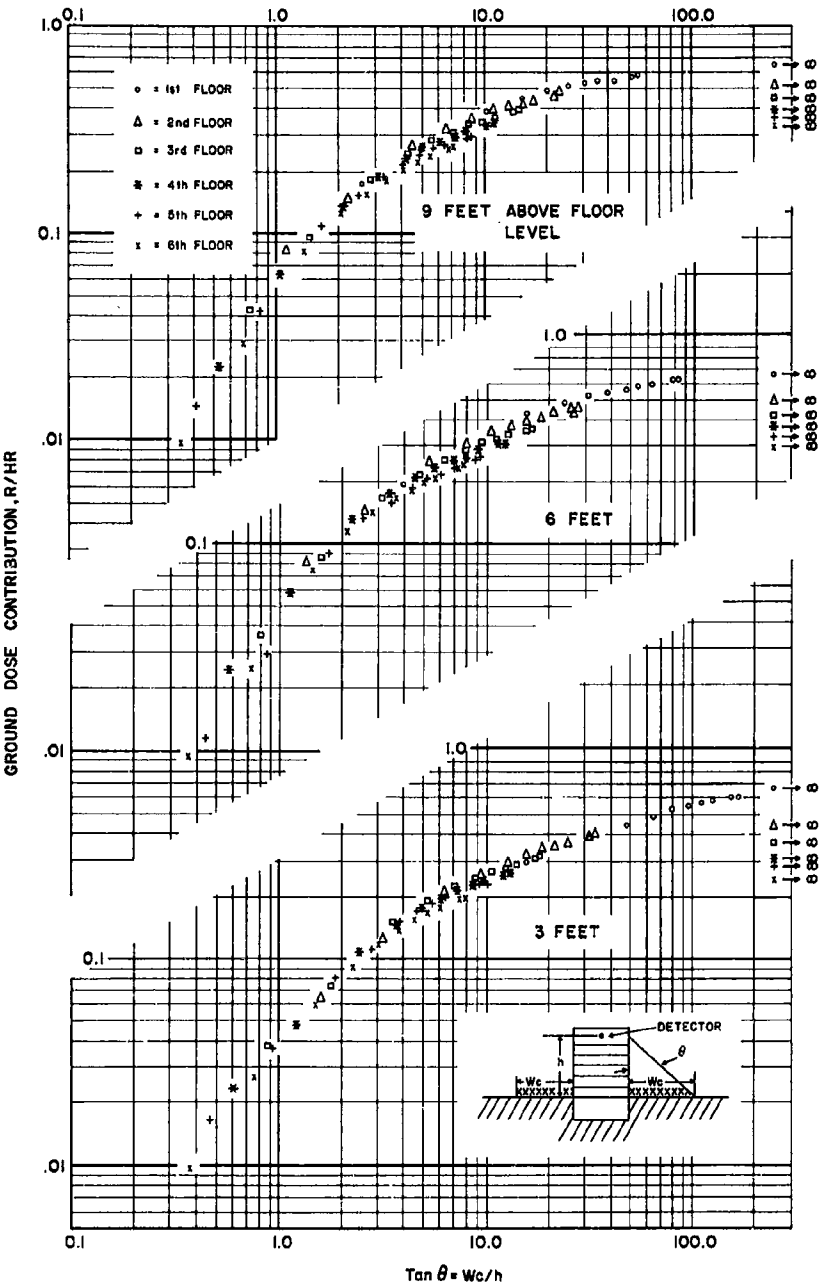

Figure 14. Full-Scale Dose Rate vs. W_c/h for Corner Position of Building with 0 psf Walls and 20 psf Floors

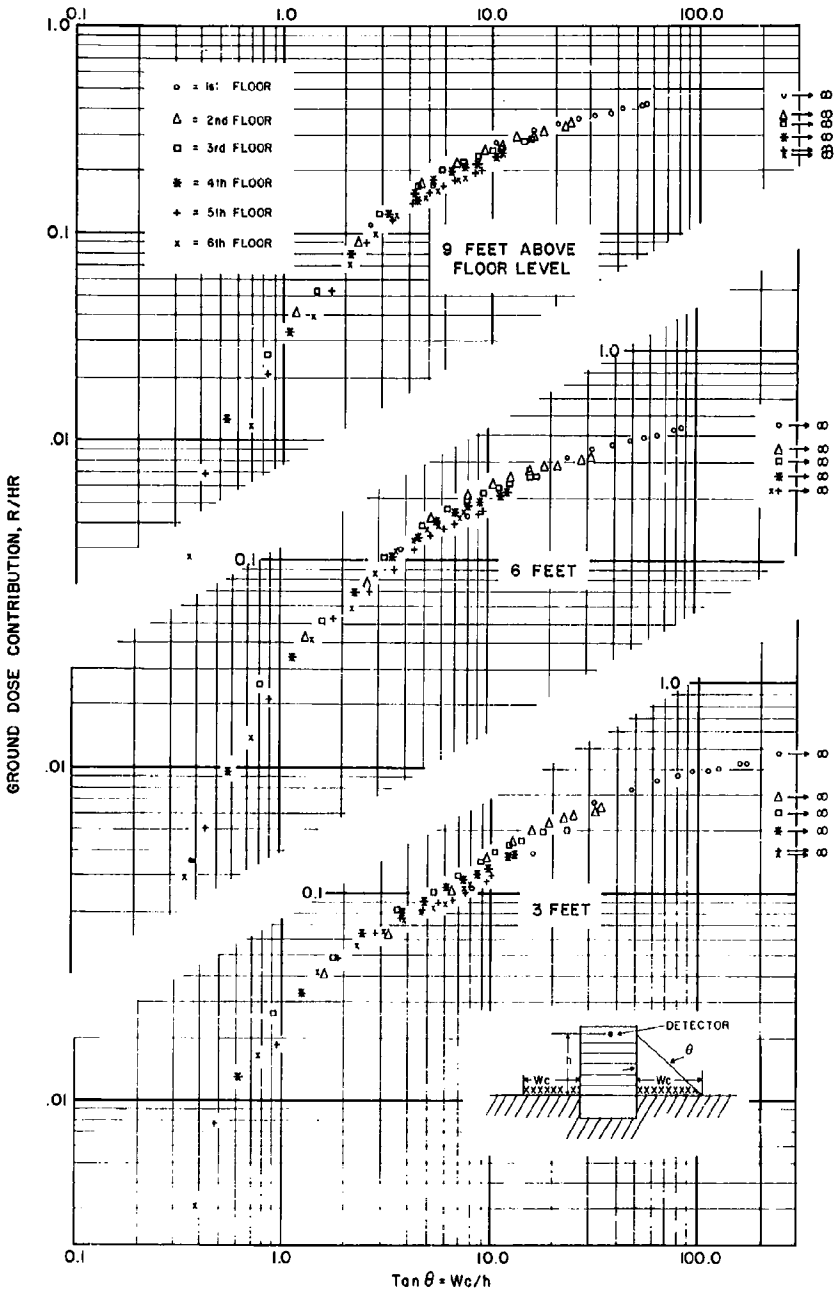

Figure 15. Full-Scale Dose Rate vs. W_c/h for Center Position of Building with 20 psf Walls and Floors

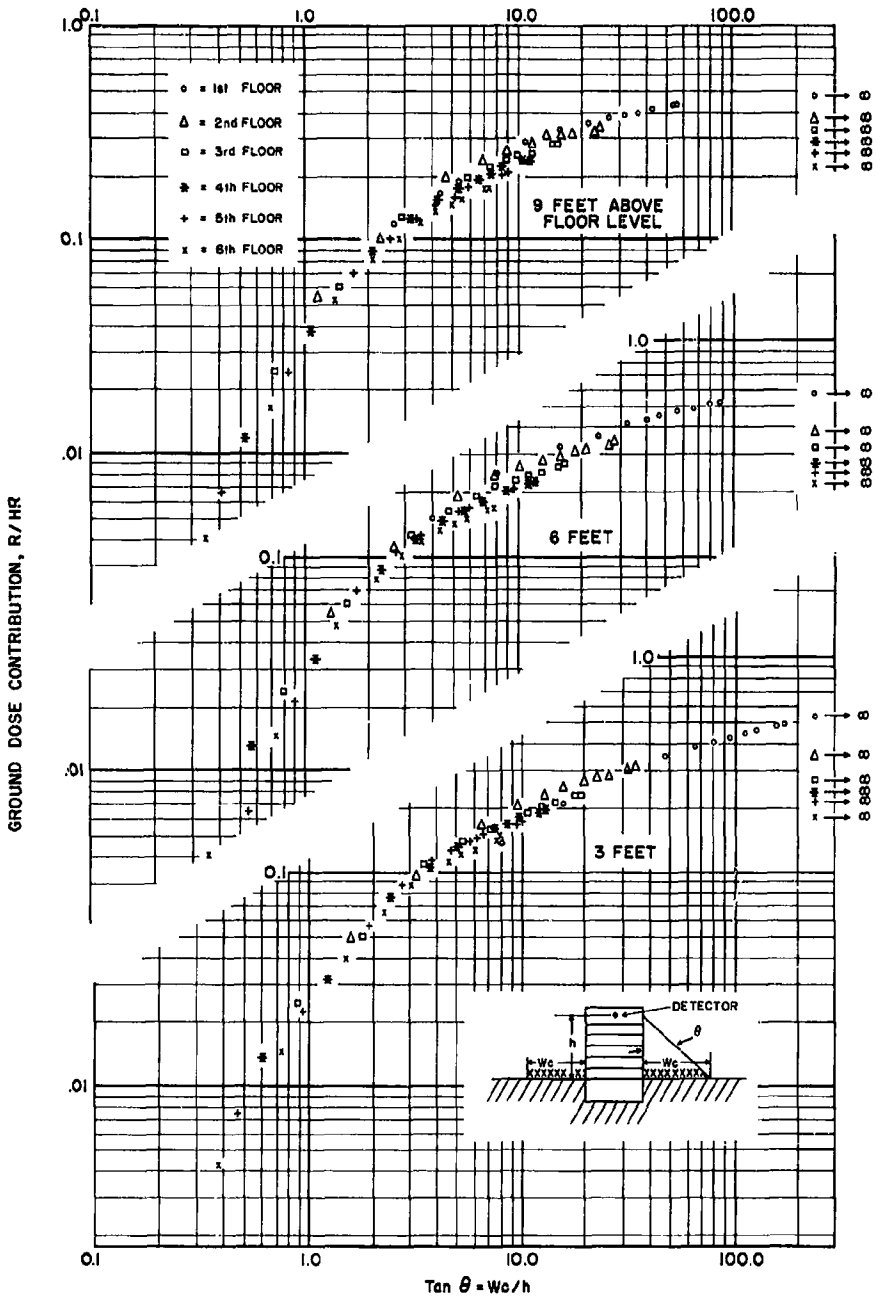

Figure 16. Full-Scale Dose Rate vs. W_c/h for Corner Position of Building with 20 psf Walls and Floors

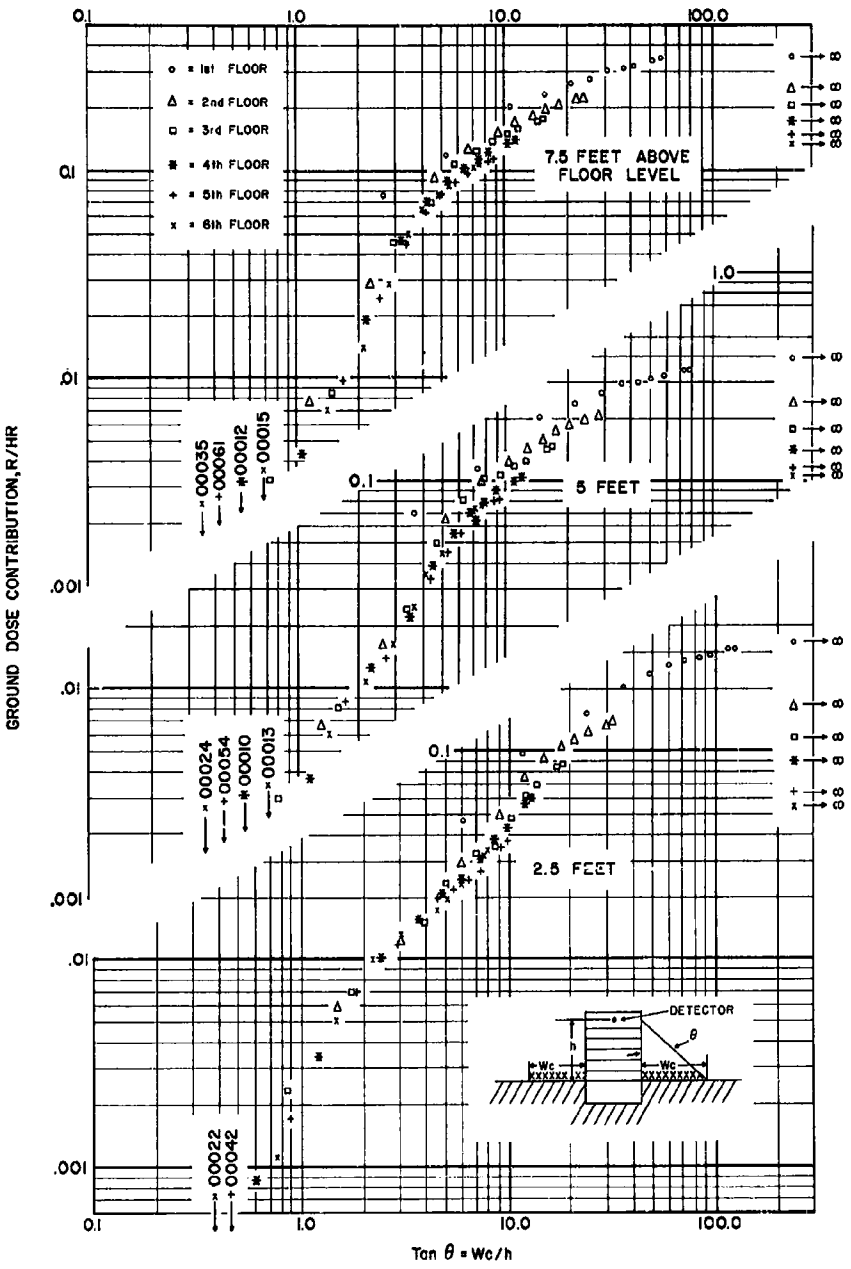

Figure 17. Full-Scale Dose Rate vs. W_c/h for Center Position of Building with 20 psf Walls and 80 psf Floors

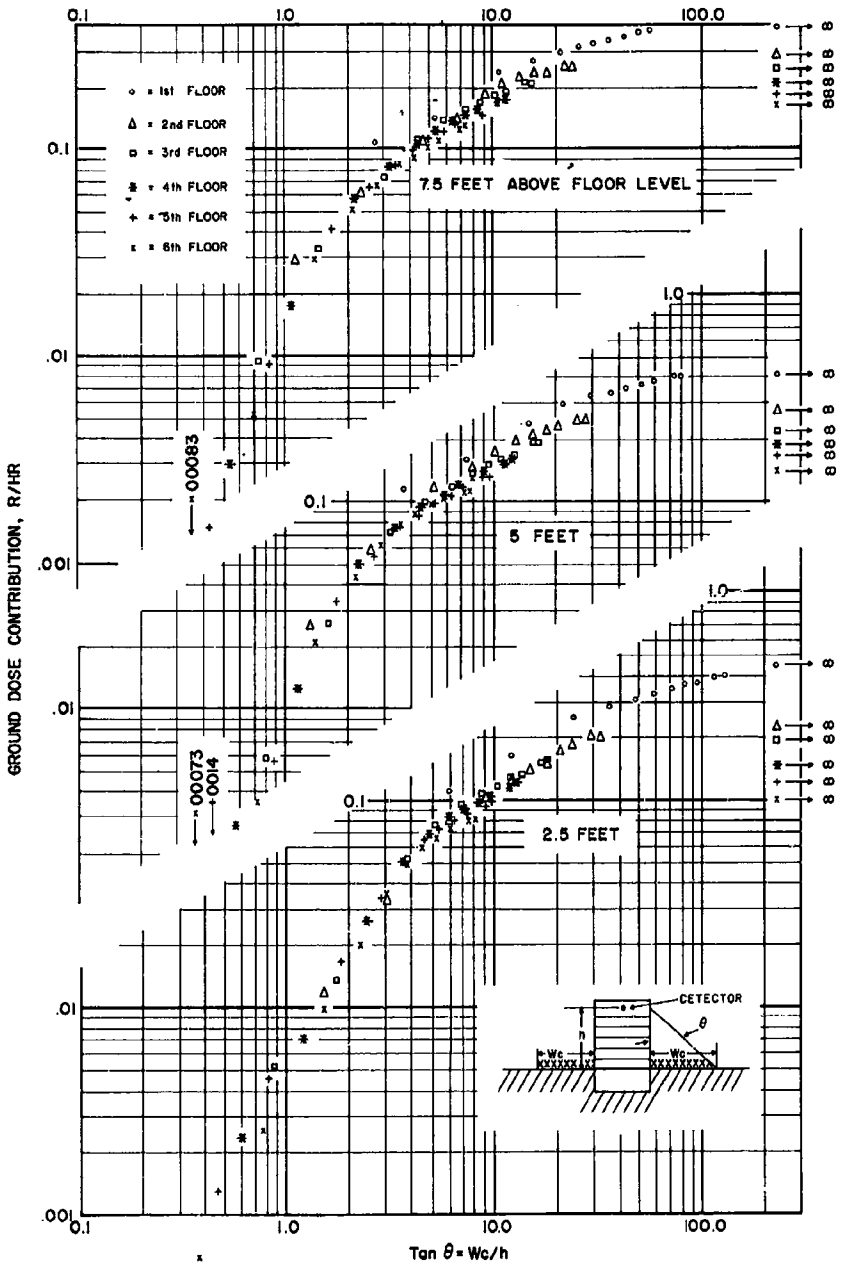

Figure 18. Full-Scale Dose Rate vs. W_c/h for Corner Position of Building with 20 psf Walls and 80 psf Floors

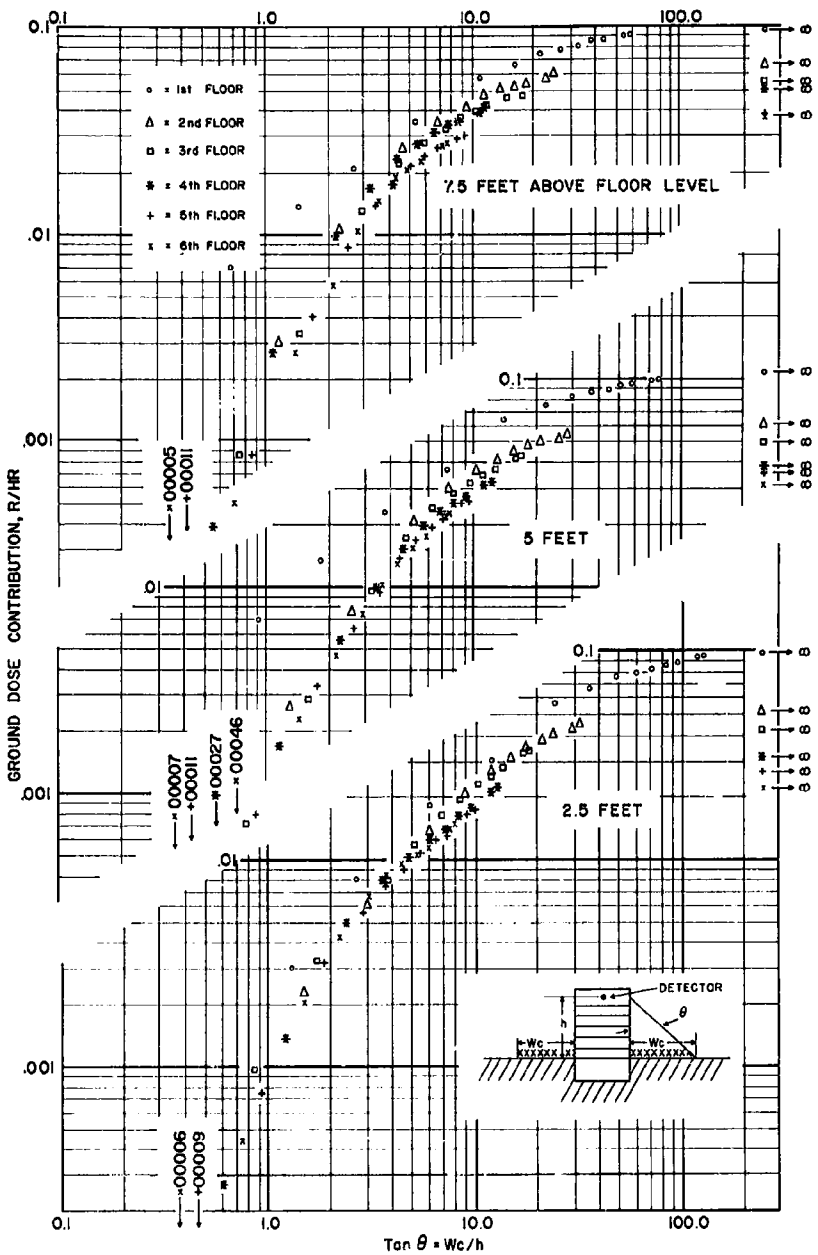

Figure 19. Full-Scale Dose Rate vs. W_c/h for Center Position of Building with 80 psf Walls and Floors

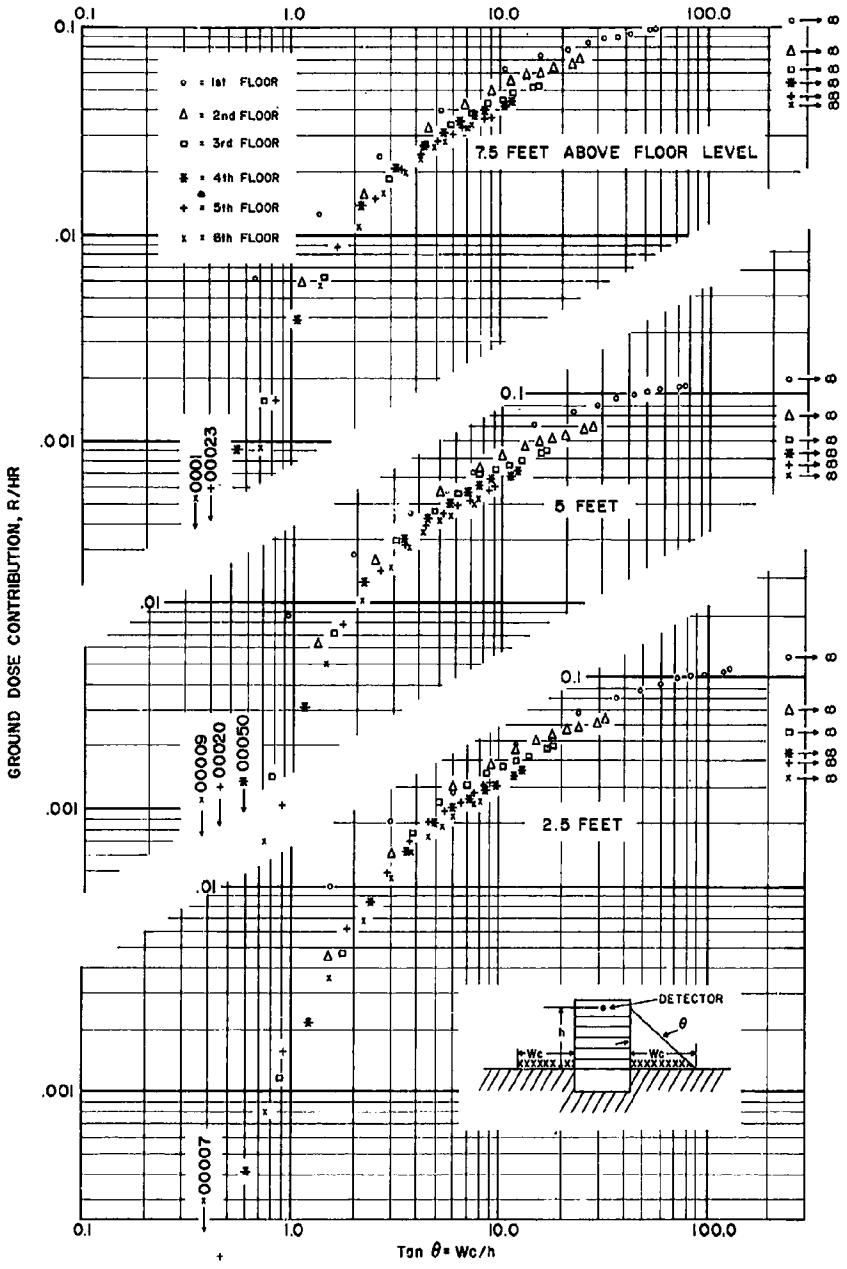

Figure 20. Full-Scale Dose Rate vs. W_c/h for Corner Position of Building with 80 psf Walls and Floors

is due to floor shadows coming into play at values of W_c/h ranging from 3 to 7.5 for center dosimeters 3 to 9 feet above floor level. The magnitude of this dip decreases with increased wall thickness and with detector height above floor level.

COMPUTATION OF A FULL-SCALE VERSION OF THE MODEL BUILDING

The computation of the radiation attenuation from ground-based sources using the methods described in the "Guide for Architects and Engineers" (GAE) and in the NSSCP is virtually identical for infinite-field sources. The major differences between these two methods of computation lie in the correction of infinite-field data to limited-field data. However, the data presented in the "Guide for Architects and Engineers" and in NSSCP are for a detector located 3 feet above the floor at the center of a structure of essentially square floor plan with a story height of 10 feet. Hence, their use to determine the expected dose rate at other locations is not strictly valid. The computational method presented in the OCD engineers' manual "Design and Review of Structures for Protection from Fallout Gamma Radiation,"[2] however, is generalized so that it may handle any detector location or height.

GAE AND NSSCP COMPUTATIONAL METHODS

The computation of the radiation contribution from ground-based sources of radiation to a detector located at a height of 3 feet in the center of a multistory building using the nomenclature of Ref. 1 is presented in Table 7. Note that the data of Ref. 1 are for a detector located 3 feet above the floor in a 10-foot story structure, and that the first floor is at ground level. Thus, the full-scale version of the model structure must be scaled to meet these criteria.

The "Guide for Architects and Engineers" specifies that the values in Table 7 should be multiplied by two factors to correct for height above the ground and width of the contaminated field. These corrections factors, reproduced from Chart 5 and Table CF-3 of the Ref. 1, are presented in Tables 8 and 9.

TABLE 7

COMPUTATION OF UNCORRECTED INFINITE-FIELD FIRST-FLOOR GROUND CONTRIBUTION
(Methods of Refs. 1 and 3)

Computation Step	Structure			
	1	2	3	4
1. Floor Plan (ft x ft)	36x48	36x48	36x48	36x48
2. Story Height (ft)	12	12	12	12
3. Scaled Story Height (ft)	10	10	10	10
4. Scaled Floor Plan (ft)	30x40	30x40	30x40	30x40
5. Scaled Detector Height (ft above floor)	3	3	3	3
6. Corresponding Detector Location in Full-Scale Building (ft above floor)	3.6	3.6	3.6	3.6
7. Exterior Wall Thickness (psf)	0	20	20	80
8. Floor Thickness (psf)	20	20	80	80
Answer: Uncorrected Dose Rate, Chart 3, Ref. 1 (r/hr*)	0.60	0.36	0.36	0.10

*From an infinite field of fallout contamination that would produce 1.0 r/hr at 3-foot height if the building were absent.

TABLE 8

EFFECT OF DOSIMETER HEIGHT
(Chart 5, "Guide for Architects and Engineers")

Detector Height, H (ft)	Multiplicative Factor	Detector Height, H (ft)	Multiplicative Factor
3	1.0	150	0.30
5	0.92	300	0.184
30	0.58	600	0.083
60	0.46	1200	0.023

TABLE 9

EFFECT OF LIMITED FIELDS OF CONTAMINATION
(Table CF-3,"Guide for Architects and Engineers")

Width of Field (W_c/ft)	Multiplicative Factor
0	0.00
10	0.08
20	0.10
50	0.20
100	0.40
200	0.60
500	0.80
1000	0.90
Infinite	1.00

The computations of infinite-field values of ground-based radiation for a detector located 3.6 feet above the floor for all floor values are presented in Table 10. Dimensionally, the floors are assumed to be of negligible thickness, with the associated mass concentrated at their mid-plane.

TABLE 10

COMPUTATION OF INFINITE-FIELD GROUND CONTRIBUTION
SIX-STORY BUILDING
(Detector 3.6 ft. above Each Floor—36x48—Plan Area
(12-Foot Story Height)

Structure	Floor	Detector Height Above Ground (ft)	Height Correction Factors	Uncorrected 1st Floor Contrib. (r/hr)	Corrected Dose Rate (r/hr)
1 0 psf Wall 20 psf Floor	1	3.85	.96	.60	.57
	2	15.85	.71	.60	.42
	3	27.85	.59	.60	.35
	4	39.85	.53	.60	.32
	5	51.85	.49	.60	.29
	6	63.85	.45	.60	.27
2 20 psf Wall 20 psf Floor	1	3.85	.96	.36	.34
	2	15.85	.71	.36	.26
	3	27.85	.59	.36	.21
	4	39.85	.53	.36	.19
	5	51.85	.49	.36	.18
	6	63.85	.45	.36	.16
3 20 psf Wall 80 psf Floor	1	4.6	.93	.36	.34
	2	16.60	.70	.36	.25
	3	28.60	.59	.36	.21
	4	40.60	.53	.36	.19
	5	52.60	.49	.36	.18
	6	64.60	.45	.36	.16
4 80 psf Wall 80 psf Floor	1	4.60	.93	.10	.093
	2	16.60	.70	.10	.070
	3	28.60	.59	.10	.059
	4	40.60	.53	.10	.53
	5	52.60	.49	.10	.049
	6	64.60	.45	.10	.045

The resulting fraction of infinite-field dose rate for a detector height 3.6 feet above the floor for the first and sixth floors (detector heights of 3.85 feet and 63.85 feet above ground, respectively) of a full-scale building (ratio of linear-dimensions model to full scale = 1/12) similar to the model structure with 20 psf floor and wall thickness is presented for illustrative purposes in Figure 21. The data are plotted versus the tangent of the angle between the building wall and a diagonal to the edge of the contaminated field at the detector height:

$$\text{Tangent } \Theta = W_c/h \tag{4}$$

where

W_c = width of contaminated field (ft)

h = detector height for floor of interest (ft).

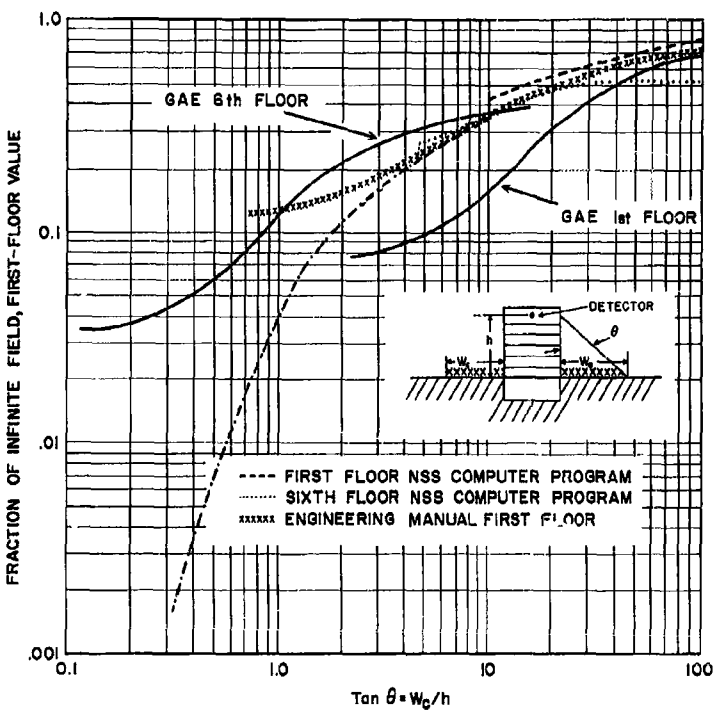

Figure 21. Computed Fraction of Infinite-Field First-Floor Dose Rate vs. W_c/h for Building with 20 psf Walls and Floors

The computer program designed for use with the National Shelter Survey corrects the infinite field by a multiplicative factor depending upon the tangent of the angle between the building face and a diagonal to the edge of the contaminated field ($\tan \Theta = W_c/h$), the mass thickness of the external building walls, and the distance from the building to the outer edge of the field. This factor, M_c, is determined as follows:

Case 1: If $\tan \Theta = W_c/h < 2$; or if $2 < \tan \Theta = W_c/h < 10$, and $W_c < 300$ feet, then:

$$M_c = M_L. \tag{5}$$

Case 2: If $2 < \tan \Theta = W_c/h \leq 10$ and $W_c > 300$ feet; or if $\tan \Theta = W_c/h > 10$, then:

$$M_c = M_h(X_e, h) \left[1 - \frac{M_h(X_e = 0, h = \sqrt{h^2 + W_c^2})}{M_h(X_e = 0, h)} \right] \tag{6}$$

where

M_L = multiplicative factor for finite-field corrections, all heights and wall thicknesses

$M_h(X_e h)$ = multiplicative factor for height correction based on air attenuation

h = detector height above ground (ft)

X_e = exterior wall thickness (psf).

Note that the NSSCP correction factor for "close-in" limited fields of contamination ($W_c/h \leq 10$ and $W_c < 300$ ft) has been computed specifically for the case of a detector height of 3 feet and a story height of 10 feet in upper-story locations of a thick-floored structure (negligible direct radiation). The factor for far-field limited strips of contamination ($W_c > 300$ ft, $W_c/h > 2$) has been based primarily upon air-attenuation results and, hence, should be valid for all locations.

The tabular values to be used in evaluating the multiplicative factor, M_c, are presented in Tables 11 and 12. These values[3] for the mass thickness of interest

TABLE 11

MULTIPLICATIVE FACTOR FOR FINITE-FIELD CORRECTION, M_L

Tan $\theta = W_c/h$	M_L			Tan $\theta = W_c/h$	M_L		
	(0 psf)	(20 psf)	(80 psf)		(0 psf)	(20 psf)	(80 psf)
0.000	0.0000	0.0000	0.00000	0.98	0.070	0.037	0.017
0.314	0.0095	0.0019	0.00039	1.33	0.109	0.068	0.040
0.436	0.0174	0.0048	0.0012	2.06	0.175	0.120	0.086
0.577	0.0293	0.010	0.0031	2.5	0.195	0.133	0.10
0.75	0.047	0.021	0.0077	5.0	0.290	0.230	0.19
				10.0	0.420	0.365	0.33

TABLE 12

MULTIPLICATIVE FACTOR FOR HEIGHT CORRECTION, $M_h(X_e, h)$

Detector Height, h (ft)	Wall Thickness X_e (psf)		
	0	50	100
3	1.00	1.00	1.00
5	0.88	0.90	0.89
30	0.58	0.56	0.54
60	0.46	0.42	0.39
150	0.30	0.24	0.23
300	0.18	0.14	0.12
600	0.083	0.059	0.051
1200	0.023	0.017	0.015

(0 psf, 20 psf, and 80 psf) are reproduced from the computer program as used in the National Shelter Survey.

For illustrative purposes, the fraction of infinite-field dose rate for the first and sixth floor detectors located 3.6 feet above the floor in a structure with 20 psf walls and floors is presented in Figure 21.

COMPUTATIONAL METHOD OF ENGINEERING MANUAL

The method of computation of the dose expected from ground sources of radiation presented in Ref. 2 is to divide the total radiation contribution into seven separate components, depending upon the mode of travel to the detector. Each of these components is computed separately, and their sum is then added. The equations required to determine these components for infinite fields of contamination using the terminology of Ref. 2 are (see Figure 22):

Skyshine radiation penetrating to the detector through the ceiling above the detector

$$D_{ss}^{U} = \left[G_a(\omega'_u) - G_a(\omega_u) \right] (1 - S_w)\, B_w(X_e, H_u)\, B'_o(X_f) \tag{7}$$

Skyshine radiation penetrating to the detector through the walls of the detector floor

$$D_{ss} = G_a(\omega_u)(1 - S_w)\, B_w(X_e, H) \tag{8}$$

Wall-scattered radiation from the story above the detector

$$D_{ws}^{U} = \left[G_s(\omega'_u) - G_s(\omega_u) \right] S_w E\, B_w(X_e, H_u)\, B'_o(X_f) \tag{9}$$

Wall-scattered radiation from the walls of the same story as the detector

$$D_{ws} = \left[G_s(\omega_u) + G_s(\omega_\ell) \right] S_w E\, B_w(X_e, H) \tag{10}$$

Wall-scattered radiation from the story below the detector

$$D_{ws}^{L} = \left[G_s(\omega'_\ell) - G_s(\omega_\ell) \right] S_w E\, B_w(X_e, H_L)\, B_o(X_f) \tag{11}$$

Direct radiation from the same story as the detector

$$D_d = \left[G_d(\omega_\ell, H) \right] (1 - S_w)\, B_w(X_e, H) \tag{12}$$

Direct radiation from the story below the detector

$$D_d^L = \left[G_d(\omega'_\ell H) - G_d(\omega_\ell, H)\right](1 - S_w)\, B_w(X_e, H)\, B_o(X_f) \qquad (13)$$

where

$G_a(\omega)$ = the directional response of atmospheric-scattered radiation

$G_s(\omega)$ = the directional response of wall-scattered radiation

$G_d(\omega, H)$ = the directional response of direct radiation

ω = a solid angle fraction (solid angle/2π)(see Figure 22)

H = detector height above ground

H_u = mid-height of floor above detector

H_L = mid-height of floor below detector

S_w = the fraction of radiation scattered by the wall

E = an eccentricity factor depending upon length-to-width ratio

$B_w(X_e, H)$ = the barrier shielding introduced by a vertical wall of thickness X_e at height H above the ground

$B'_o(X_f)$ = the barrier shielding introduced by an overhead mass of thickness X_f to atmospheric or wall-scattered radiation

$B_o(X_f)$ = the barrier shielding introduced by a barrier of thickness X_f parallel to the field of contamination between the detector and the field.

Spencer[16] evaluates these functions for cobalt radiation as well as fallout radiation. Hence, to compute the dose rate from cobalt in the center of the structure, the methods of Ref. 2 together with the functions evaluated in Ref. 16 were used. Table 13 presents the infinite-field values of ground dose contribution for both cobalt radiation and fallout for detectors located in the center of the structure.

Additional data are also presented in Ref. 2 so that the effects of limited rectangular fields of contamination may be estimated for first-floor locations. The procedure used is to neglect the wall-scatter contribution from the second story;

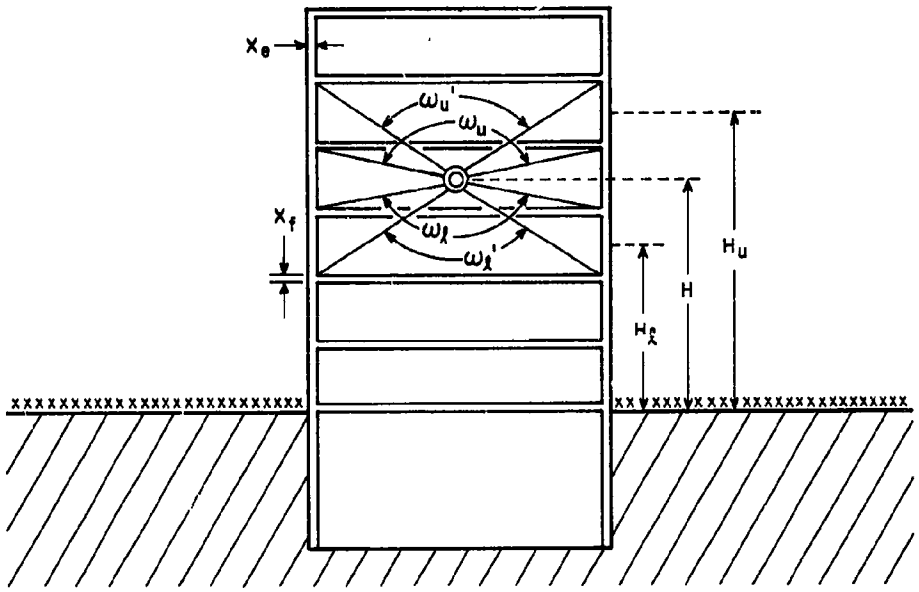

INFINITE FIELD OF CONTAMINATION

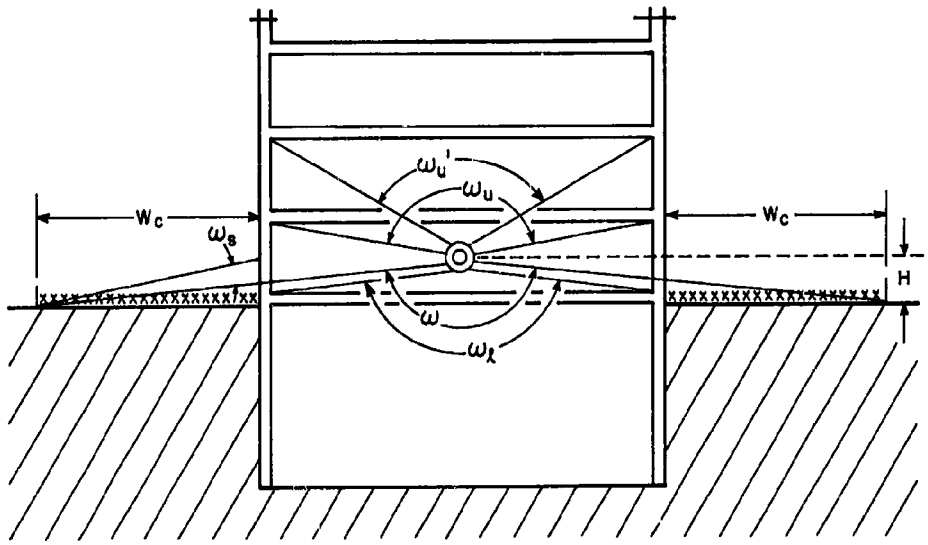

LIMITED FIELD OF CONTAMINATION

Figure 22. Application of Geometric Terminology of Engineering Manual to a Multistory Structure

TABLE 13

COMPUTED CENTER INFINITE-FIELD DOSE RATES OF FOUR MODEL STRUCTURES*

Floor	Computed Dose Rates							
	[1] 0 psf Floor 20 psf Wall		[2] 20 psf Floor 20 psf Wall		[3] 20 psf Floor 80 psf Wall		[4] 80 psf Floor 80 psf Wall	
	Detector Height Above Floor							
	3		3		2-1/2		2-1/2	
	Fallout	Co-60	Fallout	Co-60	Fallout	Co-60	Fallout	Co-60
1	.49	.49	.35	.35	.32	.32	.087	.087
2	.29	.29	.22	.22	.17	.17	.055	.049
3	.23	.23	.19	.19	.16	.16	.042	.039
4	.19	.19	.15	.15	.11	.11	.037	.033
5	.15	.15	.14	.14	.10	.10	.031	.029
6	.12	.12	.12	.12	.09	.09	.029	.025

*From an infinite field of fallout contamination that would produce 1.0 r/hr at a 3-foot height if the building were absent. Methods of Ref. 2 and functions of Ref. 16 were used.

replace the function $B_w(X_e, H)$ with a new function, $2B_{ws}(X_e \omega_s)$, in the equation for wall-scattered radiation through the first-story walls; and limit the directional response of direct radiation to the contaminated limited field. Thus Eqs. (9), (11), and (13) become identically zero while $B_w(X_e, H)$ must be replaced with $2B_{ws}(X_e, \omega_s)$ in Eq. (10) and $G_d(\omega_e, H)$ is replaced with the quantity $\left[G_d(\omega_e, H) - G_d(\omega_e^*, H) \right]$ in Eq. (12). The resulting fraction of infinite-field dose rate for a detector located 3.0 feet above the first floor of a full-scale building similar to the model building (scale ratio 12) with 20 psf walls and floors is presented for illustrative purposes in Figure 21. It is clear that none of the three presently proposed methods of computation shows good agreement with any other.

COMPARISON OF DATA

The purpose of the previous three sections is to provide the analytical tools required to correct the data obtained from model experiments to those which would be obtained from similar full-scale experiments and to outline the computational

methods presently proposed to compute the radiation from a limited field of contamination. Thus Eq. (1), evaluated in Table 5, presents the ratio of full-scale to model dose rate for any annulus of interest, and Eq. (3), evaluated in Table 6, presents the ratio of expected full-scale far-field dose to that obtained from the outer annulus of simulated contamination used in the model experiments. Similarly, the previous section presents in outline form the three computational methods presently proposed to compute the dose rate within a structure.

Let us compare the calculated infinite-field values of ground contribution for the three methods of computation with those experimentally measured. These values are given in Table 14 . It should be noted that the GAE computational method and the NSSCP computational method are virtually identical for infinite fields of contamination; however, they only allow the computation of dose rate at a height of 3/10 of the story height (or 3.6 feet) above the mid-plane of each floor.

Table 14 shows that the relative agreement between computational methods is excellent at first-floor locations, while for upper-story locations the engineering manual[2] approach consistently predicts lower dose rates than GAE or the NSSCP. Moreover, the agreement of infinite-field ground contribution between the engineering manual and the experimental results are excellent over all stories.

The major purpose of these experiments has been to evaluate the tabular correction for finite fields of contamination for above-ground areas as used in the National Shelter Survey Computer Program. It is thus of interest to present the data obtained in a fashion similar to that used in the NSSCP; that is, as a multiplicative factor to be used to correct the infinite-field ground contribution to the finite-field case. For purposes of discussion, it is convenient to divide the contaminated field into two regions: (1) near-field limited fields of contamination and (2) far-field limited fields of contamination. The NSSCP method performs the separation at values of $W_c/h = 10$ or $W_c = 300$ feet (W_c = width of contaminated field, h = detector height), whichever represents the smallest field of contamination. An examination of the experimental data (Figures 13 through 20) will show this approach to be realistic, since the data taken from similar positions in each structure from all floors with the exception of the first floor for the thick-floored cases fall on a common curve within approximately 10% for values of $W_c/h < 10$ and $W_c <$ about 300 feet.

TABLE 14

COMPARISON OF CALCULATED AND EXPERIMENTAL
INFINITE-FIELD GROUND DOSE CONTRIBUTION, CENTER POSITION
(From an infinite field of fallout contamination that would
produce 1.0 r/hr at a 3-foot height if the building were absent.)

Floor	Height Above Floor (ft)	Dose Rate							
		0 psf Wall 20 psf Floor				20 psf Wall 20 psf Floor			
		Fallout		Co-60		Fallout		Co-60	
		GAE NSSCP*	Eng. Manual†	Eng. Manual	Experiment	GAE NSSCP	Eng. Manual	Eng. Manual	Experiment
1‡	3	.58	.49	.49	.59	.35	.35	.35	.48
	6	—	.51	.51	.58	—	.36	.36	.44
	9	—	.50	.50	.58	—	.35	.35	.46
2	3	.43	.29	.29	.34	.27	.22	.22	.29
	6	—	.35	.35	.42	—	.26	.26	.35
	9	—	.39	.39	.46	—	.26	.26	.37
3	3	.35	.23	.23	.29	.21	.19	.19	.25
	6	—	.30	.30	.38	—	.22	.22	.30
	9	—	.31	.31	.43	—	.23	.23	.33
4	3	.32	.19	.19	.24	.19	.15	.15	.20
	6	—	.24	.24	.32	—	.17	.17	.26
	9	—	.26	.26	.36	—	.17	.17	.29
5	3	.29	.15	.15	.20	.18	.14	.14	.16
	6	—	.19	.19	.27	—	.16	.16	.22
	9	—	.22	.22	.33	—	.16	.16	.25
6	3	.27	.12	.12	.19	.16	.12	.12	.15
	6	—	.16	.16	.25	—	.14	.14	.22
	9	—	.19	.19	.30	—	.14	.14	.24

Floor	Height Above Floor (ft)	20 psf Wall 80 psf Floor				80 psf Wall 80 psf Floor			
		Fallout		Co-60		Fallout		Co-60	
		GAE NSSCP**	Eng. Manual	Eng. Manual	Experiment	GAE NSSCP	Eng. Manual	Eng. Manual	Experiment
1‡	2-1/2	.34	.32	.32	.36	.093	.087	.087	.098
	5	—	.34	.34	.36	—	.087	.087	.107
	7-1/2	—	.33	.33	.35	—	.082	.092	.098
2	2-1/2	.25	.17	.17	.19	.070	.055	.049	.051
	5	—	.23	.23	.24	—	.061	.055	.062
	7-1/2	—	.22	.22	.27	—	.058	.061	.067
3	2-1/2	.21	.14	.16	.12	.059	.042	.039	.040
	5	—	.18	.18	.19	—	.047	.046	.050
	7-1/2	—	.17	.17	.22	—	.044	.043	.055
4	2-1/2	.19	.11	.11	.096	.053	.037	.033	.043
	5	—	.15	.15	.15	—	.043	.039	.036
	7-1/2	—	.15	.15	.18	—	.042	.036	.050
5	2-1/2	.18	.10	.10	.068	.049	.031	.029	.025
	5	—	.13	.13	.12	—	.036	.034	.035
	7-1/2	—	.13	.13	.16	—	.031	.028	.038
6	2-1/2	.16	.09	.09	.054	.045	.029	.025	.021
	5	—	.11	.11	.11	—	.034	.031	.032
	7-1/2	—	.12	.12	.14	—	.032	.029	.037

*Height above floor surface for GAE and NSSCP computational methods is 3.35 ft.

†Ref. 2

‡The minor difference in calculated values on the first floor between the building with 20 psf walls and 20 psf floors and that with 20 psf walls and 80 psf floors is attributable to the difference in detector and wall heights caused by the increased floor thickness.

**Height above floor surface for GAE and NSSCP computational methods is 2.6 ft.

The NSSCP correction factors for limited strips of contamination in the close-in region ($W_c/h \leq 10$, $W_c \leq 300$ ft) are designed to represent the fraction of infinite-field first-floor dose rate that would be obtained 3 feet above the floor on the upper stories at the center of a thick-floored structure. Thus, the experimental data that are directly comparable with the NSSCP are those obtained at the center positions, lowest detector height, on the upper stories of the model structure. These data are given in Table 15.

TABLE 15

EFFECTS OF LIMITED FIELDS OF CONTAMINATION OF RECTANGULAR SHAPE IN THE NEAR-FIELD REGION, UPPER FLOORS
(Fraction of infinite-field first-floor dosage)

Width/Height (W_c/h)	Method						
	Exp.	NSSCP	Exp.		NSSCP	Exp.	NSSCP
	0 psf Wall 20 psf Floor	0 psf Wall Thick Floor	20 psf Wall 20 psf Floor	20 psf Wall 80 psf Floor	20 psf Wall Thick Floor	80 psf Wall 80 psf Floor	80 psf Wall Thick Floor
0.0	0.000	0.0000	0.0000	0.0000	0.0000	0.0000	0.0000
0.32	0.011	0.0095	0.0021	0.0004	0.0019	0.0003	0.0004
0.44	0.018	0.017	0.0050	0.0011	0.0048	0.0010	0.0012
0.58	0.026	0.029	0.021	0.0024	0.010	0.0023	0.0031
0.75	0.035	0.047	0.034	0.0046	0.021	0.0046	0.0077
0.98	0.050	0.070	0.051	0.0086	0.037	0.0094	0.017
1.33	0.069	0.11	0.069	0.015	0.068	0.017	0.040
2.06	0.11	0.18	0.10	0.028	0.120	0.037	0.086
2.5	0.13	0.20	0.12	0.036	0.133	0.049	0.10
5.0	0.18	0.29	0.18	0.070	0.230	0.11	0.19
10.0	0.32	0.42	0.30	0.20	0.365	0.22	0.33

Note in Table 15 that, while agreement between theory and experiment is, at best, only fair for thick floors (80 psf), the experimental data for thin floors show no resemblance to the data for thick floors. This may be attributed to the fact that, for close-in locations, the major portion of the dose received by the detector is from direct radiation that has penetrated the floor slab. For example, the comparison of the structure with 20 psf walls and floors and that with 20 psf walls and 80 psf floors indicates that a field extending to $W_c/h = 0.58$ creates 10 times higher a percentage of infinite field dose for the thin-floored structure than for the thick-floored structure. While at $W_c/h = 0.98$ the thin-floored structure receives an infinite-field dose only about 6 times as high in percentage as the thick-floored structure.

This ratio of percentages of infinite-field dose rates continues to decrease as W_c/h increases, illustrating the effect of direct radiation penetration through the floor slabs. The fraction of infinite-field dose for close-in locations of limited strips of contamination is thus dependent on both the floor and wall thicknesses. In practice, however, it is probably sufficient to specify the floor in terms of a thick floor (greater than perhaps 40 psf) or a thin floor (less than 40 psf).

During the performance of the experiments on the four model structures, data were taken at positions other than those required to evaluate the multiplicative factor for correction to limited fields of contamination for the NSSCP program. These data for all floors at all heights, including those corresponding to approximately 3 feet above floor level and for corner locations, are presented in Tables 16 through 19. From examination of these tables and the infinite field values from Figures 13 through 20, general conclusions as to the variation of dose rate with position may be drawn for limited fields of contamination, $W_c/h \leq 10$. These conclusions are best represented as the ratio of the dose rate at positions other than the center 3-foot high position to that center position. Table 20 presents these ratios. These ratios are valid to within ± 20% of the value stated.

The NSSCP correction factor for far-field ($W_c/h > 10$ and $W_c > 300$ ft) limited strips of contamination is computed from tabular values of air-attenuation functions. Thus, the correction factor basically assumes that the only difference in the fraction of the infinite-field dose received by two detectors, one slightly above the other, from a field extending from the structure to a distance of perhaps 500 feet is that introduced by the additional atmosphere that must be traversed by the radiation to reach the higher detector. It may easily be shown that this assumption is correct only for the case of a structure with floors of negligible thickness.

The argument may be made as follows. Consider two detector positions, No. 1 and No. 2, of slightly different height located on the upper floor of a structure with thick floors (see Figure 23). If the floor below the detector is assumed to be black to radiation, we may qualitatively estimate the dose rate at each detector position as a function of increasing field width. The dose detected at both positions No. 1 and No. 2 remains zero until the detector can see the field. Thus, for field width W_c^1, detectors No. 1 and No. 2 read zero; for field width W_c^2, detector No. 2 sees

TABLE 16

EFFECT OF RECTANGULAR LIMITED FIELDS OF CONTAMINATION
FRACTION OF INFINITE FIELD
(0 psf walls, 20 psf floors)

Width/Height (W_c/h)	Infinite Field Dose Rate (r/hr)*					
	.59	.58	.58	.67	.65	.62
	Center Position (ft)			Corner Position (ft)		
	3	6	9	3	6	9
	Experimental Data, First Floor					
.75	.035	.041	.043	.041	.052	.056
.98	.050	.062	.066	.061	.078	.087
1.33	.069	.088	.097	.086	.11	.12
2.06	.11	.14	.16	.13	.17	.20
2.5	.13	.17	.20	.16	.20	.24
5.0	.18	.30	.37	.25	.34	.42
10.0	.32	.46	.55	.36	.51	.60
	Experimental Data, Upper Floors					
0.0	0	0	0	0	0	0
.315	.011	.0095	.011	.010	.0092	.012
.436	.018	.017	.019	.018	.019	.023
.577	.026	.028	.029	.028	.034	.037
.75	.035	.041	.043	.041	.052	.056
.98	.050	.062	.066	.061	.078	.087
1.33	.069	.088	.097	.086	.11	.12
2.06	.11	.14	.16	.13	.17	.20
2.5	.13	.17	.20	.16	.20	.24
5.0	.18	.30	.37	.25	.34	.42
10.0	.32	.46	.55	.36	.51	.60

*From an infinite field of fallout contamination that would produce 1.0 r/hr at a 3-foot height if the building were absent.

TABLE 17

EFFECT OF RECTANGULAR LIMITED FIELDS OF CONTAMINATION
FRACTION OF INFINITE FIELD
(20 psf walls, 20 psf floors)

Width/Height (W_c/h)	Infinite Field Dose Rate (r/hr)*					
	.48	.46	.46	.53	.52	.47
	Center Position (ft)			Corner Position (ft)		
	3	6	9	3	6	9
	Experimental Data, First Floor					
.75	.034	.030	.040	.031	.038	.048
.98	.051	.049	.061	.049	.063	.055
1.33	.069	.078	.096	.070	.096	.11
2.06	.10	.14	.17	.12	.16	.18
2.5	.12	.17	.21	.14	.19	.21
5.0	.18	.31	.39	.23	.36	.37
10.0	.30	.48	.57	.34	.52	.58
	Experimental Data, Upper Floors					
0	0	0	0	0	0	0
.315	.0021	.0057	.0083	.0053	.0041	.0074
.436	.0050	.011	.014	.010	.0096	.015
.577	.021	.013	.025	.023	.021	.028
.75	.034	.030	.040	.031	.038	.048
.98	.051	.049	.061	.049	.063	.055
1.33	.069	.078	.096	.070	.096	.11
2.06	.10	.14	.17	.12	.16	.18
2.5	.12	.17	.21	.14	.19	.21
5.0	.18	.31	.39	.23	.33	.37
10.0	.30	.48	.57	.34	.50	.58

*From an infinite field of fallout contamination that would produce 1.0 r/hr at a 3-foot height if the building were absent.

TABLE 18

EFFECT OF RECTANGULAR LIMITED FIELDS OF CONTAMINATION
FRACTION OF INFINITE FIELD
(20 psf walls, 80 psf floors)

Width/Height (W_c/h)	Infinite Field Dose Rate (r/hr)*					
	.36	.36	.35	.44	.41	.38
	Center Position (ft)			Corner Position (ft)		
	2-1/2	5	7-1/2	2-1/2	5	7-1/2
	Experimental Data, First Floor					
0	0	0	0	0	0	0
2.5	.052	.11	.19	.11	.18	.25
5.0	.119	.25	.34	.21	.30	.39
10.0	.25	.42	.55	.33	.53	.58
	Experimental Data, Upper Floors					
0	0	0	0	0	0	0
.315	.0038	.00044	.00066	.00010	.00097	.0014
.436	.0011	.0011	.0017	.0020	.0030	.0039
.577	.0024	.0024	.0039	.0042	.0070	.0092
.75	.0046	.0044	.0074	.0074	.013	.018
.98	.0086	.0083	.014	.013	.027	.037
1.33	.015	.015	.027	.023	.048	.066
2.06	.028	.033	.063	.049	.100	.13
2.5	.036	.044	.088	.064	.13	.17
5.0	.070	.15	.23	.15	.27	.32
10.0	.20	.33	.43	.27	.40	.49

*From an infinite field of fallout contamination that would produce 1.0 r/hr at a 3-foot height if the building were absent.

TABLE 19

EFFECT OF RECTANGULAR LIMITED FIELDS OF CONTAMINATION
FRACTION OF INFINITE FIELD
(80 psf walls, 80 psf floors)

Width/Height (W_c/h)	Infinite Field Dose Rate (r/hr)*					
	.098	.107	.098	.124	.116	.104
	Center Position (ft)			Corner Position (ft)		
	2-1/2	5	7-1/2	2-1/2	5	7-1/2
	Experimental Data, First Floor					
0	0	0	0	0	0	0
.75	.014	.056	.085	.036	.065	.070
.98	.022	.073	.11	.048	.084	.091
1.33	.032	.095	.14	.072	.10	.12
2.06	.056	.14	.18	.10	.16	.18
2.5	.070	.17	.22	.13	.18	.22
5.0	.15	.30	.35	.21	.31	.38
10.0	.28	.48	.56	.34	.48	.58
	Experimental Data, Upper Floors					
0	0	0	0	0	0	0
.315	.00031	.00047	.00040	—	—	—
.436	.0010	.0011	.0016	.0011	.00086	.0032
.577	.0023	.0025	.0038	.0026	.0032	.0077
.75	.0046	.0049	.0080	.0060	.0086	.015
.98	.0094	.010	.016	.013	.022	.030
1.33	.017	.019	.032	.025	.044	.054
2.06	.037	.045	.075	.058	.099	.11
2.5	.049	.063	.10	.081	.13	.14
5.0	.11	.17	.25	.18	.25	.28
10.0	.22	.32	.42	.31	.41	.47

*From an infinite field of fallout contamination that would produce 1.0 r/hr at a 3-foot height if the building were absent.

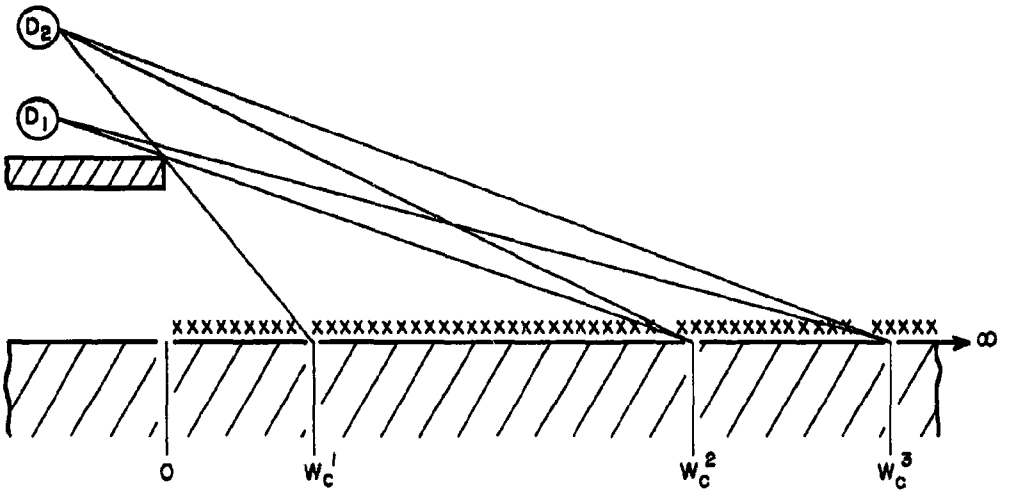

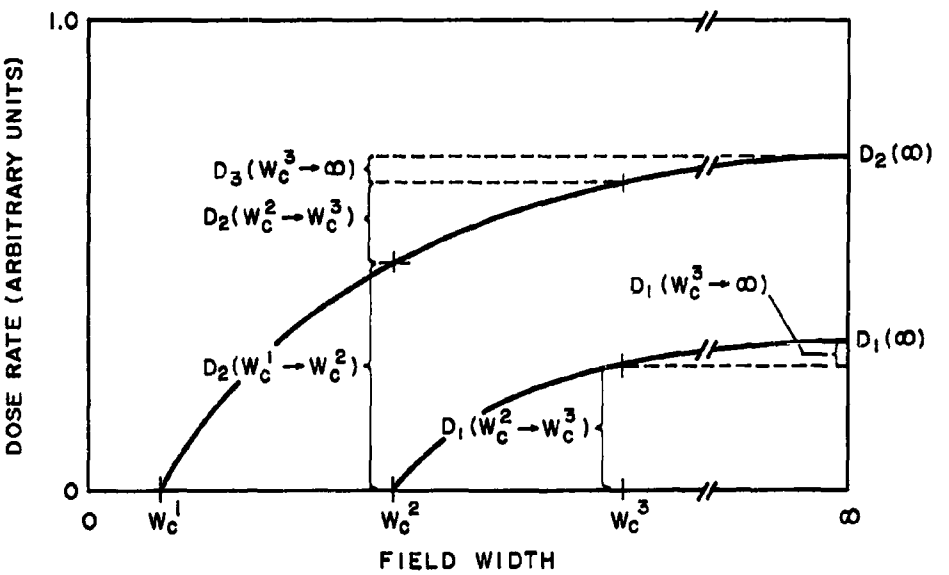

Figure 23. Geometry of Floor-Shadow Effect

TABLE 20

RATIO OF DOSE RATE AT CORNER POSITIONS TO CENTER 3 FOOT POSITIONS FOR LIMITED FIELDS OF CONTAMINATION WHERE $W_c/h \leq 10$

Position	Light-floored Structures	Heavy-floored Structures
Center (ft)		
3	1.0	1.0
6	1.4	1.7
9	1.7	2.5
Corner (ft)		
3	1.4	2.5
6	1.7	3.5
9	2.0	4.0

a contaminated field of width $W_c^2 - W_c^1$, which produces a dose rate of D_1, while detector No. 1 still sees no field and its dose rate is identically zero. When the field is extended beyond W_c^2 to W_c^3, both detectors exhibit a dose-rate increase. The incremental increase as seen by detector No. 1, however, is slightly larger than that seen by detector No. 2, since air attenuation will be greater for the upper detector position. When this argument is extended to infinity by an incremental increase in field width, the detector dose-rate increase of detector No. 2 from field width W_c^3 to infinity will be slightly lower than, but approximately the same as, detector position No. 1.

Now, by placing this argument in the same form as the NSSCP correction for far-field limited strips of contamination — the fraction of infinite-field radiation received by a detector from a given width strip of contamination — it may be easily seen that, for the same field width, the higher a detector from the structure floor, the greater its fraction of infinite-field dose rate. Quantitatively this argument is as follows:

$$D_1(0 \rightarrow \infty) = D_1(W_c^2 \rightarrow W_c^3) + D_1(W_c^3 \rightarrow \infty)$$

$$D_2(0 \rightarrow \infty) = D_2(W_c^1 \rightarrow W_c^2) + D_2(W_c^2 \rightarrow W_c^3) + D_2(W_c^3 \rightarrow \infty)$$

$$D_1(W_c^2 \rightarrow W_c^3) \approx D_2(W_c^2 \rightarrow W_c^3)$$

$$D_1(W_c^3 \rightarrow \infty) \approx D_2(W_c^3 \rightarrow \infty).$$

Thus, it follows that:

$$\frac{D_1(0 \rightarrow W_c^3)}{D_1(0 \rightarrow \infty)} << \frac{D_2(0 \rightarrow W_c^3)}{D_2(0 \rightarrow \infty)}.$$

All the experimental data obtained from the four model structures at both center and corner positions exhibit this phenomenon of increasing fraction of infinite field dose with increasing height above the floor. These data together with the fraction of infinite-field radiation computed from the tabular values of the NSSCP are presented in Tables 21 through 25. Since the NSSCP values over the range of height required vary at most a few per cent for wall thickness varying from 0 to 80 psf, these are shown as a range of values for wall thickness of 0 to 80 psf in the third column from the left in these tables.

Tables 21 through 25 also show that general agreement does exist between experimental data and computational methods. However, if the far-field limited fields of contamination were handled in a slightly different manner, even better agreement could be achieved; that is, if the effect of far-field limited strips of contamination were computed in two steps and the results added. This would first involve the computation of the radiation from the close-in areas ($W_c/h \leq 10$, $W_c \leq 300$ ft) of contamination using the methods presently proposed but with the measured values of the fraction of infinite-field dose rate as determined in this series of reports, and, secondly, the computation of radiation from the limited field of radiation beyond $W_c/h = 10$ or $W_c = 300$ feet. In the terminology of the NSSCP, the multiplicative

TABLE 21

FRACTION OF INFINITE-FIELD FIRST-FLOOR DOSE RATE FOR $W_c/h = 10$

Floor	Height Above Floor (ft)	NSSCP 0-80 psf Walls Thick Floors All Positions	Experimental				Height Above Floor (ft)	Experimental			
			0 psf Walls 20 psf Floors		20 psf Walls 20 psf Floors			20 psf Walls 80 psf Floors		80 psf Walls 80 psf Floors	
			Center	Corner	Center	Corner		Center	Corner	Center	Corner
1	3	.42 - .41	.32	.36	.30	.31	2-1/2	.23	.33	.28	.34
	6	.41 - .41	.46	.51	.48	.52	5	.41	.52	.48	.48
	9	.41 - .40	.55	.60	.57	.58	7-1/2	.54	.58	.56	.58
2	3	.41 - .39	.30	.36	.30	.34	2-1/2	.18	.27	.22	.31
	6	.41 - .38	.46	.51	.47	.48	5	.32	.39	.32	.41
	9	.40 - .38	.54	.58	.54	.56	7-1/2	.42	.49	.42	.47
3	3	.40 - .37	.30	.35	.30	.34	2-1/2	.16	.26	.21	.29
	6	.40 - .37	.44	.48	.47	.47	5	.30	.38	.30	.38
	9	.40 - .37	.53	.54	.52	.52	7-1/2	.41	.47	.40	.43
4	3	.39 - .36	.28	.33	.29	.33	2-1/2	.14	.24	.19	.25
	6	.39 - .36	.41	.44	.42	.43	5	.26	.34	.27	.34
	9	.39 - .36	.50	.51	.50	.48	7-1/2	.36	.44	.38	.40
5	3	.38 - .35	.25	.31	.25	.31	2-1/2	.11	.22	.18	.23
	6	.38 - .36	.39	.41	.38	.39	5	.23	.32	.23	.32
	9	.38 - .34	.48	.47	.48	.45	7-1/2	.33	.39	.33	.36
6	3	.38 - .33	.23	.29	.23	.28	2-1/2	.10	.18	.16	.22
	6	.37 - .33	.37	.37	.38	.37	5	.21	.29	.23	.29
	9	.37 - .33	.44	.43	.46	.39	7-1/2	.31	.36	.32	.33

TABLE 22

FRACTION OF INFINITE-FIELD FIRST-FLOOR DOSE RATE FOR $W_c/h = 25$

Floor	Height Above Floor (ft)	NSSCP 0-80 psf Walls Thick Floors All Positions	Experimental				Height Above Floor (ft)	Experimental			
			0 psf Walls 20 psf Floors		20 psf Walls 20 psf Floors			20 psf Walls 80 psf Floors		80 psf Walls 80 psf Floors	
			Center	Corner	Center	Corner		Center	Corner	Center	Corner
1	3	.59 - .56	.49	.53	.49	.51	2-1/2	.44	.57	.58	.56
	6	.57 - .57	.69	.71	.70	.71	5	.68	.72	.71	.75
	9	.56 - .56	.76	.81	.78	.79	7-1/2	.78	.82	.79	.75
2	3	.56 - .53	.46	.52	.49	.53	2-1/2	.36	.40	.39	.45
	6	.55 - .51	.62	.66	.63	.65	5	.49	.55	.48	.58
	9	.54 - .51	.72	.73	.70	.71	7-1/2	.59	.66	.57	.65
3	3	.53 - .49	.42	.46	.42	.45	2-1/2	.28	.36	.34	.39
	6	.53 - .49	.58	.59	.59	.58	5	.43	.48	.41	.48
	9	.52 - .48	.69	.66	.65	.64	7-1/2	.49	.60	.50	.54
4	3	.49 - .46	.36	.40	.38	.40	2-1/2	.23	.30	.27	.32
	6	.48 - .45	.52	.52	.50	.51	5	.34	.42	.33	.41
	9	.48 - .45	.58	.59	.59	.57	7-1/2	.43	.53	.47	.48
5	3	.46 - .42	.32	.38	.29	.36	2-1/2	.16	.26	.23	.28
	6	.46 - .42	.45	.47	.46	.47	5	.29	.37	.30	.37
	9	.45 - .41	.55	.55	.54	.51	7-1/2	.38	.47	.37	.42
6	3	.44 - .38	.29	.33	.27	.32	2-1/2	.13	.22	.21	.26
	6	.43 - .38	.43	.42	.45	.43	5	.27	.33	.29	.32
	9	.42 - .37	.50	.50	.52	.43	7-1/2	.36	.41	.36	.38

TABLE 23

FRACTION OF INFINITE-FIELD FIRST-FLOOR DOSE RATE FOR $W_o/h = 50$

Floor	Height Above Floor (ft)	NSSCP 0-80 psf Walls Thick Floors All Positions	Experimental				Height Above Floor (ft)	Experimental			
			0 psf Walls 20 psf Floors		20 psf Walls 20 psf Floors			20 psf Walls 80 psf Floors		80 psf Walls 80 psf Floors	
			Center	Corner	Center	Corner		Center	Corner	Center	Corner
1	3	.71 - .68	.63	.66	.67	.68	2-1/2	.74	.70	.78	.72
	6	.67 - .65	.84	.86	.83	.82	5	.85	.84	.87	.89
	9	.64 - .62	.90	.94	.89	.89	7-1/2	.89	.92	.92	.94
2	3	.63 - .60	.53	.60	.58	.60	2-1/2	.44	.46	.46	.52
	6	.62 - .58	.69	.71	.70	.71	5	.56	.62	.55	.64
	9	.59 - .57	.79	.78	.77	.78	7-1/2	.66	.72	.64	.71
3	3	.57 - .53	.47	.50	.46	.49	2-1/2	.31	.40	.37	.42
	6	.57 - .52	.64	.62	.64	.63	5	.45	.52	.45	.51
	9	.56 - .51	.73	.70	.70	.67	7-1/2	.53	.64	.54	.56
4	3	.51 - .48	.40	.43	.40	.42	2-1/2	.25	.32	.30	.34
	6	.50 - .47	.55	.54	.54	.54	5	.35	.43	.34	.44
	9	.49 - .46	.62	.60	.63	.59	7-1/2	.45	.55	.50	.49
5	3	.48 - .44	.33	.39	.31	.39	2-1/2	.18	.26	.24	.30
	6	.46 - .43	.47	.49	.47	.49	5	.30	.39	.31	.38
	9	.46 - .42	.57	.56	.54	.53	7-1/2	.39	.48	.38	.44
6	3	.45 - .42	.31	.34	.29	.34	2-1/2	.14	.22	.22	.27
	6	.44 - .38	.43	.44	.47	.44	5	.28	.34	.30	.33
	9	.43 - .38	.52	.51	.52	.45	7-1/2	.36	.43	.36	.40

TABLE 24

FRACTION OF INFINITE-FIELD FIRST-FLOOR DOSE RATE FOR $W_o/h = 75$

Floor	Height Above Floor (ft)	NSSCP 0-80 psf Walls Thick Floors All Positions	Experimental				Height Above Floor (ft)	Experimental			
			0 psf Walls 20 psf Floors		20 psf Walls 20 psf Floors			20 psf Walls 80 psf Floors		80 psf Walls 80 psf Floors	
			Center	Corner	Center	Corner		Center	Corner	Center	Corner
1	3	.78 - .76	.75	.78	.75	.76	2-1/2	.84	.82	.86	.82
	6	.74 - .72	.93	.95	.90	.88	5	.94	.90	.97	.92
	9	.70 - .69	.95	.97	.96	.93	7-1/2	.94	.96	.97	.95
2	3	.67 - .63	.55	.62	.60	.62	2-1/2	.47	.48	.49	.54
	6	.65 - .60	.71	.73	.73	.74	5	.58	.64	.56	.65
	9	.61 - .58	.79	.80	.79	.78	7-1/2	.67	.74	.68	.72
3	3	.58 - .54	.49	.62	.48	.61	2-1/2	.33	.41	.39	.43
	6	.57 - .53	.65	.62	.65	.63	5	.47	.52	.46	.52
	9	.57 - .52	.74	.71	.72	.67	7-1/2	.54	.64	.55	.57
4	3	.52 - .49	.41	.43	.41	.43	2-1/2	.26	.32	.30	.34
	6	.51 - .48	.55	.54	.56	.54	5	.41	.44	.34	.44
	9	.50 - .47	.62	.61	.63	.59	7-1/2	.47	.55	.51	.50
5	3	.48 - .44	.34	.39	.31	.40	2-1/2	.19	.27	.25	.30
	6	.47 - .43	.47	.49	.48	.50	5	.30	.39	.33	.39
	9	.46 - .42	.57	.56	.54	.53	7-1/2	.40	.48	.39	.45
6	3	.45 - .39	.32	.35	.29	.34	2-1/2	.14	.22	.22	.27
	6	.44 - .39	.43	.44	.48	.44	5	.28	.34	.30	.34
	9	.43 - .38	.52	.52	.52	.46	7-1/2	.36	.43	.37	.40

TABLE 25

FRACTION OF INFINITE-FIELD FIRST-FLOOR DOSE RATE FOR $W_o/h = 100$

Floor	Height Above Floor (ft)	NSSCP 0-80 psf Walls Thick Floors All Positions	Experimental				Height Above Floor (ft)	Experimental			
			0 psf Walls 20 psf Walls		20 psf Walls 20 psf Floors			20 psf Walls 80 psf Floors		80 psf Walls 80 psf Floors	
			Center	Corner	Center	Corner		Center	Corner	Center	Corner
1	3	.83 - .80	.80	.81	.81	.81	2-1/2	.91	.88	.91	.86
	6	.77 - .76	.98	.98	.93	.96	5	1.0	.95	1.0	.95
	9	.74 - .72	.99	.98	.98	.94	7-1/2	.97	.99	1.0	.96
2	3	.69 - .65	.57	.62	.60	.64	2-1/2	.48	.49	.51	.55
	6	.66 - .61	.72	.74	.74	.77	5	.59	.64	.56	.66
	9	.63 - .60	.79	.81	.80	.79	7-1/2	.68	.76	.69	.72
3	3	.59 - .55	.50	.52	.49	.51	2-1/2	.33	.42	.39	.44
	6	.58 - .54	.66	.63	.65	.63	5	.47	.52	.47	.52
	9	.57 - .52	.74	.71	.72	.68	7-1/2	.56	.64	.55	.57
4	3	.52 - .49	.41	.43	.42	.44	2-1/2	.26	.33	.31	.35
	6	.51 - .48	.55	.55	.56	.56	5	.38	.45	.35	.44
	9	.50 - .47	.62	.61	.63	.60	7-1/2	.47	.55	.51	.50
5	3	.48 - .44	.34	.39	.32	.40	2-1/2	.19	.27	.26	.31
	6	.47 - .43	.47	.49	.48	.50	5	.30	.39	.34	.39
	9	.46 - .42	.57	.56	.54	.53	7-1/2	.40	.48	.39	.45
6	3	.45 - .39	.33	.35	.30	.34	2-1/2	.15	.22	.22	.27
	6	.44 - .39	.43	.45	.48	.44	5	.28	.34	.30	.34
	9	.43 - .38	.52	.52	.52	.47	7-1/2	.36	.43	.37	.40

factor for far-field limited strips of contamination would then become (see Eqs. (5) and (6), and Table 12):

Case 2: If $2 < \tan\Theta = W_c/h \leq 10$, and $W_c > 300$ ft, or if $\tan\Theta = W_c/h > 10$.

then,

$$M_c = M_1(W_c^*/h) + \frac{M_h(X_e, h)}{M_h(X_e = 0, h)} \left[M_h(X_e = 0, h = \sqrt{h^2 + W_c^{*2}}) - M_h(X_e = 0, h = \sqrt{h^2 + W_c^2}) \right] \quad (14)$$

where

h = detector height

W_c^* = 10 h or 300 feet, whichever is the least distance

W_c = outer width of the contaminated field.

This equation is evaluated in Tables 26 to 29 for all structures for values of W_c/h extending from 10 to 25, 25 to 50, 50 to 75, and 75 to 100. These tables illustrate that excellent agreement exists between this method of computation and the experimental data.

TABLE 26

FRACTION OF INFINITE-FIELD FIRST-FLOOR DOSE INTRODUCED BY A FIELD EXTENDING FROM W_o/h = 10 TO W_o/h = 25

Floor	Height Above Floor (ft)	NSSCP 0-80 psf Walls Thick Floors All Positions	Experimental				Height Above Floor (ft)	Experimental			
			0 psf Walls 20 psf Floors		20 psf Walls 20 psf Floors			20 psf Walls 80 psf Floors		80 psf Walls 80 psf Floors	
			Center	Corner	Center	Corner		Center	Corner	Center	Corner
1	3	.17 - .17	.17	.17	.19	.22	2-1/2	.21	.24	.30	.22
	6	.16 - .16	.23	.20	.22	.19	5	.27	.20	.23	.28
	9	.15 - .15	.21	.21	.21	.21	7-1/2	.24	.24	.23	.17
2	3	.14 - .14	.16	.16	.19	.19	2-1/2	.18	.13	.17	.14
	6	.14 - .13	.16	.14	.16	.17	5	.17	.16	.16	.17
	9	.14 - .13	.18	.15	.16	.15	7-1/2	.17	.17	.15	.18
3	3	.13 - .12	.12	.11	.12	.11	2-1/2	.12	.10	.13	.10
	6	.13 - .12	.14	.11	.12	.11	5	.13	.10	.11	.10
	9	.12 - .11	.16	.11	.11	.12	7-1/2	.08	.13	.10	.11
4	3	.10 - .10	.C8	.07	.09	.07	2-1/2	.09	.06	.08	.07
	6	.11 - .09	.11	.08	.08	.09	5	.08	.08	.06	.07
	9	.11 - .09	.08	.08	.09	.09	7-1/2	.07	.09	.09	.08
5	3	.08 - .07	.07	.07	.04	.05	2-1/2	.05	.04	.05	.05
	6	.08 - .07	.06	.06	.07	.08	5	.06	.05	.07	.05
	9	.07 - .07	.07	.08	.06	.06	7-1/2	.05	.08	.04	.06
6	3	.06 - .05	.06	.04	.04	.04	2-1/2	.03	.04	.05	.04
	6	.06 - .05	.06	.05	.07	.06	5	.06	.04	.06	.03
	9	.05 - .04	.06	.07	.06	.04	7-1/2	.04	.05	.03	.05

TABLE 27

FRACTION OF INFINITE-FIELD FIRST-FLOOR DOSE INTRODUCED BY A FIELD EXTENDING FROM W_o/h = 25 TO W_o/h = 50

Floor	Height Above Floor (ft)	NSSCP 0-80 psf Walls Thick Floors All Positions	Experimental				Height Above Floor (ft)	Experimental			
			0 psf Walls 20 psf Floors		20 psf Walls 20 psf Floors			20 psf Walls 80 psf Floors		80 psf Walls 80 psf Floors	
			Center	Corner	Center	Corner		Center	Corner	Center	Corner
1	3	.12 - .10	.14	.13	.18	.17	2-1/2	.30	.13	.20	.16
	6	.10 - .08	.15	.15	.13	.14	5	.15	.12	.16	.14
	9	.08 - .07	.14	.13	.11	.10	7-1/2	.11	.10	.13	.19
2	3	.08 - .06	.07	.08	.09	.07	2-1/2	.08	.06	.07	.07
	6	.07 - .07	.07	.06	.07	.06	5	.07	.07	.07	.06
	9	.06 - .06	.07	.05	.07	.07	7-1/2	.07	.06	.07	.06
3	3	.04 - .04	.05	.04	.04	.04	2-1/2	.03	.04	.03	.03
	6	.04 - .03	.06	.03	.05	.05	5	.02	.04	.04	.03
	9	.04 - .03	.04	.05	.05	.03	7-1/2	.04	.04	.04	.02
4	3	.02 - .02	.04	.03	.02	.02	2-1/2	.02	.02	.03	.02
	6	.02 - .02	.03	.02	.04	.03	5	.01	.01	.01	.03
	9	.01 - .01	.04	.01	.04	.02	7-1/2	.02	.02	.03	.01
5	3	.02 - .02	.01	.01	.02	.03	2-1/2	.02	.00	.01	.02
	6	.00 - .01	.02	.02	.02	.02	5	.01	.02	.01	.01
	9	.01 - .01	.02	.01	.00	.02	7-1/2	.01	.01	.01	.02
6	3	.01 - .04	.02	.01	.02	.02	2-1/2	.01	.00	.01	.01
	6	.01 - .00	.00	.02	.02	.01	5	.01	.01	.01	.01
	9	.01 - .01	.02	.01	.00	.02	7-1/2	.01	.02	.01	.02

TABLE 28

FRACTION OF INFINITE-FIELD FIRST-FLOOR DOSE INTRODUCED BY A FIELD EXTENDING FROM $W_c/h = 50$ TO $W_c/h = 75$

Floor	Height Above Floor (ft)	NSSCP 0-80 psf Walls Thick Floors All Positions	Experimental				Height Above Floor (ft)	Experimental			
			0 psf Walls 20 psf Floors		20 psf Walls 20 psf Floors			20 psf Walls 80 psf Floors		80 psf Walls 80 psf Floors	
			Center	Corner	Center	Corner		Center	Corner	Center	Corner
1	3	.07 - .08	.12	.12	.08	.08	2-1/2	.10	.12	.08	.10
	6	.07 - .07	.09	.09	.07	.06	5	.09	.06	.10	.03
	9	.06 - .07	.05	.03	.07	.04	7-1/2	.05	.04	.05	.01
2	3	.04 - .03	.02	.02	.02	.02	2-1/2	.03	.02	.03	.02
	6	.03 - .02	.02	.02	.03	.03	5	.02	.02	.01	.01
	9	.02 - .01	.00	.02	.02	.00	7-1/2	.01	.02	.04	.01
3	3	.01 - .01	.02	.02	.02	.02	2-1/2	.02	.01	.02	.01
	6	.00 - .01	.01	.00	.01	.03	5	.02	.00	.01	.01
	9	.01 - .01	.01	.01	.02	.00	7-1/2	.01	.00	.01	.01
4	3	.01 - .01	.01	.00	.01	.01	2-1/2	.01	.00	.00	.00
	6	.01 - .01	.00	.00	.02	.00	5	.06	.01	.00	.00
	9	.01 - .01	.00	.01	.00	.00	7-1/2	.02	.00	.01	.01
5	3	.00 - .00	.01	.00	.00	.01	2-1/2	.01	.01	.01	.00
	6	.01 - .00	.00	.00	.01	.01	5	.00	.00	.02	.01
	9	.00 - .00	.00	.00	.00	.00	7-1/2	.01	.00	.01	.01
6	3	.00 - .03	.01	.01	.00	.00	2-1/2	.00	.00	.00	.00
	6	.00 - .01	.00	.00	.01	.00	5	.00	.00	.00	.01
	9	.00 - .00	.00	.01	.00	.01	7-1/2	.00	.00	.01	.00

TABLE 29

FRACTION OF INFINITE-FIELD FIRST-FLOOR DOSE INTRODUCED BY A FIELD EXTENDING FROM $W_c/h = 75$ TO $W_c/h = 100$

Floor	Height Above Floor (ft)	NSSCP 0-80 psf Walls Thick Floors All Positions	Experimental				Height Above Floor (ft)	Experimental			
			0 psf Walls 20 psf Floors		20 psf Walls 20 psf Floors			20 psf Walls 80 psf Floors		80 psf Walls 80 psf Floors	
			Center	Corner	Center	Corner		Center	Corner	Center	Corner
1	3	.05 - .04	.05	.03	.06	.05	2-1/2	.07	.08	.05	.04
	6	.03 - .04	.05	.03	.03	.08	5	.06	.05	.03	.03
	9	.04 - .03	.04	.01	.02	.01	7-1/2	.03	.03	.03	.01
2	3	.02 - .02	.02	.00	.00	.02	2-1/2	.01	.01	.02	.01
	6	.01 - .01	.01	.01	.01	.04	5	.01	.00	.00	.01
	9	.02 - .02	.00	.01	.01	.01	7-1/2	.01	.01	.01	.00
3	3	.01 - .01	.01	.00	.01	.00	2-1/2	.00	.01	.00	.01
	6	.01 - .01	.00	.01	.00	.00	5	.00	.00	.01	.00
	9	.00 - .00	.00	.00	.00	.01	7-1/2	.02	.00	.00	.00
4	3	.00 - .00	.00	.00	.01	.01	2-1/2	.00	.01	.01	.01
	6	.00 - .00	.00	.01	.00	.01	5	.03	.01	.01	.00
	9	.00 - .00	.00	.00	.00	.01	7-1/2	.00	.00	.00	.00
5	3	.00 - .00	.00	.00	.01	.00	2-1/2	.00	.00	.01	.01
	6	.00 - .00	.00	.00	.00	.00	5	.00	.00	.01	.00
	9	.00 - .00	.00	.00	.00	.00	7-1/2	.00	.00	.00	.00
6	3	.00 - .00	.01	.00	.01	.00	2-1/2	.01	.00	.00	.00
	6	.00 - .00	.00	.01	.00	.00	5	.00	.00	.00	.00
	9	.00 - .00	.00	.01	.00	.01	7-1/2	.00	.00	.00	.00

CHAPTER 5

ANALYSIS OF BELOW-GROUND DATA

One of the major problem areas in the modeling of structures is the inability to increase the density of the ground by the proper scale factor. Hence, geometries depending upon the ground for a major portion of their shielding effectiveness must be interpreted in the light of the increased ability of photons to penetrate the ground in the scale model as opposed to the full-scale structure. Thus, the dose rate detected in the basement of a model structure is actually the sum of the radiation penetrating the ground plus that scattered into the basement by the structure above it. Since the quantity of interest is, in general, the radiation scattered to the basement by the structure above it, two measurements must be performed. First, the total of building scatter plus ground-penetration radiation must be measured, and, secondly, the amount of ground penetration must be determined. Thus, by subtracting the latter from the former, estimates of the amount of radiation scattered to the basement detectors by the structure may be made.

In the previous series of reports,[4-7] the total contribution, including both ground-penetration and structure-scatter radiation, has been reported for the below-ground positions. To determine the effect of ground-penetration radiation on these results, an experiment was run first to measure the distance of source contamination from the building face at which ground penetration is a significant factor and, secondly, to determine the magnitude of the ground-penetration component for each experimental area of simulated contamination.

The inner 4-foot rectangular annulus of contamination surrounding the structure was simulated utilizing point sources of cobalt in a square array placed on 6-inch centers. Thus, the measurement of ground penetration was made by placing a strong source shielded in all directions except those required for ground penetration by a 4-inch thick lead shield at each point in the array and measuring the dose rate in the basement area. Figure 24a illustrates the placement of the source storage shield (to the left of the picture) and the directional ground penetration shield in preparation for an experiment. Figure 24b presents a close-up of the underside of the directional shield.

Figure 24a. Storage Shield and Directional Ground-Penetration Shield

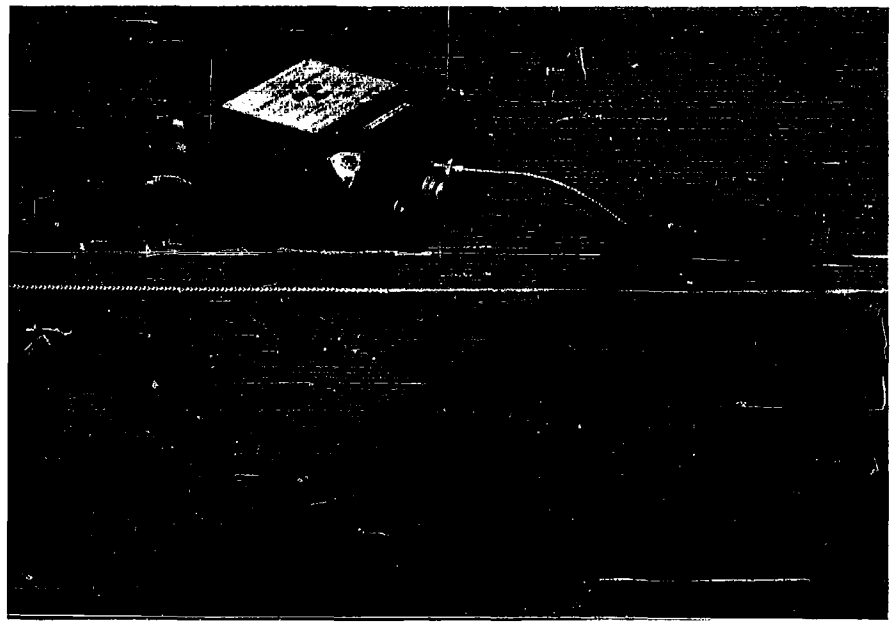

Figure 24b. Underside of Directional Ground-Penetration Shield

To determine the extent of the simulated area providing significant ground penetration, Experimental Area No. 1 was divided into eight rectangular strips parallel with the building face, and ground penetration experiments were performed upon each. Each strip was 2 feet long and 6 inches wide; thus, strips 1A1, 1A2, 1A3, and 1A4 composed Experimental Area 1A (see Figure 25); while strips 1B5

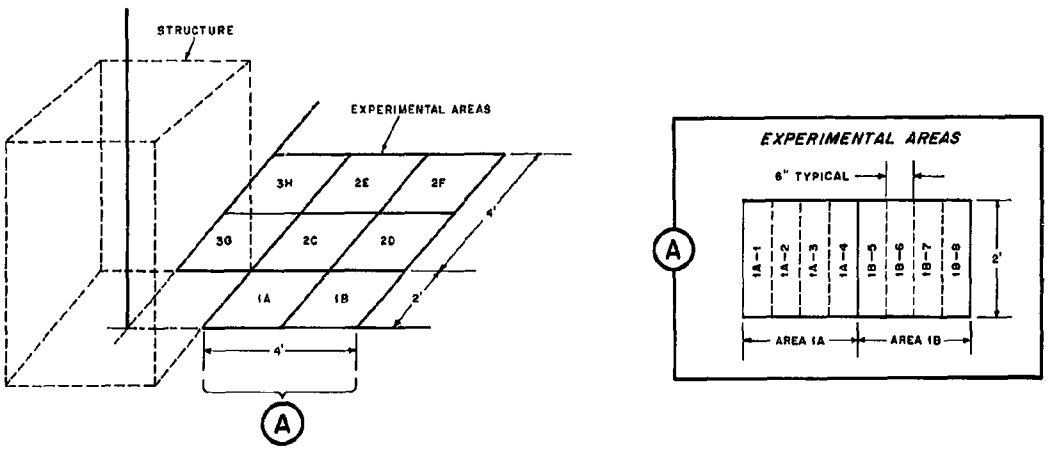

Figure 25. Diagram of Ground-Penetration Experimental Areas

1B6, 1B7, and 1B8 composed Experimental Area 1B. The data obtained from this series of experiments for the various detector positions are presented in Table 30. (Data for more than one run are reported for Areas 1A1 and 1A2.) This table shows that, in general, over 90% of the radiation received by a detector in the basement area from radiation penetrating the ground arrives from sources located in the inner rectangular annulus of 2 foot width . Thus, the data requiring correction for ground penetration are those obtained from simulated contamination in Areas 1A, 2C, and 3G.

TABLE 30

EXPERIMENTAL BASEMENT DATA GROUND PENETRATION
(mr/hr normalized to 1 curie/ft^2)

Detector Position	Dose Rate							
	Source Distance from Outer Face of Structure (inches)							
	3	9	15	21	27	33	39	45
	Simulated Contaminated Area							
	1A1	1A2	1A3	1A4	1B5	1B6	1B7	1B8
OA3*	82.1/93	3.0/2.5	0.99	.42	.33	.17	.15	.10
9	117/107	2.9/3.02	1.28	.58	.31	.15	.12	.09
15	55.4/55	3.1/3.1	1.48	.74	.33	.14	.095	.05
OB3	276	8.27/7.75	1.78	.70	.36	.13	.11	.07
9	42.0/46.5	10.9	4.44	2.18	.71	.19	.095	.06
15	17.2/17.2/17.6	12.9	9.77	4.4	1.02	.22	.095	.06
OC3	7.3/8.89/8.46	1.09/1.20	.69	.38	.33	.19	.13	.09
9	7.1/6.17/5.95	1.86/1.72	.99	.58	.31	.15	.10	.07
15	5.7/3.10/4.65	2.38/2.15	1.58	.80	.31	.13	.085	.05
OD3	14.5/23.3	1.81/1.29	.69	.38	.36	.19	.17	.11
9	45.8/37.9/42.4	1.55/1.38	.79	.42	.31	.16	.13	.09
15	22.9/20.3/26.9	1.81/1.55	.84	.48	.29	.19	.11	.08
OE1	32.5/37.9/41.4	3.72/3.44	1.18	.64	.50	.34	.27	.20
3	231	4.03/3.62	1.28	.64	.48	.24	.21	.19
6	169	4.45/4.14	1.48	.74	.43	.22	.18	.15
9	97.4/93.0	5.17/4.6	1.68	.93	.48	.19	.16	.13
12	66.9/67.2	5.17/4.65	1.91	1.09	.48	.19	.14	.11
15	45.8/44.8	5.17/4.91	2.27	1.31	.57	.20	.13	.09
18	30.6/31.0/35.2	5.17/5.0	2.68	1.98	.62	.19	.12	.07

*Position OA3 refers to a detector located at Position A in the basement a distance of 3 inches below the ground-air interface.

During the actual installation of two of the four scale models, a small amount of misalignment occurred between the inner face of the basement and the inner face of the structure. Thus, as the source areas were located from the outer building face, a total of three ground-penetration experiments were required for each simulated source area—one for the correctly aligned 20 psf and 20-80 psf building, one for the zero thickness wall building, and one for the 80 psf thickness building. The data resulting from these experiments, together with the data previously reported[4-7] containing both ground penetration and building scatter, are presented in Tables 31-34. In these tables the column marked "Difference" is thus an estimate of the radiation scattered to the basement area by the structure itself.

TABLE 31

BASEMENT DATA—20 psf BUILDING
(Normalized to r/hr from 1 curie/ft^2 source density)

Position	Dose Rate								
	Experiment 1A			Experiment 2C			Experiment 3G		
	Total	Ground Penetration	Difference	Total	Ground Penetration	Difference	Total	Ground Penetration	Difference
OA3	.21	.092	.121	.10	.0018	.098	.27	.013	.252
9	.22	.069	.151	.077	.0017	.075	.16	.012	.141
15	.18	.043	.140	.059	.0018	.057	.11	.013	.099
OB3	.75	.19	.565	.25	.013	.238	.60	.34	.258
9	.29	.058	.231	.12	.013	.105	.30	.052	.244
15	.20	.050	.150	.090	.020	.070	.17	.045	.128
OC3	.18	.0076	.167	.056	.0013	.055	.092	.019	.073
9	.12	.0086	.113	.046	.0014	.045	.17	.058	.110
15	.091	.0086	.082	.036	.0013	.037	.16	.038	.126
OD3	.14	.021	.116	.051	.0021	.049	.052	.012	.070
9	.12	.025	.097	.051	.0030	.048	.13	.039	.094
15	.12	.017	.103	.051	.0021	.049	.13	.043	.090
OE1	.27	.040	.233	.095	.0052	.090	.14	.020	.118
3	.33	.13	.201	.10	.006*	.096	.21	.099	.111
6	.33	.083	.251	.11	.0066	.103	.36	.070*	.28
9	.27	.059	.214	.11	.0046	.103	.32	.068	.253
12	.24	.043	.200	.095	.0040	.091	.27	.050	.215
15	.21	.032	.181	.085	.0039	.081	.22	.040	.179
18	.18	.028	.147	.072	.0041	.068	.17	.032	.141

*Estimated

TABLE 32

BASEMENT DATA—80 psf BUILDING
(Normalized to r/hr from 1 curie/ft^2 source density)

Position	Dose Rate								
	Experiment 1A			Experiment 2C			Experiment 3G		
	Total	Ground Penetration	Difference	Total	Ground Penetration	Difference	Total	Ground Penetration	Difference
OA3	.130	.035*	.095	.015	.0015	.013	.092	.0070*	.085
9	.089	.025	.064	.014	.0014	.013	.066	.0062	.059
15	.073	.016	.057	.015	.0016	.013	.049	.0078	.041
OB3	.310	.188	.122	.140	.0052	.135	.300	.209	.091
9	.130	.026	.104	.060	.0077	.052	.170	.026	.145
15	.110	.033	.077	.054	.017	.037	.110	.023	.087
OC3	.030	.0023	.028	.0053	.0010	.0043	.019	.010	.009
9	.038	.0028	.035	.0056	.0010	.0046	.083	.022	.061
15	.029	.0032	.026	.0071	.0010	.0061	.075	.013	.062
OD3	.032	.010	.022	.0040	.0016	.0024	.015	.0071	.008
9	.032	.0074	.025	.0048	.0017	.0029	.060	.016	.044
15	.038	.0051	.033	.0079	.0015	.0054	.064	.0087	.055
OE1	.041	.022	.019	.005	.0040	.0010	.025	.011	.014
3	.200	.050	.140	.019	.0044	.015	.099	.037	.062
6	.140	.034	.106	.023	.0032	.020	.120	.028	.092
9	.130	.023	.107	.025	.0028	.022	.130	.023	.110
12	.110	.018	.092	.025	.0028	.022	.100	.017	.083
15	.082	.014	.068	.022	.0028	.019	.084	.014	.070
18	.070	.012	.058	.018	.0031	.015	.072	.011	.061

*Estimated

TABLE 33

BASEMENT DATA--0 psf Walls, 20 psf Floors
(Normalized to r/hr from 1 curie/ft^2 source density)

Position	Dose Rate								
	Experiment 1A			Experiment 2C			Experiment 3G		
	Total	Ground Penetration	Difference	Total	Ground Penetration	Difference	Total	Ground Penetration	Difference
OA3	.163	.092	.071	.039	.0029	.036	.102	.096	.006
9	.186	.117	.069	.028	.0022	.024	.070	.040	.030
15	.122	.061	.061	.023	.0024	.021	.051	.028	.023
OB3	.452	.287	.165	.079	.023	.056	.380*	.302	.078
9	.159	.062	.097	.049	.014	.035	.138	.129*	.009
15	.112	.044	.068	.046	.024	.022	.080	.070	.010
OC3	.066	.0091	.057	.034	.0010	.033	.070	.039	.031
9	.056	.0094	.046	.028	.0011	.027	.118	.115*	.003
15	.047	.0091	.038	.023	.0012	.022	.102	.100*	.002
OD3	.089	.022	.067	.039	.0019	.037	.059	.040	.019
9	.097	.045	.052	.034	.0024	.032	.089	.085	.004
15	.074	.026	.048	.023	.0020	.026	.078	.075*	.003
OE1	.162	.041	.121	.066	.0041	.062	.097	.029	.068
3	.300	.237	.063	.060	.0052	.055	.235	.125	.110
6	.259	.176	.083	.051	.0048	.046	.235	.155	.070
9	.186	.103	.083	.044	.0046	.039	.189	.139	.050
12	.146	.075	.071	.039	.0044	.035	.162	.129*	.033
15	.122	.054	.068	.034	.0039	.030	.138	.114	.024
18	.103	.043	.060	.030	.0041	.026	.110	.085	.025

*Estimated

TABLE 34

BASEMENT DATA--20 psf Walls, 80 psf Floors
(Normalized to r/hr from a 1 curie/ft^2 source density)

Position	Dose Rate								
	Experiment 1A			Experiment 2C			Experiment 3G		
	Total	Ground Penetration	Difference	Total	Ground Penetration	Difference	Total	Ground Penetration	Difference
OA3	.087	.092	—	.014	.0018	.012	.055	.013	.042
9	.085	.069	.016	.014	.0017	.012	.048	.012	.036
15	.074	.043	.031	.013	.0018	.011	.038	.013	.025
OB3	.210	.19	.020	.110	.013	.097	.220	.34	—
9	.130	.058	.072	.058	.013	.045	.130	.052	.078
15	.086	.050	.036	.046	.020	.026	.086	.045	.041
OC3	.047	.0076	.039	.0066	.0013	.0053	.018	.019	—
9	.045	.0086	.036	.0079	.0014	.0065	.038	.058	—
15	.037	.0086	.028	.0079	.0013	.0066	.033	.038	—
OD3	.028	.021	.007	.0043	.0021	.0022	.014	.012	.002
9	.035	.025	.010	.0066	.0030	.0036	.027	.039	—
15	.037	.017	.020	.0073	.0021	.0052	.023	.043	—
OE1	.047	.040	.007	.0055	.0052	.0003	.021	.020	.001
3	.160	.130	.030	.017	.006*	.011	.084	.099	—
6	.130	.083	.047	.017	.0066	.010	.073	.080*	—
9	.120	.059	.061	.019	.0048	.014	.069	.068	.001
12	.100	.043	.057	.019	.0040	.015	.061	.050	.011
15	.089	.032	.057	.018	.0039	.014	.052	.040	.012
18	.073	.028	.045	.017	.0041	.013	.048	.032	.016

*Estimated

CONVERSION OF MODEL TO FULL-SCALE DATA

To properly scale a full-sized building to a model for radiation testing, the densities of all materials must be increased by the scaling factor in a practical way. It is difficult, if not impossible, to increase the density of the atmosphere to the extent required for perfect scaling. Hence, results obtained from modeling tests must be treated analytically to correct for this density difference artificially. The method used to correct for the discrepancy in perfect modeling of the atmosphere has been previously described in Chapter 3 and, hence, will not be repeated here. However, some ambiguity does exist as to the proper height to choose in making this correction. Radiations reaching a detector located in a basement by scattering from the building above the basement predominantly traverse paths from the location of contamination to the outer wall and ceiling of the first floor of the structure, then scatter to the basement. Thus, it is appropriate to use the model to full-scale correction factor computed for the mid-height of the first floor for all basement results. This factor is shown in Table 35 for the mid-height of the first floor.

TABLE 35

RATIO OF FULL-SCALE TO MODEL DATA
MID-FLOOR HEIGHT, FLOOR 1

Source Area (See Figure 6)	Ratio	Source Area (See Figure 6)	Ratio
1A, 2C, 3G	0.98	16, 17, 18	0.69
1B, 2D, 2E, 2F, 3H	0.96	19, 20, 21	0.63
4, 5, 6	0.91	22, 23, 24	0.57
7, 8, 9	0.85	25, 26	0.69
10, 11, 12	0.80	27	0.48
13, 14, 15	0.75	Far field*	5.50*

*Ratio is to be multiplied by model results obtained from Area 27.

Estimates of far-field radiation; that is, radiation arising from contamination beyond the outer annulus of the contamination simulated, may be made in a somewhat similar manner. The exact method of computation is to compute a ratio of far-field radiation to that received from the outer annulus simulated. This computation has been presented in Chapter 4, and, hence, will not be repeated here. Note, however, that the argument about the proper choice of height discussed above holds as well for infinite-field sources, and, hence, this estimate of far-field radiation is also based

upon the mid-height of the first floor. The resulting ratio of full-scale far-field radiation to that received from the outer annulus of simulated contamination surrounding the model is presented in Table 35 (p. 78).

The results obtained from the model structure must also be corrected for source anisotropy and the gamma-ray attenuation offered by the inner lengths of the source tubing when the source is in its outermost positions. This correction has been evaluated in Chapter 3 and is presented there as a simple multiplicative factor (see Table 3). This factor unfortunately varies over the height of the first floor (12 inches) and, hence, some ambiguity exists as to the proper selection of correction factor to be used. However, the choice of using the correction factor for the mid-height of the first floor may be defended since the majority of the radiation reaching a detector located in the basement has previously been scattered by the walls or ceiling of the first floor.

COMPARISON OF DATA

The purpose of the previous section has been to provide the analytical tools required to convert the data obtained from model experiments to those which would be obtained from a similar full-scale experiment. Thus, Table 35 presents the ratio of full-scale to model dose rate for any annulus of interest and the ratio of expected full-scale, far-field dose to that obtained from the outer annulus of simulated contamination used in the model experiments.

The data obtained from the center and corner positions have been corrected for the difference in air attenuation between the model and the full-scale building and normalized to the source density (2.01 millicuries/ft^2) that would produce 1.0 r/hr 3 feet above an infinite smooth plane. These normalized data are plotted in cumulative form in Figures 26 through 29 as a function of the width of the contaminated field divided by the mid-height of the first floor for both center and corner positions for each of the four buildings of interest. The presentation of these data on separate graphs for each structure and position (center or corner) rather than on a common graph is dictated by the difference in the effect of the "in-and-down" scattering provided by each building type. It is of interest to present these data in the form used by the National Shelter Survey Computer Program, that is, as the fraction of infinite-field dosage created by a rectangular limited field of contamination surrounding the structure. To compute this fraction, the ground dose from a limited field of contamination for any detector location is divided by the infinite-field value for the source

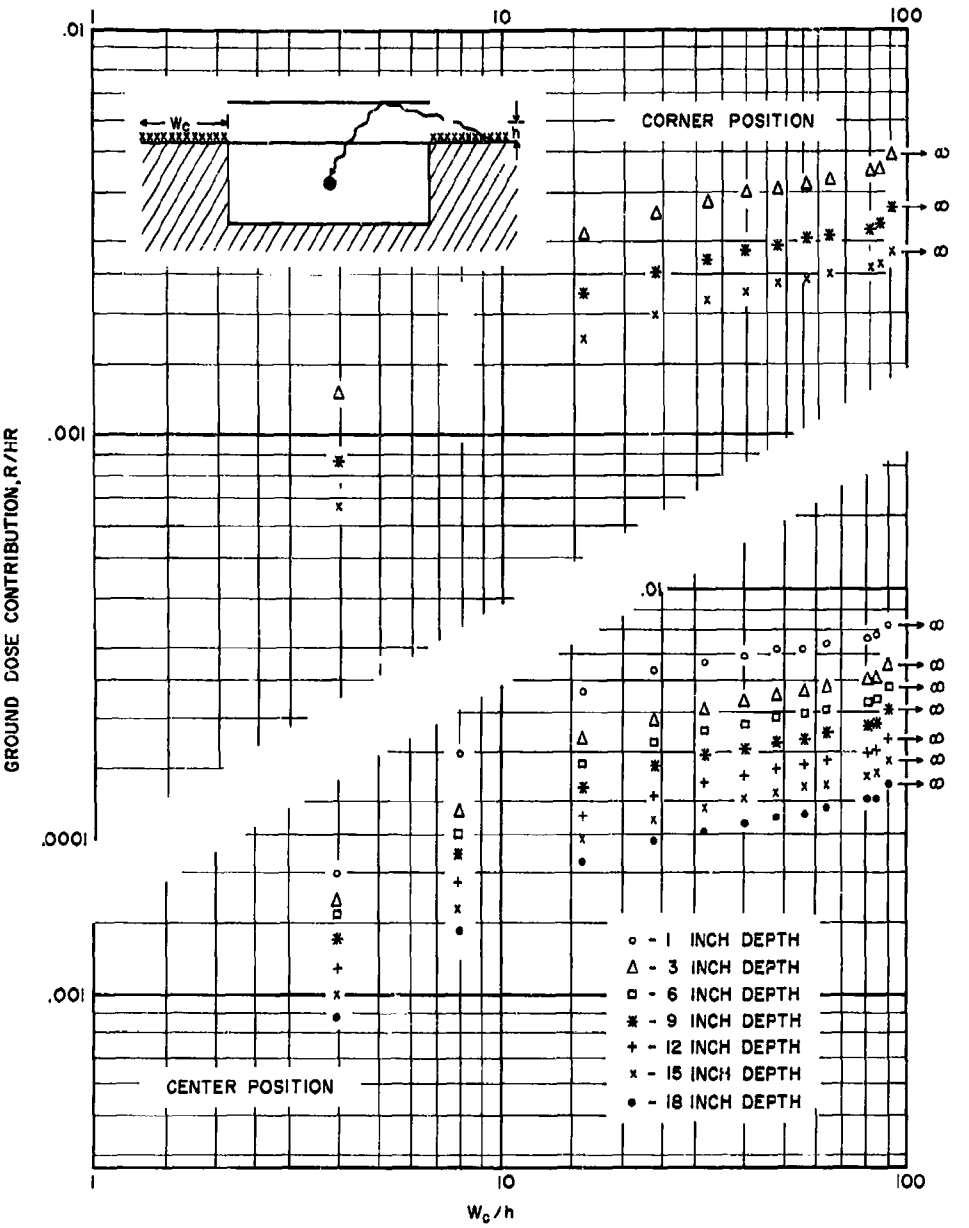

Figure 26. Ground-Dose Contribution in the Basement of Building with 0 psf Walls and 20 psf Floors

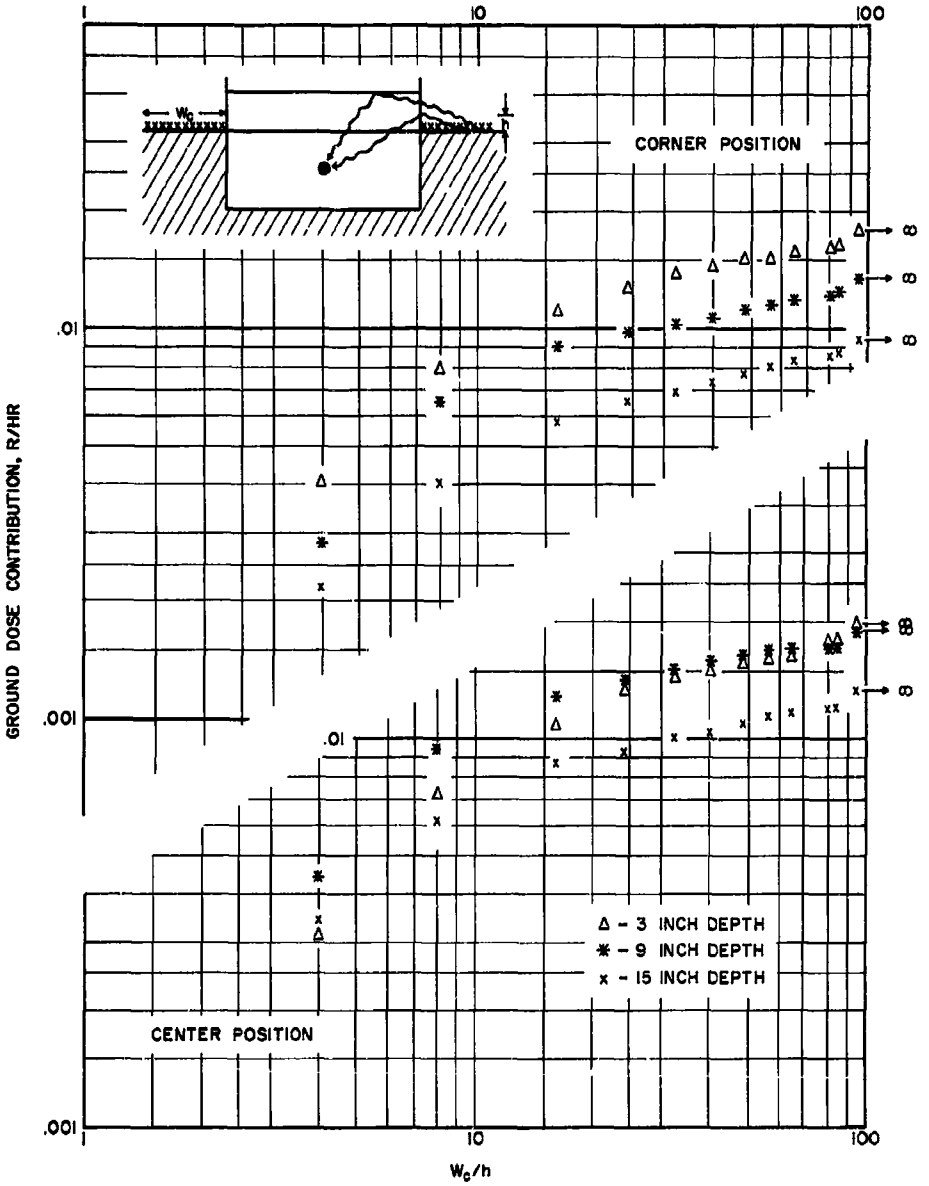

Figure 27. Ground-Dose Contribution in the Basement of Building with 20 psf Walls and Floors

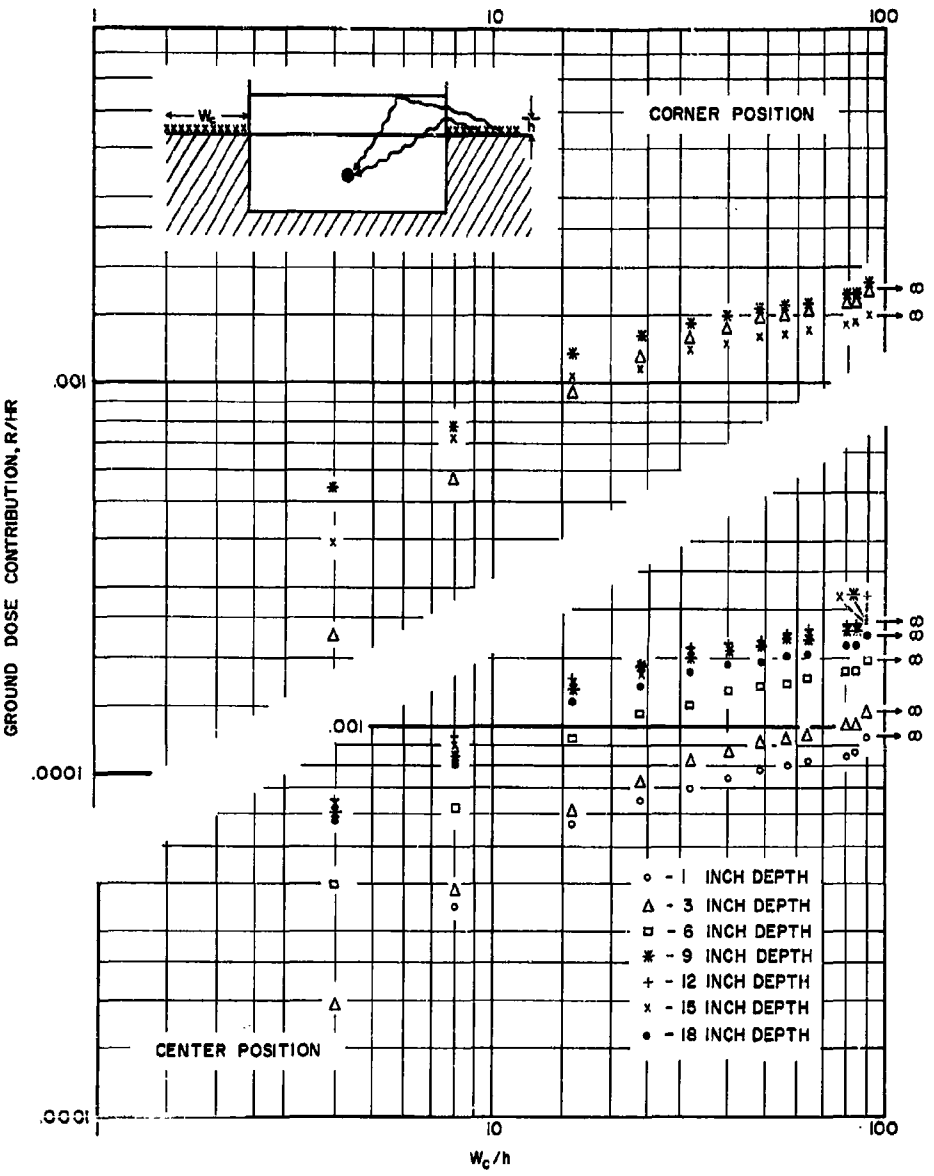

Figure 28. Ground-Dose Contribution in Basement of Building with 20 psf Walls and 80 psf Floors

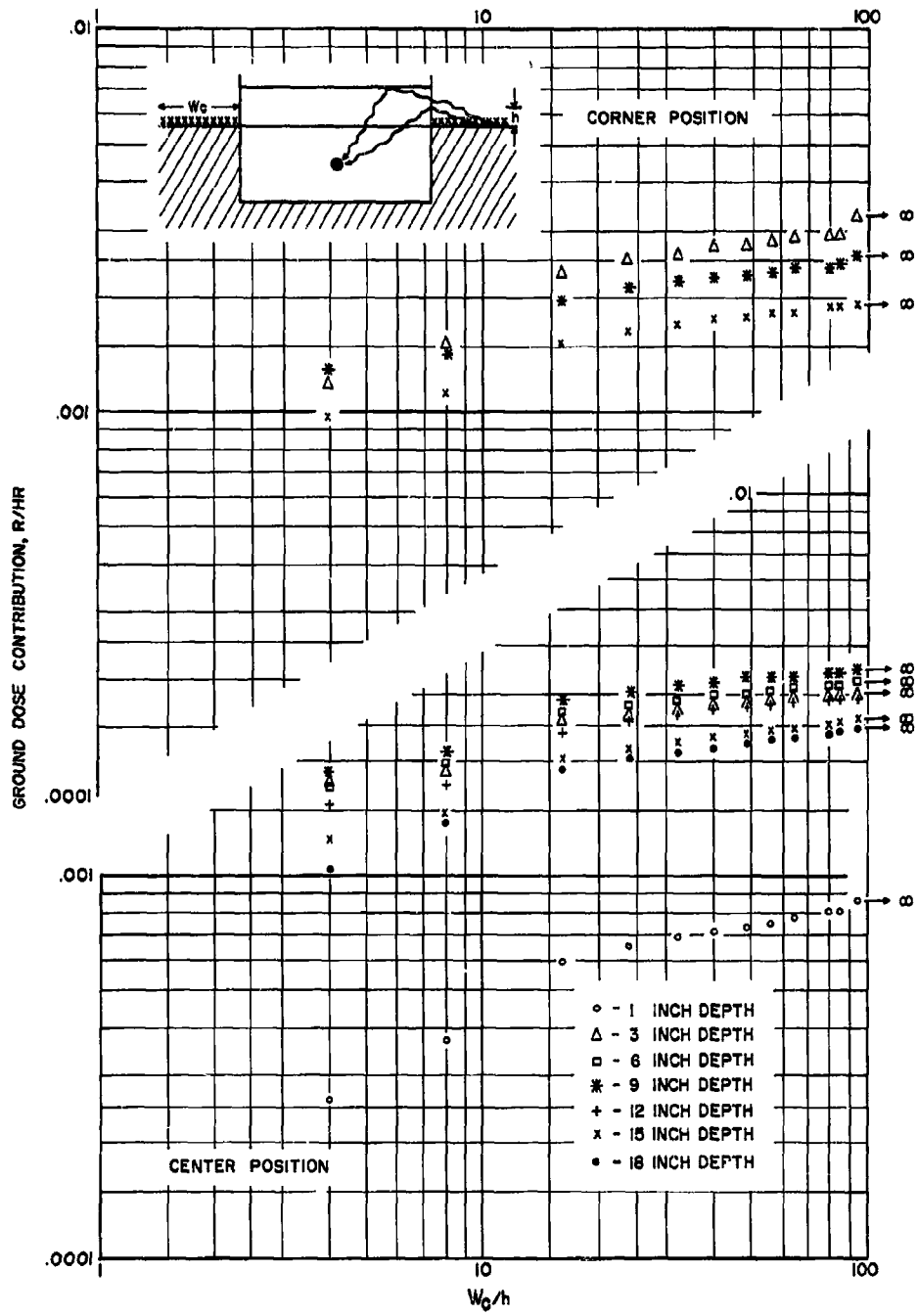

Figure 29. Ground-Dose Contribution in Basement of Building with 80 psf Walls and Floors

position. This computation has been performed for various values of W_c/h and is presented in Table 36. Since most of the radiation entering the basement region scatters from either the first-story wall or the first-story ceiling, h is here used as the mid-height of the first story, 6 inches. Note that the values of these ratios for any one building are nearly constant with both depth and position (center or corner). The maximum deviation from the average values presented in Table 36 is ±20%, with most of the data falling within ±10% of the average.

TABLE 36

FRACTION OF INFINITE-FIELD GROUND-DOSE CONTRIBUTION FOR RECTANGULAR LIMITED FIELDS (Average Values, D/D_∞)

W_c/h	Dose Rate			
	0 psf Walls 20 psf Floors	20 psf Walls 20 psf Floors	20 psf Walls 80 psf Floors	80 psf Walls 80 psf Floors
4	0.26	0.23	0.31	0.51
8	0.36	0.37	0.40	0.55
16	0.65	0.64	0.65	0.79
32	0.77	0.76	0.79	0.87
100	0.96	0.93	0.96	0.99
∞	1.00	1.0	1.0	1.0

COMPARISON OF CALCULATED AND MEASURED INFINITE-FIELD DATA

The results obtained in this series of experiments offered an ideal opportunity to evaluate the computational methods for below-ground areas suggested in the "Guide for Architects and Engineers"[1] and in the manual "Design and Review of Structures for Protection from Fallout Gamma Radiation."[2] The "Guide for Architects and Engineers" presents a simplified method of computing the dose rate in the basement at the center of a structure of essentially square floor plan. The graphical data

presented for this computation are valid only for a detector located 5 feet below the first-floor slab for structures with 10-foot story height. Since the model structures may be considered to represent a scaled version of 10-foot story height, the dose rate at the center of the basement at a depth of 6 inches should represent, upon correction to full scale, that expected at a detector located 5 feet below the first-floor slab.

The radiation contribution in the basement at a depth of 5 feet at the center of a windowless building from an infinite field of radiation emitted from ground-based sources is thus computed as shown in Table 37.

TABLE 37

COMPUTATION OF DOSE RATE IN THE BASEMENT
5-FEET BELOW THE FIRST FLOOR AT A CENTRAL LOCATION
(Methods of Ref. 1)

Computation Step	Structure			
	1	2	3	4
1. Wall Thickness (psf)	0	20	20	80
2. Floor Thickness (psf)	20	20	80	80
3. Actual Plan Area (in^2)	36x48	36x48	36x48	36x48
4. Scaled Plan Area (ft^2)	30x40	30x40	30x40	30x40
5. Uncorrected Ground Contributions, Ref. 6, Chart 4 (r/hr)	.035	.052	.052	.020
6. Floor Attenuation Ref. 6, Case 3, Chart 1	0.3	0.3	0.03	0.03
Answer: Dose Rate in Basement (r/hr)*	0.011	0.016	0.0016	0.0006

*From an infinite field of ground-based fallout contamination that would produce 1.0 r/hr at a 3-foot height if the building were absent.

The method of computation of the dose rate expected in the basement of a structure as presented in the manual entitled "Design and Review of Structures for Protection from Fallout Gamma Radiation"[2] divides the radiation contribution into two distinct fractions: (1) radiation scattered by the wall of the first floor to the basement, or "wall-scattered radiation," and (2) radiation scattered by the atmosphere to the basement, commonly called "skyshine." The equations required to determine these components, using the terminology of Ref. 2, are:

$$D_{\text{wall-scatter}} = \left[G_s(\omega'_u) - G_s(\omega_u)\right] \; S_w E \, B_w(X_e) \, B'_o(X_f)$$

$$D_{\text{skyshine}} = \left[G_a(\omega'_u) - G_a(\omega_u)\right] \; (1 - S_w) \, B_w(X_e) \, B'_o(X_f)$$

$$D_{\text{total}} = D_{\text{wall-scatter}} + G_{\text{skyshine}}$$

where

$G_s(\omega)$ = the directional response of wall-scattered radiation

$G_a(\omega)$ = the directional response of atmospheric-scattered radiation

ω'_u = the solid-angle fraction ($\frac{\text{solid angle}}{2\pi}$) as seen by the detector of the first-floor ceiling

ω_u = the solid-angle fraction ($\frac{\text{solid angle}}{2\pi}$) as seen by the detector of the basement ceiling

S_w = the fraction of direct radiation scattered by the wall

E = an eccentricity factor dependent on the length-to-width ratio of the structure

$B_w(X)_e$ = the barrier shielding introduced by a vertical wall of thickness, X_e

$B'_o(X_f)$ = the barrier shielding introduced by a basement ceiling of thickness, X_f

Spencer[16] evaluates these functions for cobalt as well as fallout radiation. Hence, to compute the expected dose rate in the center of the basement of the scale-model structures, the methods of Ref. 2 were used together with the function as evaluated for cobalt given in Ref. 16. Table 38 presents the computed values of dose rate for the basement areas of the four model structures.

For comparison, the calculated dose rates using the two methods mentioned above and the data obtained from the model experiment are presented in Figure 30. A large discrepancy between computed dose rates and measured dose rates can be seen in this figure. This discrepancy is particularly large in the case of the two buildings with 80 psf floors.

TABLE 38

COMPUTED DOSE RATES IN THE BASEMENT OF THE FOUR MODEL STRUCTURES FOR COBALT RADIATION
(Using method of Ref. 2 and functions of Ref. 16)

Center Detector Position (ft below basement ceiling)	Dose Rate (r/hr*)			
	0 psf Walls 20 psf Floors	20 psf Walls 20 psf Floors	20 psf Walls 80 psf Floors	80 psf Walls 80 psf Floors
1	.0097	.0175	.00164	.00072
3	.0074	.0142	.00133	.00058
7	.0036	.0080	.00075	.00034
10	.0025	.0055	.00052	.00023
15	.0014	.0035	.00034	.00015

*From an infinite field of ground-based cobalt contamination that would produce 1.00 r/hr at 3-foot height if the building were absent.

In the performance of the two experiments using 80 psf floors, the first-floor slab projected 2 inches above the ground-air interface (see Figure 31). Thus a major dose contribution in the basement was from photons striking the outer edge of the floor slab and scattering to the basement detectors. To illustrate this phenomenon, a series of six experiments were run with just the floor slab in place but the upper building removed. The experimental areas of simulated contamination used in these experiments were selected to cover the range of experimentation used. Thus, experimental runs were made using source Areas 4 and 6 (see Figure 6), representing sources fairly close to the building; Areas 13 and 15, representing source areas mid-way out in the quadrant of simulated contamination; and Areas 22 and 24, representing extreme radial positions. The data obtained from these experiments are presented in Table 39 together with that obtained previously from these source areas with the 80 psf floored structures in place.

From Table 39 it is clear that approximately 40% to 50% of the dose obtained in the basement of the structure with 80 psf floors and walls and 50% to 60% of the dose obtained in the structure with 80 psf floors and 20 psf walls may be directly attributable to radiation that has scattered from the edge of the first-floor slab to the basement area. If this correction is applied to the data of Figure 30 to remove the edge-scattered radiation from the dose rates, it will be noticed that, at the depth of normal computation of basement dose rate (6 feet below the basement ceiling),

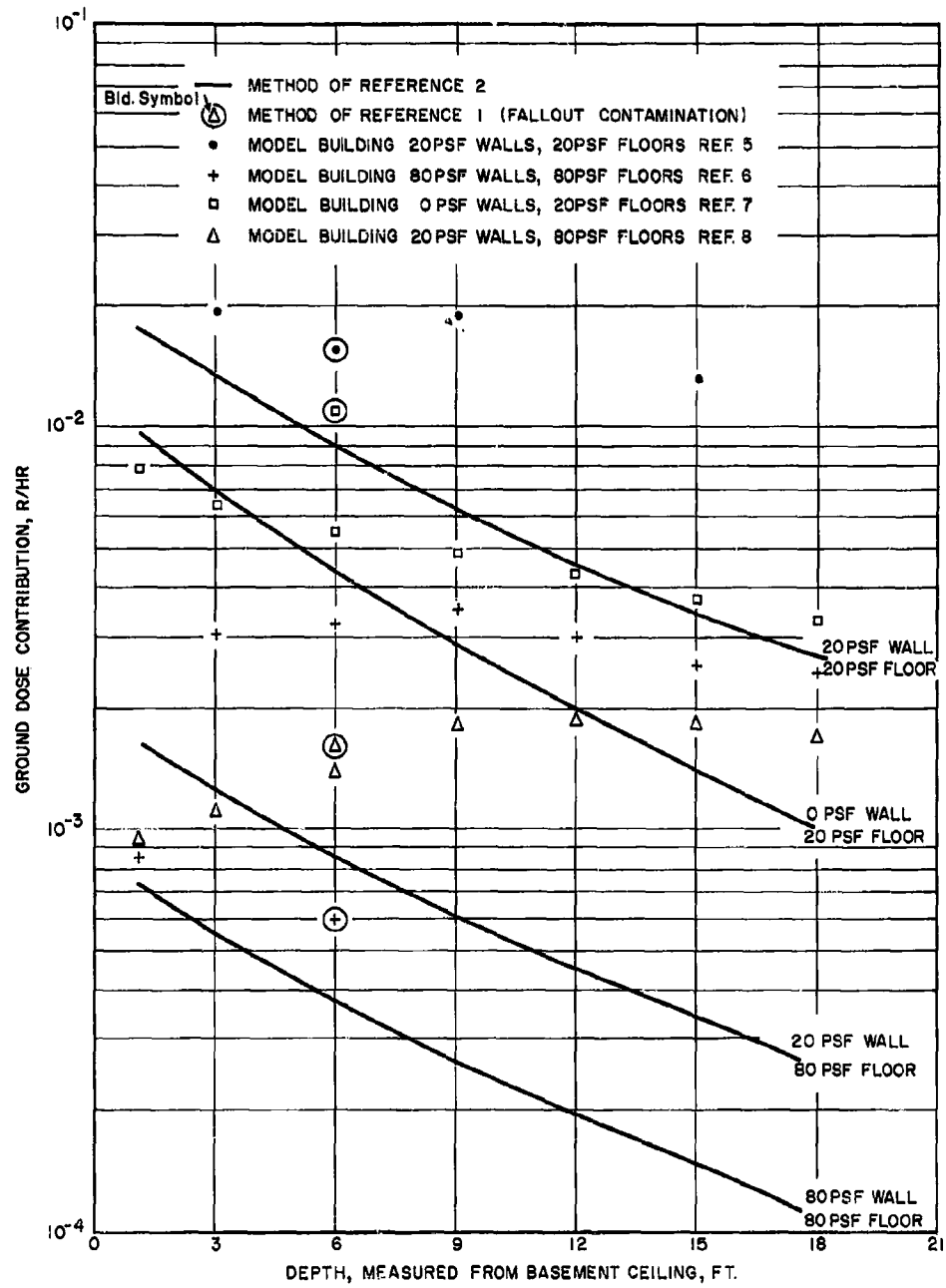

Figure 30. Comparison of Calculated and Experimental Basement Dose-Rate Values from an Infinite Source Field, Including Floor-Edge Scattered Dose

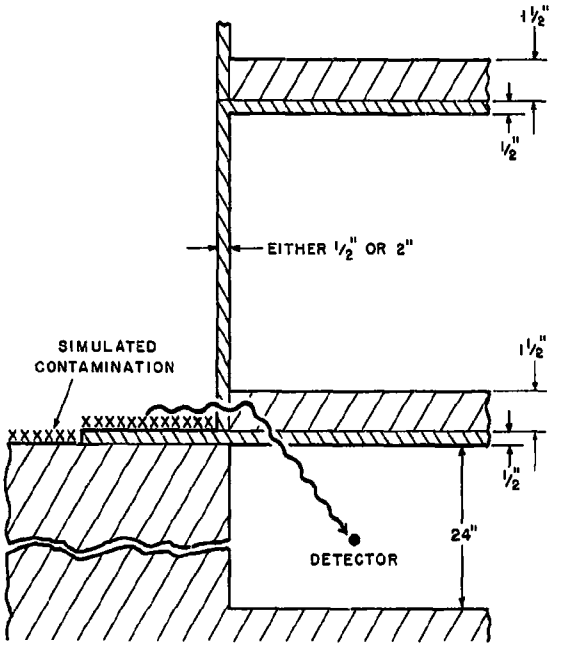

Figure 31. Diagram of Floor Geometry for 80 psf Floor Experiments

the data from all experiments except that with 80 psf walls and 80 psf floors are now roughly the same factor higher than the computed data. The data taken in the basement with the 80 psf wall and 80 psf floor structure remain, however, an unexplained factor of about 4 higher than the data computed analytically. Possibly, the structure was misaligned with the basement wall to a greater extent than was realized. Disregarding the results of the building with 80 psf walls and floors, however, the ratio of experimental results divided by computed values is approximately 1.5 and is unexplainable at this writing.

A more significant variation than the factor of 1.5, however, for basements of greater than average depth (greater than 9 or 10 feet) is the very serious discrepancy between calculated and experimental values for depths greater than 6 feet. The data from all four experiments in general follow a somewhat similar curve, with dose rate first increasing with depth and then decreasing. The methods of computation presently proposed, however, exhibit a continuing decrease in dose rate with depth. The discrepancy in curve form may be related to the neglect of radiation scattering from the underface of the first-floor ceiling (ceiling shine) to the detectors.

TABLE 39

EVALUATION OF EDGE-SCATTERING EFFECT OF FLOORS
CENTER POSITION
(mr/hr from a source density of 1 curie/ft^2)

Area	Depth Below Ground Level	Dose Rate*			Differences Per Cent of Data with Building	
		20 psf Wall 80 psf Floor	80 psf Wall 80 psf Floor	Phantom Building†	20 psf Wall 80 psf Floor	80 psf Wall 80 psf Floor
4	- 1	6.4	5.33	2.62	59	51
	- 3	11.3	11.5	5.24	53	54
	- 6	14.0*	15.0	7.67	46	49
	- 9	14.0	16.0	8.23	41	49
	-12	13.0	15.0	6.92	47	54
	-15	12.0	12.0	5.98	50	50
	-18	11.0	11.0	5.05	54	54
		Average Value			50	51
6	- 1	6.4	5.40	3.24‡	49	40
	- 3	7.0*	6.00	3.96	43	34
	- 6	7.2	7.40	4.59	37	38
	- 9	8.2	8.10	5.65	30	36
	-12	8.4	8.90	5.31	37	41
	-15	8.4	8.60	4.86	42	44
	-18	8.2	8.10	4.32	47	47
		Average Value			40	40
13	- 1	2.8	1.93	0.97	64	50
	- 3	4.0	3.85	1.84	54	52
	- 6	4.4	4.68	2.52	43	46
	- 9	4.8	4.95	2.42	50	51
	-12	4.6	4.68	2.18	52	53
	-15	4.2	3.98	1.94	54	51
	-18	3.9	3.57	1.65	58	54
		Average Value			54	51
16	- 1	1.8	1.37	0.92	49	33
	- 3	3.0	1.78	1.38	54	23
	- 6	3.2	2.47	1.73	46	30
	- 9	3.6	3.01	2.19	39	27
	-12	3.6	3.29	2.30	36	30
	-15	3.6	3.43	2.30	36	33
	-18	3.6	3.29	2.25	38	32
		Average Value			43	30
22	- 1	1.7	0.99	0.57	66	42
	- 3	1.9	1.42	0.88	55	38
	- 6	2.1	1.70	0.91	57	46
	- 9	2.1	1.85	1.02	52	45
	-12	2.2	1.70	0.96	56	44
	-15	1.8	1.56	0.88	51	44
	-18	1.8	1.42	0.82	54	42
		Average Value			56	43
24	- 1	1.1	0.88	0.53‡	52	40
	- 3	1.4	1.33	0.85	40	36
	- 6	1.5	1.62	0.90	40	45
	- 9	1.8	1.77	1.10	39	38
	-12	1.8	1.84	1.10	39	41
	-15	1.6	1.77	1.05	35	42
	-18	1.5	1.62	1.00	33	38
		Average Value			40	40

*Not corrected for source anisotropy or tubing attenuation.

† 80 psf first floor slab only.

‡ Estimated Value.

CHAPTER 6

CONCLUSIONS AND RECOMMENDATIONS

This report is the fifth and final of a series devoted to evaluating the effects of limited fields of contamination on the dose rate expected in multistory structures of different wall and floor mass thicknesses. The previous four interim reports[4-7] presented the data in preliminary form with a minimum of analysis so that they could become immediately useful to the National Shelter Survey Computer Program.

CONCLUSIONS

The major conclusions derived from this study may be summarized as follows:

Near-Field Limited Strips of Contamination ($W_c/h \leq 10$; $W_c \leq 300$ feet, upper floors)

1. The method of correction for limited fields of contamination as presently used in the National Shelter Survey Computer Program can lead to considerable error in the case of thick floors. The NSSCP presents a single multiplicative correction factor for all height positions. Experimental values indicate that when the floor thickness is not great ($X_f \leq 40$ psf) a single correction factor is adequate for all floor locations. However, where floor thicknesses exceed 40 psf, one correction factor applies for first-floor locations and a separate factor is required for upper-floor locations.
2. The multiplicative correction factors as presented in Table 6 of the NSSCP show fair agreement with experimental values. Presently used and experimentally obtained values are given in Tables 40 and 41.
3. The dose rate from limited strips of contamination ($W_c/h \leq 10$, $W_c \leq 300$ feet) at locations and heights other than that at the center of the structure at a 3-foot height may be estimated within 25% accuracy as ratios of the center-position dose rate. These dose ratios are given in Table 42.

TABLE 40

M_L, MULTIPLICATIVE CORRECTION FACTORS FOR ALL FLOORS

($W_c/h \leq 10$, $W_c \leq 300$ ft., thin floors ($X_f \leq 40$ psf))

W_c/h	0 psf Walls		20 psf Walls	
	Experimental	NSSCP	Experimental	NSSCP
0	0.000	0.0000	0.0000	0.0000
.32	0.011	0.0095	0.0021	0.0019
.44	0.018	0.017	0.0050	0.0048
.58	0.026	0.029	0.021	0.010
.75	0.035	0.047	0.034	0.021
.98	0.050	0.070	0.051	0.037
1.33	0.069	0.11	0.069	0.068
2.06	0.110	0.18	0.10	0.120
2.5	0.13	0.20	0.12	0.133
5	0.18	0.29	0.18	0.230
10	0.32	0.42	0.30	0.365

TABLE 41

M_L, MULTIPLICATIVE CORRECTION FACTORS

$W_c/h \leq 10$, $W_c \leq 300$ feet, thick floors ($X_f \geq 40$ psf)

W_c/h	20 psf Walls			80 psf Walls		
	Experimental		NSSCP	Experimental		NSSCP
	First Floor	Upper Floors	All Floors	First Floor	Upper Floors	All Floors
0	0.0000	0.0000	0.000	0.0000	0.0000	0.0000
0.32	—	0.0004	0.0019	—	0.0003	0.0004
0.44	—	0.0011	0.0048	—	0.0010	0.0012
0.58	—	0.0024	0.010	—	0.0023	0.0031
0.75	—	0.0046	0.021	0.014	0.0046	0.0077
0.98	—	0.0086	0.037	0.022	0.0094	0.017
1.33	—	0.015	0.068	0.032	0.017	0.040
2.06	0.043	0.028	0.120	0.056	0.037	0.086
2.5	0.052	0.036	0.133	0.070	0.049	0.10
5	0.12	0.070	0.230	0.15	0.11	0.19
10	0.25	0.20	0.365	0.28	0.22	0.33

TABLE 42

RATIO OF DOSE RATE AT POSITIONS OTHER THAN THE CENTER 3 FT POSITIONS TO THAT AT THE CENTER 3 FT POSITIONS

Position	Light-Floored Structures ($X_f \leq 40$ psf)	Heavy-Floored Structures ($X_f > 40$ psf)
Center (ft)		
3	1.0	1.0
6	1.4	1.7
9	1.7	2.5
Corner (ft)		
3	1.4	2.5
6	1.7	3.5
9	2.0	4.0

Far-Field Limited Strips of Contamination ($W_c/h \leq 10$, $W_c > 300$ feet)

4. The present method used in the NSSCP to compute the effect of far-field limited strips of contamination is to compute a factor and multiply this factor times the infinite-field dosage. This factor, the ratio of the dose expected from the limited field to that expected from an infinite-field, is computed from air-attenuation functions. The experimentally measured values in general agree within 30% of those computed. Better agreement between theory and experiment may be obtained, however, if the computation is performed in two steps. These are: (1) compute the effect of near-field contamination ($W_c/h \leq 10$, $W_c \leq 300$ feet) using the methods mentioned above and (2) add to this the effect of contamination existing beyond $W_c/h = 10$ or $W_c = 300$ feet, computing this effect as before. The equation for far-field limited strips of contamination thus becomes (using the nomenclature of Chapter 4):

$$M_c = M_L\,(W_c^*/h) + \frac{M_h(X_e, h)}{M_h(X_e, =0, h)}\left[M_h\,(X_e = 0, h = \sqrt{h^2 + W_c^{*2}} - M_h\,(X_e = 0, h = \sqrt{h^2 + W_c^2})\right]$$

where

M_c = fraction of infinite-field dose rate obtained from a limited strip of contamination extending from the building to the far field.

M_L = tabular values from Table 40 or 41

h = detector height

W_c^* = 10 h or 300 feet, whichever is the least dimension

W_c = actual width to outer edge of field.

Infinite-Field Dose Rates

5. The agreement between experimentally measured values of infinite-field dose rate and those computed using the methods of the "Guide for Architects and Engineers,"[1] the National Shelter Survey Computer Program,[3] and the manual entitled "The Design and Review of Structures for Protection from Fallout Gamma Radiation"[2] is excellent.

Below-Ground Dose Rate

6. The data obtained from measurements of the dose rate at a distance corresponding to 6 feet below ground level were in general somewhat higher than those predicted by the methods of Ref. 1, 2, and 3. This discrepancy increased slightly with increasing depth.

7. The fraction of infinite-field dose rate in basement locations obtained from limited strips of contamination fell on a common curve for all detector depths within approximately 10%. The mean values as obtained experimentally in each of the four structures are presented in Table 43.

TABLE 43

FRACTION OF INFINITE FIELD GROUND DOSE RATE FOR RECTANGULAR LIMITED FIELDS OF CONTAMINATION

W_c/h^*	Dose Rate			
	0 psf Walls 20 psf Floors	20 psf Walls 20 psf Floors	20 psf Walls 80 psf Floors	80 psf Walls 80 psf Floors
0	0.00	0.00	0.00	0.00
4	0.26	0.23	0.31	0.51
8	0.36	0.37	0.40	0.55
16	0.64	0.64	0.64	0.79
32	0.78	0.76	0.79	0.87
100	0.96	0.94	0.96	0.99
∞	1.00	1.00	1.00	1.00

*h is taken here as the mid-height of the first story.

Model to Full-Scale Agreement

8. Excellent agreement (within 5%) is shown between the dose rate obtained from modeling technique on a phantom structure (no building present) and those previously obtained in similar full-scale geometry by Rexroad.[13]

RECOMMENDATIONS

The major recommendations of this study are:

1. Since floor thickness plays a critical role in the dose obtained from limited strips of contamination, the present series of experiments should be extended to cover the cases of: 0 psf walls and 80 psf floors and 80 psf walls and 20 psf floors.

2. Since the agreement between infinite-field values of experimental and theoretical data obtained in basement regions is poor, further experiments on both model and full-scale structures should be carried out.

3. The effect of floor-edge scattering (radiation scattering from the edge of a thick floor to a detector) should be thoroughly investigated and analytical methods should be developed to compute this radiation component.

REFERENCES

1. Office of Civil Defense, "Guide for Architects and Engineers," NP-10-2 (May, 1960).
2. Office of Civil Defense, "The Design and Review of Structures for Protection from Fallout Gamma Radiation," rev. ed. (1 October 1961).
3. L. V. Spencer and C. Eisenhauer,"Calculation of Protection Factors for the National Fallout Shelter Survey," National Bureau of Standards, Report No. 7539 (July, 1962).
4. J. F. Batter and A. W. Starbird, "The Effect of Limited Strips of Contamination on the Dose Rate in a Multistory Windowless Building, Volume I, 20 psf Wall and Floor Thickness," Technical Operations Research, Report No. TO-B 62-26 (30 April 1962).
5. J. F. Batter and A. W. Starbird, "The Effect of Limited Strips of Contamination on the Dose Rate in a Multistory Windowless Building, Volume II, 80 psf Wall and Floor Thickness," Technical Operations Research, Report No. TO-B 62-29 (15 May 1962).
6. J. F. Batter, A. W. Starbird, and M. Dwonczyk, "The Effect of Limited Strips of Contamination on the Dose Rate in a Multistory Windowless Building, Volume III, 0 psf Wall and 20 psf Floor Thickness," Technical Operations Research, Report No. TO-B 62-40 (30 June 1962).
7. N. York, R. MacNeil, R. Brodeur, "The Effect of Limited Strips of Contamination on the Dose Rate in a Multistory Windowless Building, Volume IV, 20 psf Wall and 80 psf Floor Thickness," Technical Operations Research, Report No. TO-B 62-49 (July, 1962).
8. A. W. Starbird, J. F. Batter, and H. A. Mehlhorn, "Modeling Techniques as Applied to Fallout Simulation on Residential-Type Structures and Some Preliminary Results," Technical Operations Research, Report No. TO-B 61-35 (8 July 1961).

9. J. F. Batter and E. T. Clarke, "Modeling as a Technique for Determining Radiation Shielding," Shielding Symposium Proceedings, NRDL-OCDM Reviews and Lectures No. 110 (31 October - 1 November 1960).

10. E. T. Clarke, J. F. Batter, and A. L. Kaplan, "Measurement of Attenuation in Existing Structures of Radiation from Simulated Fallout," Technical Operations, Inc., Report No. TO-B 59-4 (27 April 1959).

11. J. F. Batter, and others, "An Experimental Evaluation of Radiation Protection Afforded by a Large Modern Concrete Office Building," Technical Operations, Inc., Report No. TO-B 59-5 (CEX 59. 1 AEC) (May, 1959).

12. E. T. Clarke and J. F. Batter, "Gamma-Ray Scattering by Nearby Surfaces," ANS Transactions 5 (1962).

13. R. E. Rexroad and M. A. Schmoke, "Scattered Radiation and Far-Field Dose Rates from Distributed Cobalt-60 and Cs-137 Sources," U. S. Army Chemical Corps, Nuclear Defense Laboratory, Report No. NDL-TR-2 (September, 1960).

14. L. R. Solon, and others, "Measurements of the Scatter Component from a Kilocurie Co-60 Source," U. S. AEC NYO-2065 (June, 1957).

15. B. L. Jones, J. W. Harris, and W. P. Kunkel, "Air and Ground Scattering of Co-60 Gamma Radiation," CVAC-170 (March, 1955).

16. L. V. Spencer, "Structure Shielding Against Fallout Radiation from Nuclear Weapons," National Bureau of Standards, Monograph 42 (1 June 1962).

Rept No. TO-B 62-58
Batter, J. F., Starbird, A. W., and York, N., FINAL REPORT, THE EFFECT OF LIMITED STRIPS OF CONTAMINATION ON THE DOSE RATE IN A MULTISTORY, WINDOWLESS BUILDING, Technical Operations Research, Burlington, Mass. Office of Civil Defense, Department of Defense, Washington, D. C. August, 1962, 109 p. incl. 31 figs., 43 tables.

Unclassified Report

This final report of a series of five evaluates the effects of limited fields of contamination on the dose rate within multistory structures. Comparisons are made between experimentally determined results and those obtained through use of the OCD "Guide for Architects and Engineers," the National Shelter Survey Computer Program, and the

(over)

1. The Effect of Limited Strips of Contamination on the Dose Rate in a Multistory, Windowless Building
2. Simulated Fallout
3. Co-60
4. Modeling Technique
5. Radiation Shielding
6. Batter, J. F.
7. Starbird, A. W.
8. York, N.
9. Office of Civil Defense
10. Contract OCD-OS-62-14

Rept No. TO-B 62-58
Batter, J. F., Starbird, A. W., and York, N., FINAL REPORT, THE EFFECT OF LIMITED STRIPS OF CONTAMINATION ON THE DOSE RATE IN A MULTISTORY, WINDOWLESS BUILDING, Technical Operations Research, Burlington, Mass. Office of Civil Defense, Department of Defense, Washington, D. C. August, 1962, 109 p. incl. 31 figs., 43 tables.

Unclassified Report

This final report of a series of five evaluates the effects of limited fields of contamination on the dose rate within multistory structures. Comparisons are made between experimentally determined results and those obtained through use of the OCD "Guide for Architects and Engineers," the National Shelter Survey Computer Program, and the

(over)

1. The Effect of Limited Strips of Contamination on the Dose Rate in a Multistory, Windowless Building
2. Simulated Fallout
3. Co-60
4. Modeling Technique
5. Radiation Shielding
6. Batter, J. F.
7. Starbird, A. W.
8. York, N.
9. Office of Civil Defense
10. Contract OCD-OS-62-14

OCD Manual entitled "The Design and Review of Structures for Protection from Fallout Gamma Radiation."

The National Shelter Survey Computer Program method for correction to account for near-field limited strips of contamination contains appreciable error, because it does not differentiate between thin- and thick-floor correction factors. Recommended experimentally obtained multiplicative correction factors for both thin and thick floors are presented. Further investigation of the effects of floor thickness and floor-edge scattering is recommended. An improved computation procedure for determining the fraction of infinite-field dose rate obtained from far-field limited strips of contamination is described. Agreement is excellent between experimentally measured and computed infinite-field dose rates. The measured dose rates in the basement are higher than predicted by computational procedures. Further below-ground-level investigation is recommended on a full-scale basement. Excellent agreement is shown between results obtained from the modeling technique on a phantom structure and previous full-scale results.

OCD Manual entitled "The Design and Review of Structures for Protection from Fallout Gamma Radiation."

The National Shelter Survey Computer Program method for correction to account for near-field limited strips of contamination contains appreciable error, because it does not differentiate between thin- and thick-floor correction factors. Recommended experimentally obtained multiplicative correction factors for both thin and thick floors are presented. Further investigation of the effects of floor thickness and floor-edge scattering is recommended. An improved computation procedure for determining the fraction of infinite-field dose rate obtained from far-field limited strips of contamination is described. Agreement is excellent between experimentally measured and computed infinite-field dose rates. The measured dose rates in the basement are higher than predicted by computational procedures. Further below-ground-level investigation is recommended on a full-scale basement. Excellent agreement is shown between results obtained from the modeling technique on a phantom structure and previous full-scale results.

Rept No. TO-B 62-58
Batter, J. F., Starbird, A. W., and York, N., FINAL REPORT, THE EFFECT OF LIMITED STRIPS OF CONTAMINATION ON THE DOSE RATE IN A MULTISTORY, WINDOWLESS BUILDING, Technical Operations Research, Burlington, Mass. Office of Civil Defense, Department of Defense, Washington, D. C. August, 1962, 109 p. incl. 31 figs., 43 tables.

Unclassified Report

This final report of a series of five evaluates the effects of limited fields of contamination on the dose rate within multistory structures. Comparisons are made between experimentally determined results and those obtained through use of the OCD "Guide for Architects and Engineers," the National Shelter Survey Computer Program, and the

(over)

OCD Manual entitled "The Design and Review of Structures for Protection from Fallout Gamma Radiation."

The National Shelter Survey Computer Program method for correction to account for near-field limited strips of contamination contains appreciable error, because it does not differentiate between thin- and thick-floor correction factors. Recommended experimentally obtained multiplicative correction factors for both thin and thick floors are presented. Further investigation of the effects of floor thickness and floor-edge scattering is recommended. An improved computation procedure for determining the fraction of infinite-field dose rate obtained from far-field limited strips of contamination is described. Agreement is excellent between experimentally measured and computed infinite-field dose rates. The measured dose rates in the basement are higher than predicted by computational procedures. Further below-ground-level investigation is recommended on a full-scale basement. Excellent agreement is shown between results obtained from the modeling technique on a phantom structure and previous full-scale results.

1. The Effect of Limited Strips of Contamination on the Dose Rate in a Multistory, Windowless Building
2. Simulated Fallout
3. Co-60
4. Modeling Technique
5. Radiation Shielding
6. Batter, J. F.
7. Starbird, A. W.
8. York, N.
9. Office of Civil Defense
10. Contract OCD-OS-62-14

Rept No. TO-B 62-58
Batter, J. F., Starbird, A. W., and York, N., FINAL REPORT, THE EFFECT OF LIMITED STRIPS OF CONTAMINATION ON THE DOSE RATE IN A MULTISTORY, WINDOWLESS BUILDING, Technical Operations Research, Burlington, Mass. Office of Civil Defense, Department of Defense, Washington, D. C. August, 1962, 109 p. incl. 31 figs., 43 tables.

Unclassified Report

This final report of a series of five evaluates the effects of limited fields of contamination on the dose rate within multistory structures. Comparisons are made between experimentally determined results and those obtained through use of the OCD "Guide for Architects and Engineers," the National Shelter Survey Computer Program, and the

(over)

OCD Manual entitled "The Design and Review of Structures for Protection from Fallout Gamma Radiation."

The National Shelter Survey Computer Program method for correction to account for near-field limited strips of contamination contains appreciable error, because it does not differentiate between thin- and thick-floor correction factors. Recommended experimentally obtained multiplicative correction factors for both thin and thick floors are presented. Further investigation of the effects of floor thickness and floor-edge scattering is recommended. An improved computation procedure for determining the fraction of infinite-field dose rate obtained from far-field limited strips of contamination is described. Agreement is excellent between experimentally measured and computed infinite-field dose rates. The measured dose rates in the basement are higher than predicted by computational procedures. Further below-ground-level investigation is recommended on a full-scale basement. Excellent agreement is shown between results obtained from the modeling technique on a phantom structure and previous full-scale results.

1. The Effect of Limited Strips of Contamination on the Dose Rate in a Multistory, Windowless Building
2. Simulated Fallout
3. Co-60
4. Modeling Technique
5. Radiation Shielding
6. Batter, J. F.
7. Starbird, A. W.
8. York, N.
9. Office of Civil Defense
10. Contract OCD-OS-62-14

Rept No. TO-B 62-58
Batter, J. F., Starbird, A. W., and York, N., FINAL REPORT, THE EFFECT OF LIMITED STRIPS OF CONTAMINATION ON THE DOSE RATE IN A MULTISTORY, WINDOWLESS BUILDING, Technical Operations Research, Burlington, Mass. Office of Civil Defense, Department of Defense, Washington, D. C. August, 1962, 109 p. incl. 31 figs., 43 tables.

Unclassified Report

This final report of a series of five evaluates the effects of limited fields of contamination on the dose rate within multistory structures. Comparisons are made between experimentally determined results and those obtained through use of the OCD "Guide for Architects and Engineers," the National Shelter Survey Computer Program, and the

(over)

1. The Effect of Limited Strips of Contamination on the Dose Rate in a Multistory, Windowless Building
2. Simulated Fallout
3. Co-60
4. Modeling Technique
5. Radiation Shielding
6. Batter, J. F.
7. Starbird, A. W.
8. York, N.
9. Office of Civil Defense
10. Contract OCD-OS-62-14

Rept No. TO-B 62-58
Batter, J. F., Starbird, A. W., and York, N., FINAL REPORT, THE EFFECT OF LIMITED STRIPS OF CONTAMINATION ON THE DOSE RATE IN A MULTISTORY, WINDOWLESS BUILDING, Technical Operations Research, Burlington, Mass. Office of Civil Defense, Department of Defense, Washington, D. C. August, 1962, 109 p. incl. 31 figs., 43 tables.

Unclassified Report

This final report of a series of five evaluates the effects of limited fields of contamination on the dose rate within multistory structures. Comparisons are made between experimentally determined results and those obtained through use of the OCD "Guide for Architects and Engineers," the National Shelter Survey Computer Program, and the

(over)

1. The Effect of Limited Strips of Contamination on the Dose Rate in a Multistory, Windowless Building
2. Simulated Fallout
3. Co-60
4. Modeling Technique
5. Radiation Shielding
6. Batter, J. F.
7. Starbird, A. W.
8. York, N.
9. Office of Civil Defense
10. Contract OCD-OS-62-14

OCD Manual entitled "The Design and Review of Structures for Protection from Fallout Gamma Radiation."

The National Shelter Survey Computer Program method for correction to account for near-field limited strips of contamination contains appreciable error, because it does not differentiate between thin- and thick-floor correction factors. Recommended experimentally obtained multiplicative correction factors for both thin and thick floors are presented. Further investigation of the effects of floor thickness and floor-edge scattering is recommended. An improved computation procedure for determining the fraction of infinite-field dose rate obtained from far-field limited strips of contamination is described. Agreement is excellent between experimentally measured and computed infinite-field dose rates. The measured dose rates in the basement are higher than predicted by computational procedures. Further below-ground-level investigation is recommended on a full-scale basement. Excellent agreement is shown between results obtained from the modeling technique on a phantom structure and previous full-scale results.

OCD Manual entitled "The Design and Review of Structures for Protection from Fallout Gamma Radiation."

The National Shelter Survey Computer Program method for correction to account for near-field limited strips of contamination contains appreciable error, because it does not differentiate between thin- and thick-floor correction factors. Recommended experimentally obtained multiplicative correction factors for both thin and thick floors are presented. Further investigation of the effects of floor thickness and floor-edge scattering is recommended. An improved computation procedure for determining the fraction of infinite-field dose rate obtained from far-field limited strips of contamination is described. Agreement is excellent between experimentally measured and computed infinite-field dose rates. The measured dose rates in the basement are higher than predicted by computational procedures. Further below-ground-level investigation is recommended on a full-scale basement. Excellent agreement is shown between results obtained from the modeling technique on a phantom structure and previous full-scale results.

Rept No. TO-B 62-58
Batter, J. F., Starbird, A. W., and York, N., FINAL REPORT, THE EFFECT OF LIMITED STRIPS OF CONTAMINATION ON THE DOSE RATE IN A MULTISTORY, WINDOWLESS BUILDING, Technical Operations Research, Burlington, Mass. Office of Civil Defense, Department of Defense, Washington, D. C. August, 1962, 109 p. incl. 31 figs., 43 tables.

Unclassified Report

This final report of a series of five evaluates the effects of limited fields of contamination on the dose rate within multistory structures. Comparisons are made between experimentally determined results and those obtained through use of the OCD "Guide for Architects and Engineers," the National Shelter Survey Computer Program, and the

(over)

1. The Effect of Limited Strips of Contamination on the Dose Rate in a Multistory, Windowless Building
2. Simulated Fallout
3. Co-60
4. Modeling Technique
5. Radiation Shielding
6. Batter, J. F.
7. Starbird, A. W.
8. York, N.
9. Office of Civil Defense
10. Contract OCD-OS-62-14

Rept No. TO-B 62-58
Batter, J. F., Starbird, A. W., and York, N., FINAL REPORT, THE EFFECT OF LIMITED STRIPS OF CONTAMINATION ON THE DOSE RATE IN A MULTISTORY, WINDOWLESS BUILDING, Technical Operations Research, Burlington, Mass. Office of Civil Defense, Department of Defense, Washington, D. C. August, 1962, 109 p. incl. 31 figs., 43 tables.

Unclassified Report

This final report of a series of five evaluates the effects of limited fields of contamination on the dose rate within multistory structures. Comparisons are made between experimentally determined results and those obtained through use of the OCD "Guide for Architects and Engineers," the National Shelter Survey Computer Program, and the

(over)

1. The Effect of Limited Strips of Contamination on the Dose Rate in a Multistory, Windowless Building
2. Simulated Fallout
3. Co-60
4. Modeling Technique
5. Radiation Shielding
6. Batter, J. F.
7. Starbird, A. W.
8. York, N.
9. Office of Civil Defense
10. Contract OCD-OS-62-14

OCD Manual entitled "The Design and Review of Structures for Protection from Fallout Gamma Radiation."

The National Shelter Survey Computer Program method for correction to account for near-field limited strips of contamination contains appreciable error, because it does not differentiate between thin- and thick-floor correction factors. Recommended experimentally obtained multiplicative correction factors for both thin and thick floors are presented. Further investigation of the effects of floor thickness and floor-edge scattering is recommended. An improved computation procedure for determining the fraction of infinite-field dose rate obtained from far-field limited strips of contamination is described. Agreement is excellent between experimentally measured and computed infinite-field dose rates. The measured dose rates in the basement are higher than predicted by computational procedures. Further below-ground-level investigation is recommended on a full-scale basement. Excellent agreement is shown between results obtained from the modeling technique on a phantom structure and previous full-scale results.

OCD Manual entitled "The Design and Review of Structures for Protection from Fallout Gamma Radiation."

The National Shelter Survey Computer Program method for correction to account for near-field limited strips of contamination contains appreciable error, because it does not differentiate between thin- and thick-floor correction factors. Recommended experimentally obtained multiplicative correction factors for both thin and thick floors are presented. Further investigation of the effects of floor thickness and floor-edge scattering is recommended. An improved computation procedure for determining the fraction of infinite-field dose rate obtained from far-field limited strips of contamination is described. Agreement is excellent between experimentally measured and computed infinite-field dose rates. The measured dose rates in the basement are higher than predicted by computational procedures. Further below-ground-level investigation is recommended on a full-scale basement. Excellent agreement is shown between results obtained from the modeling technique on a phantom structure and previous full-scale results.